



# QEX

July/August 2007

\$5

## A Forum for Communications Experimenters

Issue No. 243



**W1FR** is the project coordinator for "The ARRL 500-kHz Experiment." The Mackay 2017 Reserve Transmitter shown at the top is part of WD2XSH-10, operated by W4DEX.

**ARRL** *The national association for*  
**AMATEUR RADIO**

225 Main Street  
Newington, CT USA 06111-1494



# TOKYO HY-POWER



## HL-1.5KFX

### HF Amp, HF/50MHz Linear Power Amplifier

This compact and lightweight 1kW desktop HF/50MHz linear power amplifier has a maximum input power of 1.75kW. Our solid-state broadband power amp technology makes it the smallest and lightest self-contained amplifier in its class.

Typical output power is 1kW PEP/SSB on HF and 650W on 6m band with the drive power of 85-90W. Bands set automatically with the built-in band decoder. You can forget about the band setting when the amplifier is connected to your modern radio through supplied band data cables for ICOM CI-V, DC voltage (ICOM, Yaesu), and RS-232C (Kenwood). Manual band setting selectable as well.

All these data cables are included with the amplifier.

Complies with New FCC Rules.

## — Two More Fine Products from TOKYO HY-POWER —



## HC-200AT

### HF/50MHz 200W Auto Antenna Tuner

HC-200AT works with a variety of antennas such as short whip, vertical, half lambda dipole, random length dipole with ladder type open feeder.

#### Features

- HC-200AT is a compact 200W HF/6m auto antenna tuner. Works with any radio having a frequency coverage of 1.8-54MHz, and power output of 2-200W.
- With a wire antenna of 7.5m (25 feet) or longer, the tuner will tune from 3.5 through 54MHz. For 1.8MHz (160M), a minimum length wire of 30m (95 feet) is recommended.
- The advanced 16 bit MPU (micro processor) calculates the ratio of forward and reflected power. Our newly developed computing algorithm produces world class tuning speed.
- 256 capacitors (C) and inductors (L) are combined to form the inverted L-shape circuit. Depending on antenna, capacitances may be switched from one end of inductors to the other to form the reversed inverted-L shape circuit. Over 131,072 combinations of L & C. High current capacity relays are used in the L and C tuning network.
- Tuned data of L and C are stored in the ten channel memory. Tuning under memory mode using the same antenna on the same frequency is finished within 0.2 second after the initial tuning.
- Tuning will be accomplished by tapping the "TUNE" button, and/or pressing the "TUNER" (or "TUNE") button of the radio, if the tuner is connected to the Radio Interface cable. (See Connection Section.)
- Analog meter monitors the forward power (PF) and SWR. SWR is indicated automatically with the modern processor IC.

#### Specifications

**Frequency Range:**  
1.8 - 54MHz

**Output Impedance Range:**  
5 - 500 ohms (3.5 - 54MHz)  
15 - 500 ohms (1.8 MHz)

**Maximum Handling Power:**  
200W (P.E.P./CW)

**Input Impedance:**  
50 ohms

**Tuning Power:**  
2 - 20W  
Minimum and most adequate power

**Tuning Time:**  
1.5 sec. (typ.) for initial tuning for SWR= 3.5:1  
4 sec. (max.)  
0.2 sec. for memory mode

**DC Power Voltage:**  
DC 12V - 14V

**Current Drain:**  
0.8A max.  
**Quiescent Current:**  
0.1A

**Operating Temp. Range:**  
0 deg. to +40 deg. C

**VSWR (Max.):**  
1.5 (typ.) or lower \*  
After tuning

**Number of Memory:**  
10 ch.

**Dimension:**  
195 x 60 x 242 mm (WxHxD)  
7.7 x 2.4 x 9.5 inches

**Weight:**  
Approx. 1kg. (2.2 lbs.)

**Accessories:**  
DC power cable, 3.5mm dia. Plug \*\*  
\*\* Ear-phone plug

**Optional Parts:**  
1: 4 Unbal. To Bal. Balun  
Model HBL-100  
Remote control Cable for ICOM Radio  
HTC-100AT/ICOM5 (5 meter)  
Remote control Cable for ICOM Radio  
HTC-100AT/ICOM10 (10 meter)

\* This tuner does not tune wire antennas length with multiples of half a lambda or its vicinity.



## HC-1.5KAT

### HF 1.5KW Auto Tuner

Fast and Quiet, Auto Band Set!!

#### Features

- HC-1.5KAT is a high power HF auto antenna tuner designed to work with Tokyo HyPower HL-1.5KFX and HL-2.5KFX linear amplifiers.
- When combined with these THP amplifiers, band change is automatically made through the band data signal from the radio and the amplifier. It also works with other amplifiers as well, in manual mode.
- Tuning time is typically within one second, (2.5 sec. max.). It handles maximum power of 1.5kW pep/cw when the intrinsic antenna SWR is no more than 2.0
- Maximum impedance matching range is SWR of 4 to 1, there are three antenna connectors.
- Two of high quality 3kV rating 200pF air variable capacitors are employed to form a "T" match circuit being driven by high speed stepping motors.
- Our own tuning algorithm together with an advanced 16 bit micro-processor enables an extremely fast tuning.

#### Specifications

**Frequency Range:**  
1.8 - 29.7MHz

**Output Impedanc. Range:**  
12.5 - 200 ohms: Reduced range at lower band edges

**Maximum Handling Power:**  
1.5kW (P.E.P./CW) RTTY 1kW

**Input Impedance:**  
50 OHM

**Tuning Power:**  
50W (80W max.)

**Tuning Time:**  
1 sec. (typ.)  
2.5 sec. (max.): Under typical worst SWR condition  
4.0 sec. (max.): Under absolute worst SWR condition

**DC Power Voltage:**  
DC 12V - 14 V: From External AC adaptor

**Current Drain:**  
1.5A max.

**Quiescent Current:**  
0.7A

**Display:**  
LCD Module: 16 characters x 2 rows

**Operating Temp. Range:**  
0 deg. to +40 deg. C

**VSWR (Max.):**  
1.5 (typ.) or lower: Alter tuning band edges

**Circuit Type:**  
T-match network

**Driving Motors:**  
Stepping Motors for Two Air Variable: 0.25 deg. resolution/step

**Matching Algorithm:**  
Analog Control with MPU: Phase and IZI Magnitude Detected

**Dimension:**  
Approx. 8x5.6x12 inches (WxHxD)

**Weight:**  
Approx. 11 lbs.

**Input Connector:**  
SO-239 (UHF)

**Output Connectors:**  
Three SO-239's

**Cooling:**  
Partial air forced cooling with fan.

**Accessories:**  
DC power cable, 3.5mm dia. plug, Band Control Cable with DIN 7 pin plugs.



TOKYO HY-POWER LABS., INC. - USA  
487 East Main Street, Suite 163  
Mount Kisco, NY 10549  
Phone: 914-602-1400  
e-mail: thpusa@optonline.net

TOKYO HY-POWER LABS., INC. - JAPAN  
1-1 Hatanaka 3chome, Niiza Saitama 352-0012  
Phone: +81 (48) 481-1211 FAX: +81 (48) 479-6949  
e-mail: info@thp.co.jp  
Web: http://www.thp.co.jp

Exclusively from



www.hamradio.com

Western US/Canada 1-800-854-6045  
Mountain/Central 1-800-444-9476  
Southeast 1-800-444-7927

Mid-Atlantic 1-800-444-4799  
Northeast 1-800-644-4476  
New England/Eastern Canada 1-800-444-0047

# QEX

QEX (ISSN: 0886-8093) is published bimonthly in January, March, May, July, September, and November by the American Radio Relay League, 225 Main Street, Newington, CT 06111-1494. Periodicals postage paid at Hartford, CT and at additional mailing offices.

POSTMASTER: Send address changes to: QEX, 225 Main St, Newington, CT 06111-1494 Issue No 243

Harold Kramer, WJ1B  
*Publisher*

Doug Smith, KF6DX  
*Editor*

Larry Wolfgang, WR1B  
*Managing Editor*

Lori Weinberg, KB1EIB  
*Assistant Editor*

L. B. Cebik, W4RNL  
Zack Lau, W1VT  
Ray Mack, W5IFS  
*Contributing Editors*

**Production Department**  
Steve Ford, WB8IMY  
*Publications Manager*

Michelle Bloom, WB1ENT  
*Production Supervisor*

Sue Fagan, KB1OKW  
*Graphic Design Supervisor*

Devon Neal, KB1NSR  
*Technical Illustrator*

Joe Shea  
*Production Assistant*

**Advertising Information Contact:**

Janet L. Rocco, W1JLR  
*Business Services*  
860-594-0203 direct  
800-243-7768 ARRL  
860-594-4285 fax

**Circulation Department**

Cathy Stepina, QEX Circulation

**Offices**

225 Main St, Newington, CT 06111-1494 USA  
Telephone: 860-594-0200  
Fax: 860-594-0259 (24 hour direct line)  
e-mail: [qex@arrl.org](mailto:qex@arrl.org)

Subscription rate for 6 issues:

In the US: ARRL Member \$24,  
nonmember \$36;

US by First Class Mail:  
ARRL member \$37, nonmember \$49;

Elsewhere by Surface Mail (4-8 week delivery):  
ARRL member \$31, nonmember \$43;

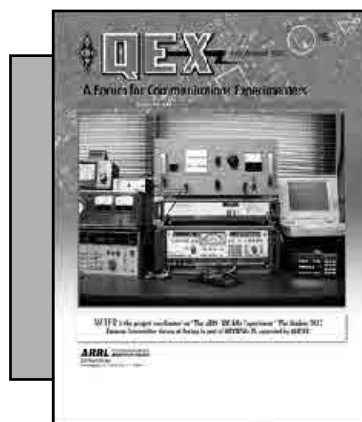
Canada by Airmail: ARRL member \$40,  
nonmember \$52;

Elsewhere by Airmail: ARRL member \$59,  
nonmember \$71.

Members are asked to include their membership control number or a label from their QST when applying.

In order to ensure prompt delivery, we ask that you periodically check the address information on your mailing label. If you find any inaccuracies, please contact the Circulation Department immediately. Thank you for your assistance.

Copyright ©2007 by the American Radio Relay League Inc. For permission to quote or reprint material from QEX or any ARRL publication, send a written request including the issue date (or book title), article, page numbers and a description of where you intend to use the reprinted material. Send the request to the office of the Publications Manager ([permission@arrl.org](mailto:permission@arrl.org)).



## About the Cover

Fritz Raab, W1FR, is the project coordinator for "The ARRL 500-kHz Experiment." The article in this issue describes the work done so far, and describes some of the equipment and antennas used by participating stations, such as this Mackay 2017 transmitter used by W4DEX.



## Features

- 3 The ARRL 500-kHz Experiment: WD2XSH**  
*By Frederick H. "Fritz" Raab, W1FR*
- 12 Voltage-Magnitude Impedance Measurement**  
*By F. N. Eddy*
- 20 Introduction to Class D Tuned RF Amplification**  
*By Jukka Vermasvuori, OH2GF*
- 31 High-Performance Audio Speech Low-Pass and CW Band-Pass Filters in SVL Design**  
*By Werner Rahe, DC8NR*
- 40 Transmission Line Paradigm**  
*By Richard F. Thompson, W3ODJ*
- 45 Microsoft Excel for Antenna Modeling**  
*By Brian B. Turner, K2SJM*

## Columns

- 52 Antenna Options**  
*By L. B. Cebik, W4RNL*
- 58 Upcoming Conferences**
- 59 Letters**
- 62 Next Issue**

## Jul/Aug 2007 QEX Advertising Index

American Radio Relay League: 44, 62, 64  
Array Solutions: 39, Cov III  
Atomic Time: 44  
Communications Specialists, Inc: 19  
Down East Microwave Inc: 11  
Elkins Marine Training International: 57  
Kenwood Communications: Cov IV

National RF, Inc: 39  
Naval Explosive Ordinance Disposal  
Tech Div.: 63  
Nemal Electronics International, Inc: 39  
Teri Software: 39  
Tokyo Hy-Power Labs, Inc: Cov II  
Tucson Amateur Packet Radio: 30



The American Radio Relay League, Inc. is a noncommercial association of radio amateurs, organized for the promotion of interest in Amateur Radio communication and experimentation, for the establishment of networks to provide communications in the event of disasters or other emergencies, for the advancement of the radio art and of the public welfare, for the representation of the radio amateur in legislative matters, and for the maintenance of fraternalism and a high standard of conduct.

ARRL is an incorporated association without capital stock chartered under the laws of the state of Connecticut, and is an exempt organization under Section 501(c)(3) of the Internal Revenue Code of 1986. Its affairs are governed by a Board of Directors, whose voting members are elected every three years by the general membership. The officers are elected or appointed by the Directors. The League is noncommercial, and no one who could gain financially from the shaping of its affairs is eligible for membership on its Board.

"Of, by, and for the radio amateur," ARRL numbers within its ranks the vast majority of active amateurs in the nation and has a proud history of achievement as the standard-bearer in amateur affairs.

A *bona fide* interest in Amateur Radio is the only essential qualification of membership; an Amateur Radio license is not a prerequisite, although full voting membership is granted only to licensed amateurs in the US.

Membership inquiries and general correspondence should be addressed to the administrative headquarters:

ARRL, 225 Main Street, Newington, CT 06111 USA.

Telephone: 860-594-0200

FAX: 860-594-0259 (24-hour direct line)

#### Officers

**President:** JOEL HARRISON, W5ZN

528 Miller Rd, Judsonia, AR 72081

**Chief Executive Officer:** DAVID SUMNER, K1ZZ

#### The purpose of QEX is to:

- 1) provide a medium for the exchange of ideas and information among Amateur Radio experimenters,
- 2) document advanced technical work in the Amateur Radio field, and
- 3) support efforts to advance the state of the Amateur Radio art.

All correspondence concerning QEX should be addressed to the American Radio Relay League, 225 Main Street, Newington, CT 06111 USA. Envelopes containing manuscripts and letters for publication in QEX should be marked Editor, QEX.

Both theoretical and practical technical articles are welcomed. Manuscripts should be submitted in word-processor format, if possible. We can redraw any figures as long as their content is clear. Photos should be glossy, color or black-and-white prints of at least the size they are to appear in QEX or high-resolution digital images (300 dots per inch or higher at the printed size). Further information for authors can be found on the Web at [www.arri.org/qex/](http://www.arri.org/qex/) or by e-mail to [qex@arri.org](mailto:qex@arri.org).

Any opinions expressed in QEX are those of the authors, not necessarily those of the Editor or the League. While we strive to ensure all material is technically correct, authors are expected to defend their own assertions. Products mentioned are included for your information only; no endorsement is implied. Readers are cautioned to verify the availability of products before sending money to vendors.

## Rights and Responsibilities

Many view the rights guaranteed under the First Amendment to our Constitution in the USA to freedom of speech and freedom of the press as absolute. They're not and our Supreme Court has consistently ruled that to be so.

Most First Amendment cases involve a clash between an individual or group and a government agency or official. That situation arises from the wording of the Amendment itself: "Congress shall make no law abridging..." as it begins. It is a negative check on federal power over freedom of expression that the Court has broadened over the years to include state and local governments, as well.

You can no more falsely yell, "Fire!" in a crowded theater than you can utter words on a street corner that incite a riot. Defamatory statements made over the radio are libelous and are not protected, as allegedly demonstrated recently by Don Imus and others. Political parody and other satirical remarks, however, are protected and must be viewed in context, which is not always easy or pleasant.

To show the flexibility of the "...make no law..." clause, the famous "Pentagon Papers" case in 1971 comes to mind. During oral arguments, Solicitor General Erwin Griswold, arguing for the United States, looked up at Justice Hugo Black — who was known as a First Amendment absolutist — and said, "You say that 'no law' means 'no law,' and that should be obvious." Black dryly replied, "I rather thought that." Griswold continued, "And I can only say, Mr. Justice, that to me it is equally obvious that 'no law' does not mean 'no law.' And I would seek to persuade the Court that that is true."

In that case, Griswold did not persuade the Court to allow the government to block further publication of the secret history of the Vietnam War. But in countless other cases, the Supreme Court has recognized — and often crafted — exceptions to the 'no law' mandate of the First Amendment. Government may "accommodate" the interests of religious groups; it may penalize or punish the "free exercise" of religious practices such as polygamy or use of peyote; it may punish speech that incites "imminent lawless action" (such as inciting that riot) or that constitutes "fighting words;" it may criminalize obscenity and provide liquidated damages for libel; it may censor certain

publications; and it may impose "time, place and manner" limitations on public assembly and demonstrations.

Amateur Radio has a long and beautiful history of promoting national and international goodwill by giving us the opportunity to make new friends. Yet the rules, by international agreement, say: "Transmissions to a different country, where permitted, shall be limited to communications incidental to the purposes of the amateur service and to remarks of a personal character." We're also limited by the above-listed precedents that establish the boundaries of our free speech rights. Nonetheless, we must rededicate ourselves to that one founding purpose that is so important. Because we're free to move around the bands, we must conduct ourselves as ladies and gentlemen and sometimes yield, even when it's inconvenient; sometimes apologize; and sometimes give thanks. After all, we do have mutual interests at heart.

Every ham should learn and follow *The Amateur's Code*, originally written by Paul M. Segal, W9EEA, in 1928. It's reproduced here from the 2007 edition of *The ARRL Handbook*:

The Radio Amateur is:

CONSIDERATE...never knowingly operates in such a way as to lessen the pleasure of others.

LOYAL...offers loyalty, encouragement and support to other amateurs, local clubs and the American Radio Relay League, through which Amateur Radio in the United States is represented nationally and internationally.

PROGRESSIVE...with knowledge abreast of science, a well-built and efficient station and operation above reproach.

FRIENDLY...slow and patient operating when requested; friendly advice and counsel to the beginner; kindly assistance, cooperation and consideration for the interests of others. These are the hallmarks of the amateur spirit.

BALANCED...radio is an avocation, never interfering with duties owed to family, job, school or community.

PATRIOTIC...station and skill always ready for service to country and community.

The moral of the story? It's that what we communicate is perhaps as important or more important than how we communicate it.

**QEX**



# The ARRL 500-kHz Experiment: WD2XSH

*Twenty-one radio amateurs begin exploration of a historic part of the radio spectrum.*

Frederick H. "Fritz" Raab, W1FR

## Introduction

The first International Wireless Telegraph Convention, held in Berlin on November 3, 1906, designated 500 kHz as the maritime international distress frequency. This same convention also designated "SOS" to replace "CQD" as the distress signal.

For nearly 100 years, the "600-meter band" (495 to 510 kHz) served as the primary calling and distress frequency for maritime communication. In the 1980s, a transition began to the Global Maritime Distress Signaling System (GMDSS), which uses UHF communication via satellite. In the 1990s, most countries ceased using and monitoring CW communications. Today, the 600-meter band is idle with the exception of occasional transmissions by historical maritime stations.

The frequencies below 1.8 MHz have been little explored by radio amateurs since our banishment to "200 meters and down" in 1912. The 600-meter band is located near the geometric mean of the 2200-m (137 kHz) and 160-m (1.8 MHz) amateur bands. See Figure 1. This band is of interest to radio

amateurs for quite a number of reasons:

- Ultra-reliable emergency communications via ground wave,
- Unique propagation and noise environment, and
- Experimental work with antennas, modulation, and signal processing.

The WD2XSH experimental license allows a group of 21 amateurs to begin exploration of this unique part of the spectrum, possibly paving the way for a future amateur band. The two key objectives of the license are:

- Demonstration of noninterference with other services, and
- Experimentation with regional ground-wave communication.

Naturally, the participants also want to determine what kind of DX can be achieved using both normal CW and QRSS, and this will add further to our understanding of the capabilities of this band. [QRSS is very slow speed CW, designed to be copied using a computer program. — Ed.]

## Ground-Wave Communication

Amateur Radio has proven its value to society by providing communication in the aftermath of Hurricane Katrina and other

natural disasters. As Katrina demonstrated, natural disasters can destroy or render inoperative most of, or the entire normal communication infrastructure (land-line telephone, cell phone, land mobile). Amateur radio is a "distributed system" that does not depend upon fixed infrastructure, hence it is well suited to providing post-disaster communications. Luckily, following Katrina the Sun was not having an "event," the ionosphere was behaving, and HF communications worked well.

Ground-wave (also called "surface-wave") propagation at low and medium frequencies can provide reliable communication over significant ranges. Ground-wave signals propagate along the surface of the Earth. Such communication is omnidirectional and continuous, and is therefore well-suited for "party-line" communication among all terminals in a network. Since the ground-wave signal is not dependent upon the ionosphere, communications based upon ground waves are not interruptable by solar events (sunspots, solar storms, coronal mass ejection) or a high-altitude nuclear detonation that disturb the ionosphere. A recent burst of solar activity (November 2003) produced significant aurora and disrupted HF ionospheric communication for several days.

240 Staniford Rd  
Burlington, VT 05408  
f.raab@ieee.org

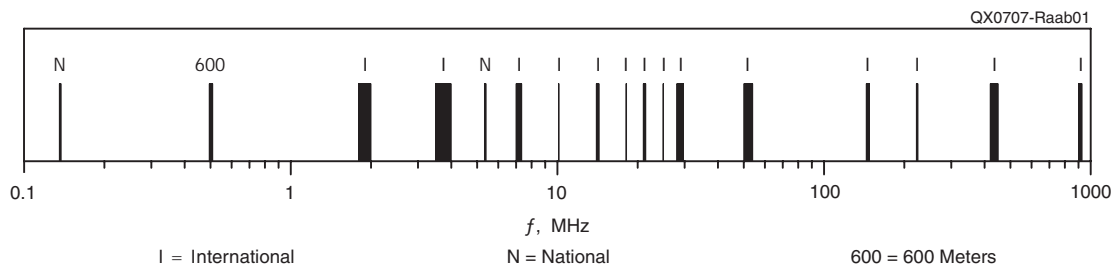


Figure 1 — Amateur bands.

The optimum frequency for ground-wave communication depends upon antenna efficiency, ground-wave propagation loss, and atmospheric noise. Vertical antennas with heights of 40 to 50 ft are readily constructed from aluminum tubing. For communication with such an antenna over average ground over distances of 100 to 300 km (60 to 200 miles), the best signal-to-noise ratio (SNR) per watt of transmitter output (see Appendix A) occurs in the range of 400 to 600 kHz, as shown in Figure 2. The 600-m amateur band is therefore ideal for amateur ground-wave emergency communications.

An Amateur Ground-Wave Emergency Net operating in the 600-m band would provide uninterrupted emergency/disaster/homeland-security communication across a midwestern-sized state (such as Iowa). Fixed nodes will be established in major cities (for example, Waterloo, Des Moines, Sioux City) and will interface with local VHF/UHF amateur networks. Transportable units could be deployed to the site of an emergency, such as a tornado. Such units could be transported by pick-up truck or van, and would consist of 100 to 500 W transmitters, laptop computers, and 40 to 50 ft vertical antennas assembled from aluminum tubing.

No current amateur frequency allocations provide this kind of coverage. The 160, 80, 60, and 40 meter bands provide regional coverage through near-vertical-incidence sky waves (NVIS). Different frequencies are required to communicate over different distances, however, and communication is subject to ionospheric disturbances. Troposcatter at VHF and UHF can also provide coverage over significant distances. Directional antennas are required, however; hence, coverage is point-to-point rather than regional. The proposed 137-kHz band is not suitable, as it has a very limited frequency allocation and the efficiency of realistic amateur antennas is very low for 137 kHz.

### Experiments

A band at 600 meters would offer radio amateurs unique opportunities for experimentation in several areas:

- Electrically short antennas,
- Propagation and noise,
- Modulation and signal processing.

At first thought, it may seem that all of those issues have been fully explored and documented. Indeed, many aspects are explained in textbooks and engineering literature. There has been little to no application of modern technology to this frequency range, however, and few textbooks treat the real issues that confront radio amateurs operating from limited real estate with limited power and resources. The brief discussion below highlights some areas for exploration by amateurs.

### Electrically Short Antennas

Virtually all amateurs will be using electrically short — and often very short — antennas. The issue for a radio amateur is not simply how to maximize radiation resistance or gain: It is how to maximize the radiated signal from an antenna constructed in a limited space, built on a limited budget, and unavoidably placed near trees and other objects. Having the capability to set up nodes for emergency communications adds portability and ease of deployment to the list of design issues.

Short, top-loaded monopoles are generally used with nondirectional beacons (NDBs) that operate at low and medium frequencies. These antennas work well in clear areas at the NDB sites; but as some low-frequency experimenters (“lowfers”) have recently discovered, nearby trees appear to cause significant losses, especially when wet. The most likely explanation is that the electric-field intensity increases as the frequency decreases and the antenna becomes shorter electrically. The electric field applied to the trees causes the losses, which are



Photo A — Here is the loading coil and ground-radial connection in use at WD2XSH/20, Rudy Severns, N6LF.

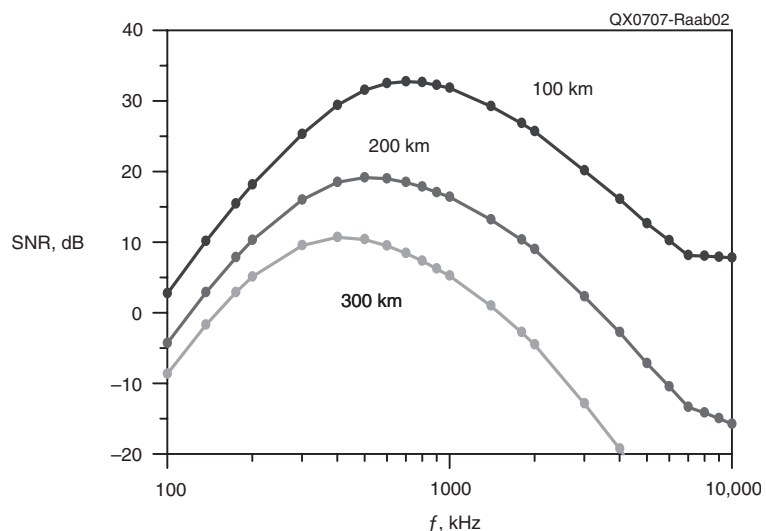


Figure 2 — Ground-wave SNR as a function of frequency for typical amateur use.



negligible at HF but significant at MF and LF. This problem has not been well explored.

In contrast, loop antennas create intense magnetic near fields. This allows them to be placed in forested areas without significant loss from the trees. Magnetic fields flowing in the conducting ground cause losses much as do the fields surrounding a monopole antenna. Little exploration has been done on these losses or ground-radial systems for minimizing the loss at MF for short antennas in the amateur literature.

The limited real estate available to the average amateur precludes the installation of ideal grounding systems. In poor soil, the common ground to the power grid and water system are likely to be more effective than ground rods and radial systems of limited size. This has implications for both modeling antennas and for determining what grounding system to use. Grounding systems are yet another area for experimentation.

#### Propagation and Noise

Virtually all long-range HF operation by amateurs relies on sky-wave (ionospheric) propagation. At 500 kHz, however, both sky-wave and ground-wave propagation can be used. The effects of the D layer are much more pronounced at 500 kHz than at higher frequencies, resulting in almost a complete absence of useable sky wave propagation during the daylight. Atmospheric noise is more impulsive, and the level of man-made noise is higher.

#### Modulation and Signal Processing

The limited bandwidth available at 500 kHz makes narrowband digital modes of great interest. BPSK and QPSK provide the lowest bit-error rates for a given amount of signal power. PSK-31 is therefore a natural candidate for this application.

Improvements may be possible. PSK-31 uses sine-wave shaping of its data pulses to provide synchronization as well as to keep the signal in a very narrow bandwidth. This amplitude modulation necessitates a linear RF-power amplifier and results in an average transmitted power that is only half of the peak power capability of the amplifier.

Minimum-shift keying (MSK) is a form of QPSK that (like PSK-31) employs sinusoidally shaped data pulses to constrain bandwidth. Delaying the modulation on the quadrature carrier by half a bit results in a constant-amplitude composite signal. The average power is the same as the peak power, and the signal can be amplified by a nonlinear power amplifier. Establishing synchronization is, however, more difficult. The Spectran software contains an MSK-31 mode that otherwise follows PSK-31 protocols. MSK has been little used in amateur applications, so evaluation of its capabilities is certainly an area for investigation.

Development of a synchronization scheme suited to short amateur-type transmissions will probably be needed. This might be embodied in software tailored to this frequency range, much as the WSJT software is tailored to me-

teor-burst and EME communications.

At 500 kHz, signals may travel significant distances by both ground-wave and sky-wave propagation. In some cases, the resultant "multipath" signal reception may make it



Photo B — This is the 500-kHz antenna tuner used at the author's station, WD2XSH/14.

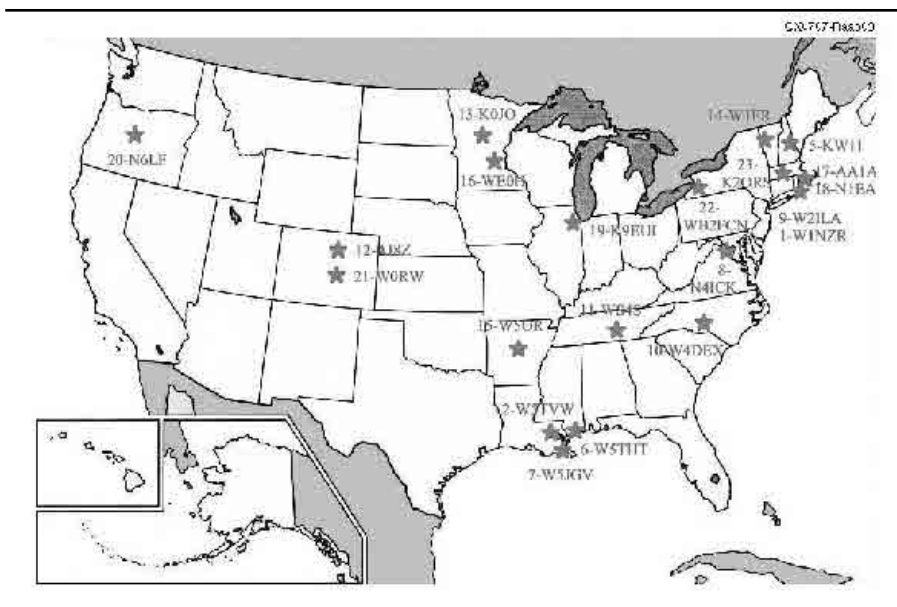


Figure 3 — Locations of WD2XSH stations.

Table 1  
Band Plan for Experimental Transmissions

Frequency, kHz	Use
505.0 - 505.2	DX window
505.250 - 505.255	QRSS — 0.25-Hz spacing
505.300 - 506.300	CW beacons — 50-Hz spacing
506.5	Rotating beacon, 1-minute time slots
507.5	Calling frequency

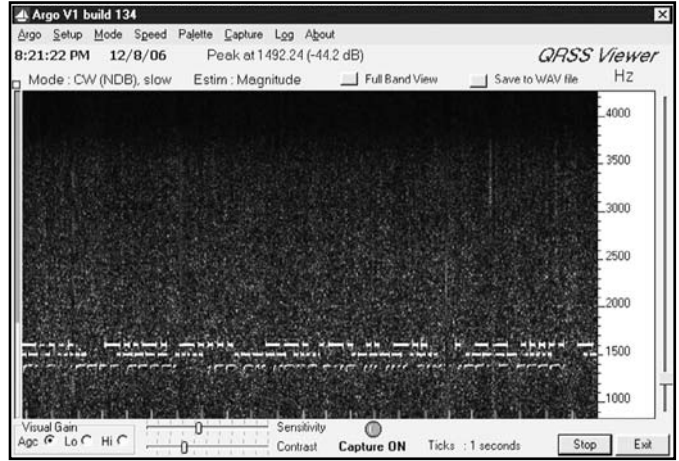
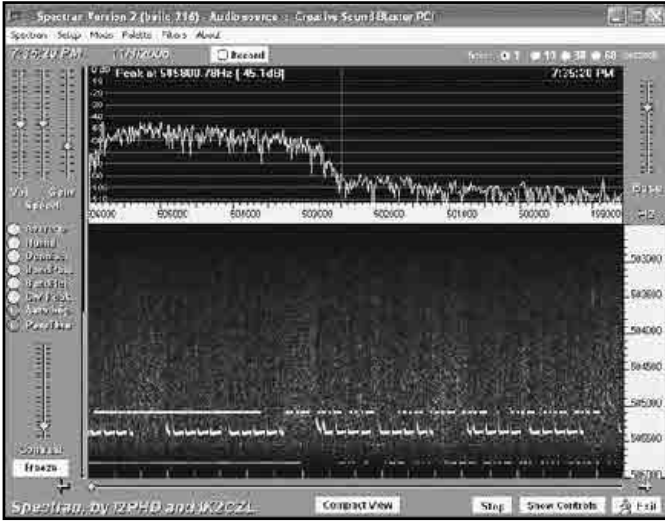


Figure 4 — Screen captures of WD2XSH signals.



Photo C — The 42-ft vertical used by Fritz Raab, W1FR, at WD2XSH/14 is almost hidden among the trees.

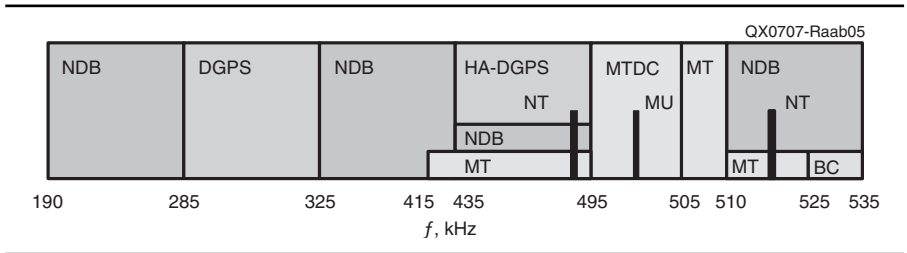


Figure 5 — Simplified MF allocations.

through nonlinear signal processing such as clipping and blanking. The presence of higher levels of man-made noise makes techniques such as noise cancellation of great interest.

**WD2XSH License**

WD2XSH is an experimental license issued to the ARRL under Part 5 of the FCC rules. The locations of the 21 stations currently authorized to operate are shown in Figure 3, with details in Appendix B. (Two other stations originally included in the FCC grant dropped out.) The basic parameters of the license are:

- Period: 09/13/2006 to 09/01/2008
- Radiated power: 20 W ERP
- Frequencies: 505 to 510 kHz
- Modulation: CW (including QRSS)

As the experiment coordinator, I have — for the time being — restricted the mid-west stations to 505 to 508 kHz to ensure there is no interference to non-directional beacon (NDB) “OF” in Nebraska.

Planned activities include:

- CW QSOs,
- CW beacon transmissions, and
- QRSS beacon transmissions.

Tests will be conducted during both day-light and nighttime conditions to ascertain capabilities of both ground-wave and sky-

wave communication. The initial band plan for experimentation (which may be changed) is given in Table 1.

CW is the only transmission mode currently authorized for WD2XSH. CW QSOs will demonstrate the capabilities of amateurs to communicate on this band. PSK-31 and similar modes should provide an even greater communication range for the same signal and noise conditions.

CW beacons enable widespread monitoring of the transmissions. Transmissions typically consist of a repeated pattern like: “VVV VVV de WD2XSH/14 14 14.” The subband from 505.3 to 506.3 kHz is used for CW beacons. Signals are separated by 50 Hz and stations in proximity are separated by about 200 Hz. A planned “rotating beacon” transmission at 506.5 kHz will place all stations on the same frequency but in different time slots. This will allow receivers to be left on one frequency while the listener monitors or records.

QRSS allows detection of signals with SNRs well below those needed for detecting real-time CW. This makes it a very useful tool for evaluating propagation. The QRSS frequencies are separated by 0.25 Hz so that all QRSS transmissions fit into a 5-Hz bandwidth from 505.050 to 505.055 kHz. This allows a single Argo window to capture all of them at once. In QRSS mode, stations transmit



“XSHm” (with occasional full ID by CW).

The center frequency of 507.5 kHz is the designated calling frequency. The rest of the band is open for use at the discretion of the various station operators.

*Participants*

The operators have excellent qualifications for participation in this experiment. Most have Advanced or Extra Class amateur licenses. Most are experienced electronics professionals, and many have maritime-radio backgrounds. Many have operated Part-5 or Part-15 stations at 137 kHz or 160 to 190 kHz.

*Equipment*

In the finest tradition of amateur radio, WD2XSH stations are using a wide variety of approaches to produce their signals. Transmitters include state-of-the-art high-efficiency switching-mode power amplifiers, converted amateur gear, test equipment, marine surplus transmitters, and retired NDB transmitters. Most commercial ham receivers have poor sensitivity at 500 kHz and require preamps or converters. Antennas include simple vertical antennas, top-loaded verticals, shunt-fed towers, and loops. Each station has its own unique equipment and approach, and in many cases they are combinations of test equipment, modern solid-state circuits, and modified vintage vacuum-tube equipment.

**Early Results**

Sixteen stations have been able to get on the air during the first six months of the license. Several stations are usually on the air on any given evening. Over 4600 transmitting hours were logged in the first six months.

Most communications to date have been by nighttime sky-wave propagation. Transmissions have included both CW and QRSS. Seventy-five CW QSOs have been reported at distances ranging from 81 to 884 miles (New Hampshire to Tennessee). Our Web site had over 3100 reception reports. Distances of 500 miles are readily achieved, and 1000 mile distances are not uncommon. Three stations have been received in Europe and one has been received in Hawaii. Day-time ground-wave communication has been demonstrated at distances of 80 to 120 miles in New England, Mississippi/Louisiana and Colorado.

The strongest signals are, of course, produced by the couple of stations with 100-ft antennas. Even those with modest 30 to 40 ft verticals, however, have been heard over significant distances. Screen captures of WD2XSH signals by Argo and Spectran software are shown in Figure 4. The first capture (A) shows /14 (VT), /19 (IL), /17 (MA), and /11 (TN) being received in Conneaut, Ohio on 11/03/06 by Fred Temple, KN8AZN. The second (B) shows /6 (MS), /15 (AR),

and /19 (IL) in Seneca, Missouri received on 12/08/06 by David Bixler, W0CH.

Fast fading (possibly due to multipath) has been observed. It spreads the bandwidth of the signal beyond the 0.25-Hz spacing in the current QRSS assignments. A slower fading has been observed that makes it difficult to copy complete call signs in the QRSS10 and QRSS30 modes.

The Web site at [www.500kc.com](http://www.500kc.com) provides current information and status, as well as a way to file reception reports. The Web site includes links to several “Grabbers” that allow you to see real-time Argo displays of the band at different locations.

**Future**

During the first year, the principal objectives were to get on the air and to prove that we do not create harmful interference. After successfully completing the first season, we

will consider requesting modifications in four areas:

- Addition of a small number of participants to expand our coverage, particularly in the southwest, KH6, KL7 and KP4;
- The use of modern narrow-band digital modes such as PSK-31;
- Communication with amateur experimenters in other countries; and
- Emergency-communication tests with maritime museum stations.

**Other MF Experimental Stations**

The Six-Hundred-Meter Research Group (600MRG) was organized by Ken Gordon, W7EKB, in 2001. It initially included 35 members at various locations across the USA. In December 2001, the 600MRG was granted experimental license WC2XSR and authorized to use 440, 470, 480, 495, and

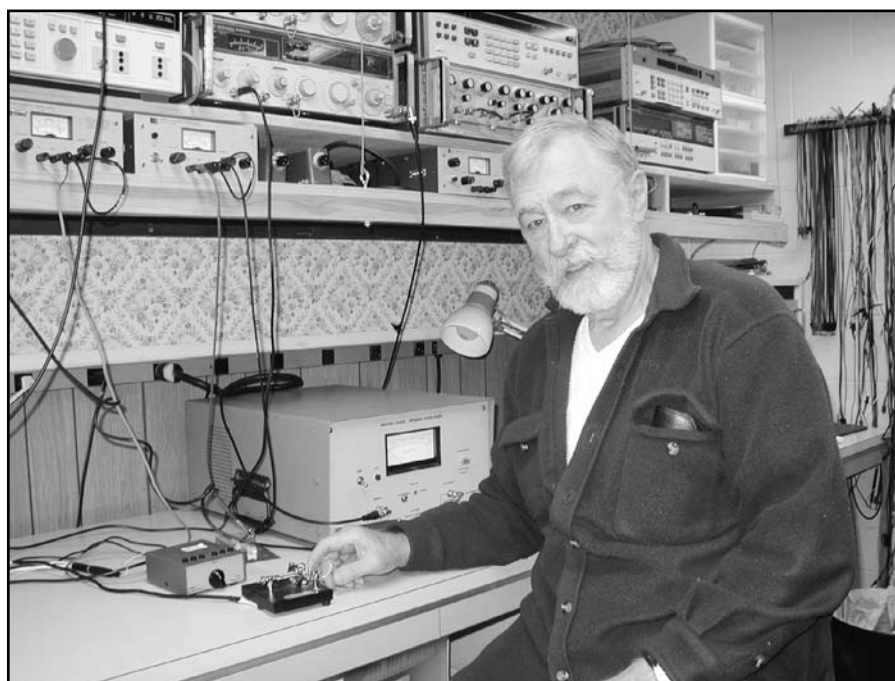


Photo D — Rudy Severns, N6LF, operating his 500-kHz station, WD2XSH/20.

**Table 2**  
**Simplified MF Allocations in Region 2**

Band Ref*	Frequency, kHz	Use	User
A	190 - 285	Aeronautical NDBs	FAA
B	285 - 325	Marine DGPS	USCG
C	325 - 435	Aeronautical NDBs	FAA
D	435 - 495	High-accuracy DGPS	USCG
E	495 - 505	Maritime calling and distress	Museum
F	505 - 510	Maritime Mobile	None
G	510 - 535	Aeronautical NDBs	FAA
H	490, 518	NAVTEX	USCG

\*Used in this note only, not universal.

166.5 kHz. Several members began experimental transmissions almost immediately. Within a week or two, however, the US Coast Guard complained to the FCC and the authorization for 440 to 495 kHz was withdrawn.

US experimental station WA2XRM is located in Colorado Springs, Colorado and operated by Paul Sigornelli, WØRW. It operates on 480 kHz with an ERP of up to 100 W. It has been operating since 2004 and has been renewed through 2009.

Brent "Gus" Gustafson, SM6BHZ, received permission from the Swedish Posts and Telecommunications to operate between 505.0 and 505.2 kHz with an EMRP (effective monopole radiated power) of 20 W. This special permission runs from Dec. 1, 2006 to Nov. 30, 2007.

Two German experimental stations are authorized to transmit with an ERP of 9 W. Walter Staubach, DJ2LF, has been operating D12AG from Dormitz near Nuernberg since late 2005. Geri Holger, DK8KW, was issued experimental license D12BO in 2006. He is located in Peine near Hannover. These stations originally were transmitting on 440 kHz, but were authorized in December 2006 to switch to 505.0 to 505.2 kHz to match the authorization for SM6BHZ.

Effective March 1, 2007, UK amateurs may apply for a special permit for transmission from 501 to 504 kHz with an ERP of 0.1 W. Interest in experimental or special access to frequencies near 500 kHz has also been expressed by the Irish Radio Transmitters Society, the Wireless Institute of Australia, as well as amateur organizations in New Zealand, Canada, and Belgium.

At the San Marino IARU Region 1 Conference in December 2002, the RSGB presented recommendation REC/02/SM/C4.11 to the HF committee. As a result, a working group was formed to investigate "the possibility of a frequency allocation of approximately 10 kHz between 470 to 490 kHz to investigate propagation and the use of new communication technologies." The IARU Region I continues to coordinate international efforts in this area.

### Current Frequency Allocations

The current uses of the MF spectrum include nondirectional beacons (NDBs), Differential Global Positioning System (DGPS), NAVTEX and historical maritime-telegraphy operations.<sup>1</sup> See Figure 5 and Table 2.

#### Aeronautical Nondirectional Beacons

Nondirectional Beacons (NDBs) are the principal occupants in 190 to 285 kHz, 325 to 435 kHz and 510 to 535 kHz (Bands A, C, and G). See Appendix C. A few NDBs can

also be found in Band D (435 to 495 kHz). A few NDBs in Eastern Europe and Asia can even be found in the distress/calling band (495 to 505 kHz).

NDBs act as non-precision approach aids and compass-type locators and are used at ranges up to 50 to 100 miles. They typically transmit an ID via modulated CW (MCW). The FAA currently operates about 225 NDBs.<sup>2</sup> Approximately 50 are operated by the Department of Defense and another 1300 are privately operated. Some NDBs are stand-alone types, while others are associated with an Instrument Landing System (ILS).

The Federal Radionavigation Plan (FRP, Section 3.1.9) calls for phasing out the federally operated stand-alone NDBs. See Note 2. The phase-out is in progress and will take about ten years. Those NDBs associated with an ILS will continue to be operated until the ILS is retired. The FAA will have no further use for these frequencies once the NDBs have been decommissioned. Private operators may continue operation of their NDBs as long as they wish, however, and it appears that a number of NDBs have been transitioned from FAA to local operation.

#### Differential Global Positioning System (DGPS)

The marine nondirectional beacons in Band B (285 to 325 kHz) have been phased out and replaced by marine DGPS beacons. In the US, these are also known as National DGPS or NDGPS. They use 200 bps MSK to relay information from a GPS monitoring

station to allow significant improvement in the accuracy of a GPS position fix of a nearby receiver. The format has been standardized by RTCM, and DGPS beacons are also found in this band in Regions 1 and 3.

The US Coast Guard (USCG), in cooperation with six other federal agencies such as highways (FHWA) and railroads (FRA), is undertaking a significant expansion of the differential GPS (DGPS) system.<sup>3</sup> This includes a faster data rate (500 or 1000 bps, versus the 200 bps) for the DGPS beacons at 300 kHz. The plan is to have coverage from at least two beacons everywhere in the continental US. The higher data rate allows the use of more monitors and the use of carrier phase. This gives them centimeter accuracy and accurate velocity for "real-time kinematics" (RTK). There is a wide variety of applications ranging from tracking vehicles to guiding crop dusters. Many of the applications are for terrestrial navigation such as tracking cars and trains and knowing which lane or track they are on. The MF transmissions are well suited for this because they can be received at all altitudes beyond line of sight. Two such transmitters (Pennsylvania and Virginia, 454 and 456 kHz) have recently been put on the air.

The USCG plans to use the entire Band D from 435 to 495 kHz for these new high-accuracy DGPS beacons. This frequency allocation has been cleared through the NTIA.

#### Maritime Telegraphy Bands

The frequencies from 435 to 525 kHz were once widely used for maritime telegraph-



Photo E — Tom Mackie, W2ILA, with his 500-kHz station, WD2XSH/9.

<sup>1</sup>Notes appear on page 11.



raphy. The band from 495 to 505 kHz was reserved for calling and distress communication. In Region 2, 505 to 510 kHz served as a guard band for the distress/calling band. These frequencies were monitored by both ships and shore stations.

Maritime communication is now handled by HF, VHF, and satellite communication. The Global Maritime Distress and Safety System (GMDSS) has supplanted MF marine telegraphy for both routine and distress communication.<sup>4</sup> Marine telegraphy is no longer used in the Western Hemisphere except by a few “museum” stations. The USCG no longer monitors 500 kHz, nor do the corresponding agencies of most nations.

China and Indonesia remain on the Admiralty List as users, but there are no reports of activity. A number of shore and ship stations retain their licenses for MF. None use these frequencies for regular commercial, military, or distress traffic, however.

The only known users of the distress/calling band (495 to 505 kHz) in Region 2 are the “museum” stations. The Maritime Radio Historical Society (MRHS) operates KPH and KSM from Bolinas, California.<sup>5</sup> The MRHS makes weekly transmissions of weather and other information, calling first on 500 kHz and then transmitting messages on a working frequency. The MRHS has also helped several other stations to resurrect their 500-kHz transmitters. Their annual “Night of Nights” (July 12) commemorates the last commercial telegraphy transmission on 500 kHz in 1999, and several other historical maritime stations sometimes participate.

Band E (495 to 505 kHz) is allocated for maritime distress and calling. As such, it is subject to special protections embodied in Appendix 13 of the ITU Radio Regulations. Subsection 13 states “... any emission capable of causing harmful interference ... is prohibited.” Subsection 15 further states “Apart from the transmissions authorized on 500 kHz, and taking account of No. 52.28, all transmissions on the frequencies included between 495 kHz and 505 kHz are forbidden. Until 1 February 1999, this applied to frequencies between 490 kHz and 510 kHz.

The prohibitions against other transmissions from 495 to 505 kHz remain in force in spite of the absence of users. These regulations have not prevented several NDBs in Eastern Europe and Asia from operating in this band.

Band F (505 to 510 kHz) is allocated for maritime telegraphy in Region 2. As noted above, it is no longer subject to the same restrictions as 495 to 505 kHz. Two US NDBs (OF in Norfolk Virginia, NE and FA in Fairbanks, Alaska) operate on 510 kHz and their sidebands extend into Band F. (Those assignments are inconsistent with the previous prohibition against signals

in this band). Otherwise, there are no known users in Region 2. In Regions 1 and 3, this band is allocated for NDBs.

NAVTEX provides automated distribution of weather and navigation-system information to mariners.<sup>6</sup> Worldwide, transmissions are authorized on 490 and 518 kHz, but only 518 kHz is used in the United States. A dozen transmitters provide coverage of most of the coast to a distance of 400 nautical miles (740 km). NAVTEX uses AMTOR protocol (100-baud FSK 170-Hz shift). NAVTEX broadcasting was implemented between 1983 and 1993 and appears to be mature and stable. Since NAVTEX is part of the GMDSS, it is likely to remain in operation for the foreseeable future.

#### Power-Line Communication

LF and MF carriers are used on long-distance transmission lines for monitoring and control. These power-line communication (PLC) systems are unlicensed and operate under Part 15 of the FCC rules. Their frequencies are no higher than 490 kHz because of prohibitions on incidental radiation in the maritime distress/calling band. In spite of their unlicensed status, concerns about interference to the power grid have caused the FCC to deny access to 137 kHz to US radio amateurs.

#### Mystery Signal

From time to time, we have heard an NDB-type signal on 505 kHz indentifying itself as NEED. This signal appears to originate from somewhere near Norfolk, Virginia. Anyone with knowledge of this signal should contact the author.

#### A New Amateur Band?

This section discusses the possibilities for a new “600-meter” amateur band. It does not necessarily represent ARRL policy.

Obtaining new amateur bands takes sev-

eral years, but it can be done. The 30, 24, 17 and 60 meter bands are examples. Generally, new bands are first authorized at the national level and eventually become recognized by the ITU.

#### Frequencies

The above review of the current uses of the MF band make it clear that the former maritime-telegraphy frequencies from 495 to 510 kHz offer the possibility of a new 600-meter amateur band.

The portion of this band from 505 to 510 kHz (currently being used by WD2XSH) is not used in Region 2 except for two NDBs on the top edge. See Appendix C. This makes it a logical starting point for an amateur allocation. Many NDBs operate on the same or adjacent frequencies, so exclusion zones with radii of 200 to 300 miles will provide sufficient protection of the NDBs.

In Regions 1 and 3, the band from 505 to 510 kHz is allocated for NDBs. Use of this band by NDBs is generally light and limited to Eastern Europe. See Appendix D. It should be feasible for amateurs to use this band, at least in most countries, by establishing exclusion zones around these NDBs.

Overall, the best option for an international amateur allocation is in the distress/calling band at 495 to 505 kHz. This band is essentially unused except by the museum stations and will significantly expand the spectrum available to amateurs. Modification of the ITU regulations that protect this band as a distress frequency may be required.

#### Modulation Modes

The limited spectrum available precludes the use of AM, SSB, AMTOR, and other wideband modes except perhaps for special events. Modulation modes suitable for a 600-meter amateur band are CW (including QRSS) and narrowband digital modes such as PSK-31, FSK-31, and MSK-31.

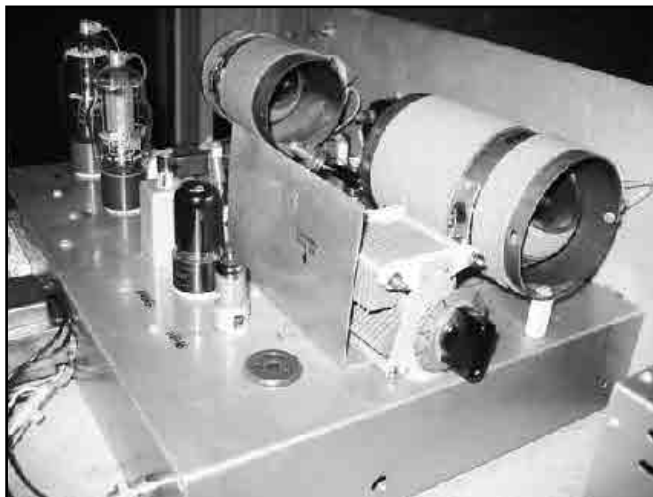


Photo F — Back view of the SAC H-25 NDB transmitter that Don Reaves, W5OR, uses at WD2XSH/15.

## Museum Stations

The museum stations preserve an important part of our radio history. These stations could also help with emergency communications. A provision should therefore be made for their continued access to 495 to 505 kHz on a shared basis. To facilitate joint use, a band plan should reserve 499 to 501 kHz for museum-radio operations, amateur emergency communications, and amateur special events.

## Uses

The need to make or to adapt equipment and the larger antennas required make it unlikely that a 600-meter amateur band will become anything close to as popular as the HF bands. The author anticipates that it will be occupied by a combination of experimenters and amateurs with historical interests and ties to maritime radio. The 600-meter amateur band will also be an ideal place for special events of a historical nature. One example is a Fessenden commemoration on Christmas Eve during which AM would be permitted. Another example is a maritime commemoration (on November 3 to mark the anniversary of the Berlin Convention that created SOS and the 500-kHz distress/calling band). During this event, MCW transmission and cross-service contacts with museum stations would be permitted.

## Conclusion

It seems fitting that a hundred years after 500 kHz was designated the international distress frequency, we are working to find new uses for the band for emergency communication as well as experimentation. We are looking forward to applying modern technology to this historic part of the spectrum, and to working with the maritime historical groups to see that it is preserved.

## Appendix A

### SNR Predictions

The SNR of a ground-wave signal depends upon a combination of

- Antenna gain,
- Surface-wave attenuation, and
- Atmospheric-noise level.

Figure 5 shows these effects as a function of frequency for communication over a range of 200 km.

The predictions used in this paper (Figure 2 and Figure A1) are based upon the following:

- 15 m (50 ft) monopole with sixteen 30 m radials,
- Ground with  $\sigma = 0.01$  S/m and  $\epsilon_r = 10$ ,
- 1 W delivered to the antenna,

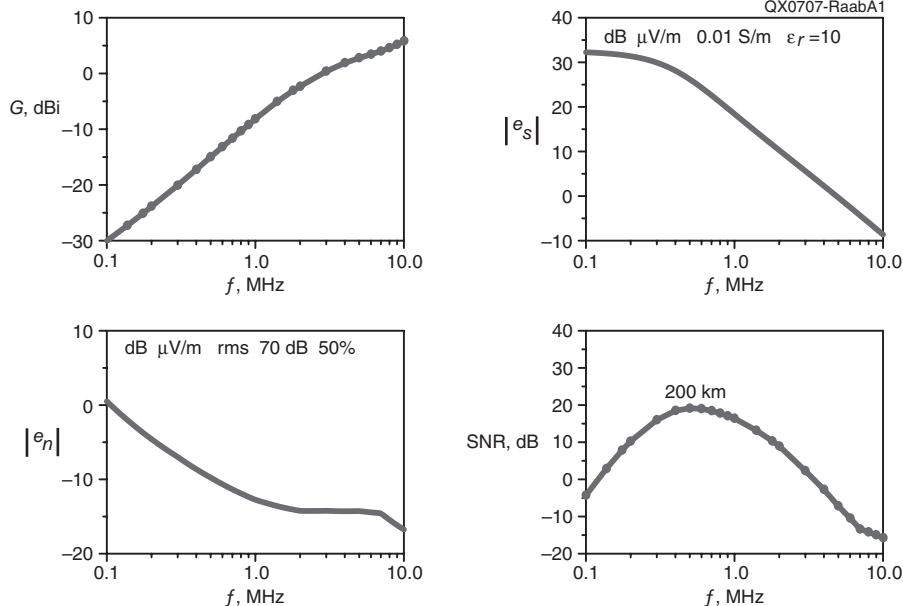


Figure A1 — Factors contributing to the SNR of a ground-wave signal.

## Appendix B

### WD2XSH Stations

Station	Ham Call	Name	Location
WD2XSH/1	W1NZR	Brown Beezer	Jamestown, RI
WD2XSH/2	W5TVW	Sandy Blaize	Hammond, LA
WD2XSH/5	KW1I	Dale Gagnon	Bow, NH
WD2XSH/6	W5THT	Pat Hamel	Long Beach, MS
WD2XSH/7	W5JGV	Ralph Hartwell	Jefferson, LA
WD2XSH/8	N4ICK	André Kesteloot	McLean VA 22101
WD2XSH/9	W2ILA	Tom Mackie	Jamestown, RI
WD2XSH/10	W4DEX	Joe McIntyre	Stanfield NC
WD2XSH/11	WS4S	Conard Murray	Cookeville, TN
WD2XSH/12	A18Z	Mike Mussler	Nederland, CO
WD2XSH/13	K0JO	John Oehlenschlager	Verndale, MN
WD2XSH/14	W1FR	Fritz Raab	Colchester, VT
WD2XSH/15	W5OR	Don Reaves	Roland, AR
WD2XSH/16	WE0H	Mike Reid	St. Francis, MN
WD2XSH/17	AA1A	Dave Riley	Marshfield, MA
WD2XSH/18	N1EA	David Ring	Green Harbor, MA
WD2XSH/19	K9EUI	Bob Roehrig	Batavia, IL
WD2XSH/20	N6LF	Rudy Severns	Cottage Grove, OR
WD2XSH/21	W0RW	Paul Signorelli	Colorado Springs, CO
WD2XSH/22	WB2FCN	James Walker	Buffalo, NY
WD2XSH/23	K2ORS	Warren Ziegler	Wayland, MA

- 1 Hz bandwidth,
- Median atmospheric-noise factor for fall and spring (70 dB), and
- Median atmospheric-noise level (50%).

Antenna gain is predicted by simulation with the Numerical Electromagnetics Code.<sup>A1</sup> The gain increases with the square of frequency until the electrical length becomes a significant part of a wavelength. This holds

for any electrically short antenna. The predicted antenna gain at 500 kHz is -15 dBi.

The amplitude of the surface wave is then predicted by a combination of standard Sommerfeld and spherical-Earth theory.<sup>A2</sup> The noise levels are based upon standard tables.<sup>A3</sup> As shown, the combination of antenna gain, surface-wave attenuation, and noise level favors frequencies near 500 kHz for distances from 100 to 300 km.

## Appendix C

### North American NDBS From 510 to 530 kHz

From [www.airnav.com](http://www.airnav.com), [www.worldaerodata.com](http://www.worldaerodata.com), and [www.classaxe.com](http://www.classaxe.com).

f, kHz	ID	LOCATION	OPERATOR	f, kHz	ID	LOCATION	OPERATOR
510	OF	Norfolk, NE	FAA	521	TO	Topeka, KA	FAA
510	FA	Fairbanks, AK	FAA	521	FEU	Frankfort, KY	Local
512	HMY	Lexington, OK	?	521	INE	Missoula, MT	FAA
513	PP	Omaha, NE	?	521	DWH	Houston, TX	Local
515	RRQ	Rock Rapids, IA	Local, possibly off air	521	GF	Cleveland, OH	
515	ONH	Jefferson City, MO	FAA	521	GM	Greenville, SC	
515	SAK	Kalispell, MT	FAA	523	JJH	Johnstown, NY	Local
515	OS	Columbus, OH	FAA	524	MNL	Mineral Creek AK	FAA
515	PN	Ponca City, OK	FAA	524	UOC	Iowa City, IA	Local
515	PKV	Port Lavaca, TX	Local	524	AJG	Mt. Carmel IL	Local
515	CL	Port Angeles, WA	FAA	524	HEH	Newark, OH	Local
516	YWA	Petawawa, ONT	RCAF	524	HRD	Kountze Silsbee, TX	Local
517	FN	Clinton, IA		525	ICW	Nenana AK	FAA
517	GKB	Kansas City, MO		526	RWE	San Miguel, CA	
518	GCT	Guthrie Center, IA	Local	526	OJ	Olathe, KS	
519	IQS	Sallisaw, OK	Local	526	ZLS	Stella Maris, Bahamas	USCG
520	F9	Miramichi, NB		529	SQM	Sumner Strait, AK	FAA
520	IQS	Sallisaw, OK		529	FDV	Ft. Davis, AK	FAA
521	ORC	Orange City, IA	Local	530	ADK	Adak Island, AK	FAA
521	TVX	Greencastle, IN	Local				

## Appendix D NDBS Heard in Europe

From [www.classaxe.com/dx/ndb/rna/index.php](http://www.classaxe.com/dx/ndb/rna/index.php), Nov 2006. Unidentified stations (possibly military) are not included.

f, kHz	ID	LOCATION
495	PA	Pancevo, Serbia
495	HU	Engels, Russia
495	ZK	Engles, Russia
496	ER	Yerevan, Russia
497	QZ	Bolshaya Murta, Russia
499.3	BDN	Pirate station heard in Europe
507	ND	Bolshevic, Russia
508	Z	Zilina/Hlinik, Slovakia
509	K	Mykolaivka, Ukraine
509	M	Taraz, Kazhakistan
509	R	Chernivtsi, Ukraine
510	CE	Poltava, Ukraine
510	CR	Cheboksary, Russia
510	DU	Tokol, Hungary
510	LA	Cheboksary, Russia
510	LJ	Gromovo, Russia
510	MB	Poltava, Ukraine
510	NK	Novokazalinsk, Kazakhstan

### Notes

<sup>1</sup>The text of 47CFR2.106 is available at [www.fcc.gov](http://www.fcc.gov)

<sup>2</sup>The "2005 Federal Radionavigation Plan," DOT-VNTSC-RSPA-05-12/DoD-4850.5, US Department of Defense and US Department of Transportation, 2005.

<sup>3</sup>Meetings of the Civil Global Positioning System Service Interface Committee (CGSIC). [www.navcen.uscg.gov/cgsic/meetings](http://www.navcen.uscg.gov/cgsic/meetings)

<sup>4</sup>"Global Maritime Distress and Safety System," US Coast Guard, [www.navcen.uscg.gov/marcomms/gmdss](http://www.navcen.uscg.gov/marcomms/gmdss)

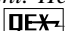
<sup>5</sup>The Web site for the Maritime Radio Historical Society is [www.radiomarine.org](http://www.radiomarine.org)

<sup>6</sup>"NAVTEX in the United States," Downloaded from [www.navcen.uscg.gov/Default.htm](http://www.navcen.uscg.gov/Default.htm), March 17, 2004.

<sup>A1</sup>*The Numerical Electromagnetics Engineering Design System*, Monterey, CA: The Applied Computational Electromagnetics Society, 1989.

<sup>A2</sup>L. Boithias, *Radiowave Propagation*. New York, Wiley, 1987.

<sup>A3</sup>A. D. Spaulding and J. S. Washburn, "Atmospheric radio noise: World-wide levels and Other Characteristics," Report 85-173 (PB85-212 942), National Telecommunications and Information Administration, Boulder, CO, April 1985.

"Fritz" (Frederick H.) Raab, *W1FR*, has been licensed since 1961 and holds an Amateur Extra Class license. He primarily operates CW on the 160 to 10-meter bands. Fritz received BS, MS, and PhD degrees in electrical engineering from Iowa State University. He is an electronics engineer and designs RF power amplifiers through his consulting company, Green Mountain Radio Research in Colchester, Vermont. A number of his designs have appeared in Amateur Radio publications. He is the project coordinator for the ARRL-sponsored 500-kHz experiment. He can be reached at [f.raab@ieee.org](mailto:f.raab@ieee.org). 

## Down East Microwave Inc.

We are your #1 source for 50MHz to 10GHz components, kits and assemblies for all your amateur radio and Satellite projects.

Transverters & Down Converters, Linear power amplifiers, Low Noise preamps, coaxial components, hybrid power modules, relays, GaAsFET, PHEMT's, & FET's, MMIC's, mixers, chip components, and other hard to find items for small signal and low noise applications.

**We can interface our transverters with most radios.**

Please call, write or see our web site [www.downeastmicrowave.com](http://www.downeastmicrowave.com) for our Catalog, detailed Product descriptions and interfacing details.

Down East Microwave Inc.  
954 Rt. 519  
Frenchtown, NJ 08825 USA  
Tel. (908) 996-3584  
Fax. (908) 996-3702



# Voltage-Magnitude Impedance Measurement

*Determine impedance through accurate measurement of voltage magnitude using a method developed by the author.*

F. N. Eddy

Voltage-magnitude measurements enable rapid, low-cost and accurate complex impedance measurements at VLF through UHF, using simple fundamental principles first described by Charles Proteus Steinmetz well over 100 years ago. Low-clock-rate PCs and digitally-controlled synthesizers enable a pure-real four-voltage (four-V) Z-sensor to plot and record  $Z(\omega)$  rapidly, accurately, and unambiguously. This can be accomplished over preselected very low frequency to ultra high frequency bands, with resistance and reactance measurement ranges and accuracies exceeding those of conventional noise bridges.

## Introduction

Professor Steber's fascinating "LMS Impedance Bridge" paper combined glitzy *Visual Basic* software with the earlier three-voltage technique to enable accurate inductance measurements at a 1-kHz test frequency.<sup>1,2</sup> His method used the efficient least mean square (LMS) parameter estimation procedure (adapted by Professor Widrow and his students at Stanford, using earlier work by Wiener of MIT, on optimal estimation theory). By itself, this three-voltage technique suffers from a fundamental ambiguity: It cannot distinguish between positive and negative reactances. That is, the unaided three-V technique is unable to distinguish capacitors from inductors. Having independently discovered a version of the three-V scheme many years ago, I was motivated in the early 1970s to extend the technique to a four-V version that overcomes that ambiguity, and which may warrant wider use. Although

this four-V scheme seems in retrospect to be quite obvious, I have been unable to find any reference to it in the literature. In any case, few amateurs seem to be aware of the fact that pure-real (absolute magnitude) voltage measurements do enable simple high-accuracy, unambiguous measurements of complex impedance.

Because the Wheatstone bridge requires time-consuming manual nulling, and most present-day alternatives involve expensive phase-matched quadrature channels, these three- and four-V concepts hold great promise for amateurs with less than infinite test-equipment budgets.<sup>3</sup> A fundamental purpose of this paper is, therefore, to describe the techniques in greater detail and even to suggest that perhaps groups of dedicated amateurs might band together, somewhat like special-interest groups sponsoring *GNU/LINUX* "freeware" software development, for coordinating test equipment design.<sup>4</sup> That would make possible the assembly of accurate, yet low-cost, gear with validated performance capabilities for their own noncommercial use. Possibly the ARRL might play a significant role in such an effort.

In the following discussion, it is suggested that a fundamental limitation to the accuracy of both the three- and four-V schemes (as well as more conventional bridge circuits and other higher frequency equipment) is the distributed inductance and capacitance of available components (as the result of the so-called "Boella Effect").<sup>5</sup> To obtain high accuracy over a wide range of impedance values at frequencies above roughly 10 MHz, it is necessary to minimize or correct for these undesired distributed parameters. Accordingly, this paper has the additional objective of both characterizing the inductance and capacitance of ordinary low-cost resistors and capacitors and then going on to describe techniques allowing compensated bandwidths extending above 500 MHz. It is hoped that

these component discussions may be found useful beyond their obvious impacts on three- and four-V measurement accuracy.

## Geometric Plots of Complex Impedance to Illustrate the Three- and Four-V Concepts

Steinmetz, armed with a good European foundation in complex variable theory in the 1890s, popularized geometrical (vector) plots of alternating currents and voltages. In a highly influential text, he showed that the complex voltages across series-connected components resulting from a current could be plotted simply in an *Argand* format (positive real components horizontally to the right, positive imaginary components up, along the vertical axis).<sup>6</sup> As he was careful to point out, the precision attainable from such analog plotting was limited, but the resulting mental picture could guide subsequent, more accurate numerical computation, thereby minimizing the risk of error. That approach is still valid today.

Consider an unknown impedance  $Z_x = R_x + jX_x$ , where  $R$  denotes resistance,  $X$  reactance,  $j$  is the imaginary operator (and the subscript  $x$  denotes an unknown), in series with a known resistance  $R_m$  (where the subscript  $m$  denotes measurement) as shown in Figure 1A. If there are no sneak paths (such as stray capacitance, mutual inductance, leakage resistance), the current,  $i$ , through this circuit is everywhere the same, and Kirchhoff's Laws apply. (The currents into and out of any node sum to zero, and the voltage across the entire network is given by the complex sum of the voltages across the individual branches.) Given these ground rules, the voltages across the components are simply:  $e_{01} = iR_m$ ,  $e_{13} = i(R_x + jX_x)$ , and  $e_{03} = i(R_m + R_x + jX_x)$ . Here, subscript 0 denotes the reference (ground) node, subscript 1 the junction between  $R_m$  and  $Z_x$ , and subscript 3 the other unknown (output) node.

<sup>1</sup>Notes appear on page 19.

40 Finn Rd  
Harvard, MA 01451-1923  
fneddy@charter.net

Node  $N_2$  is hidden and is presumed inaccessible. Accordingly,  $e_{01}$  is the voltage between nodes  $N_0$  and  $N_1$ , and so forth.

The current through this circuit is then simply  $|i| = |e_{01}| / R_m$ , where that magnitude is given by the square root of the summed squares of the variable's real and imaginary components. For simplicity, we assume  $R_m$  to be pure real (an ideal resistor with no capacitance or inductance). Later on we will show that  $R_m$  can, in fact, be complex (possess a frequency-dependent reactive component).

By plotting  $|e_{01}|$ ,  $|e_{13}|$ , and  $|e_{03}|$ , it is immediately evident that we can compute  $R_x$  and  $|X_x|$ . Specifically, from Figure 1A, we see that we can draw a circle with radius  $|e_{13}|$  from the tip of  $R_m$  (from Node  $N_1$ , at potential

$e_{01}$ ), and that this circle, in general, intersects with another circle of radius  $|e_{03}|$  drawn from node  $N_0$  (at ground potential). So long as  $|X_x| > 0$ , the circles intersect at two points corresponding to  $X_x$  and  $-X_x$ . By applying the scale factor,  $Z = e / i$ , where  $|i| = e_{01} / R_m$ , the resulting complex vector defined by this geometry uniquely defines  $R_x \pm jX_x$ .

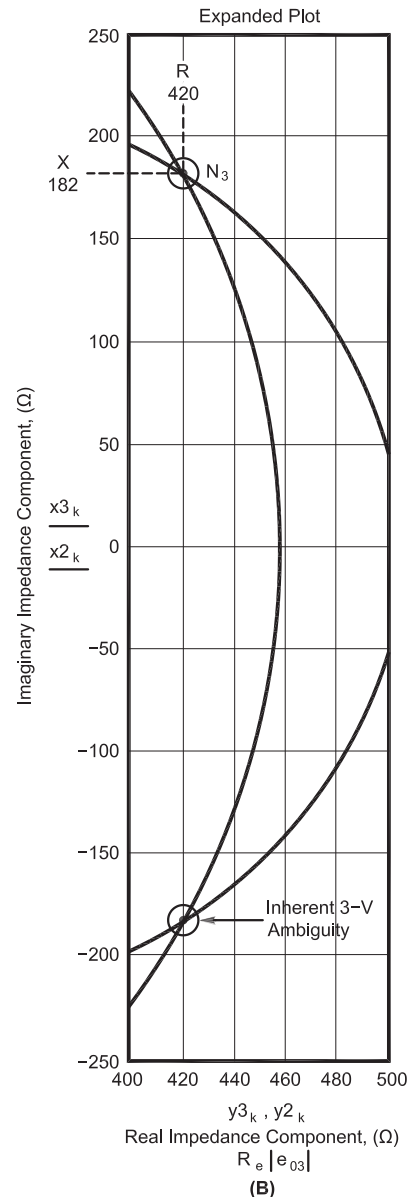
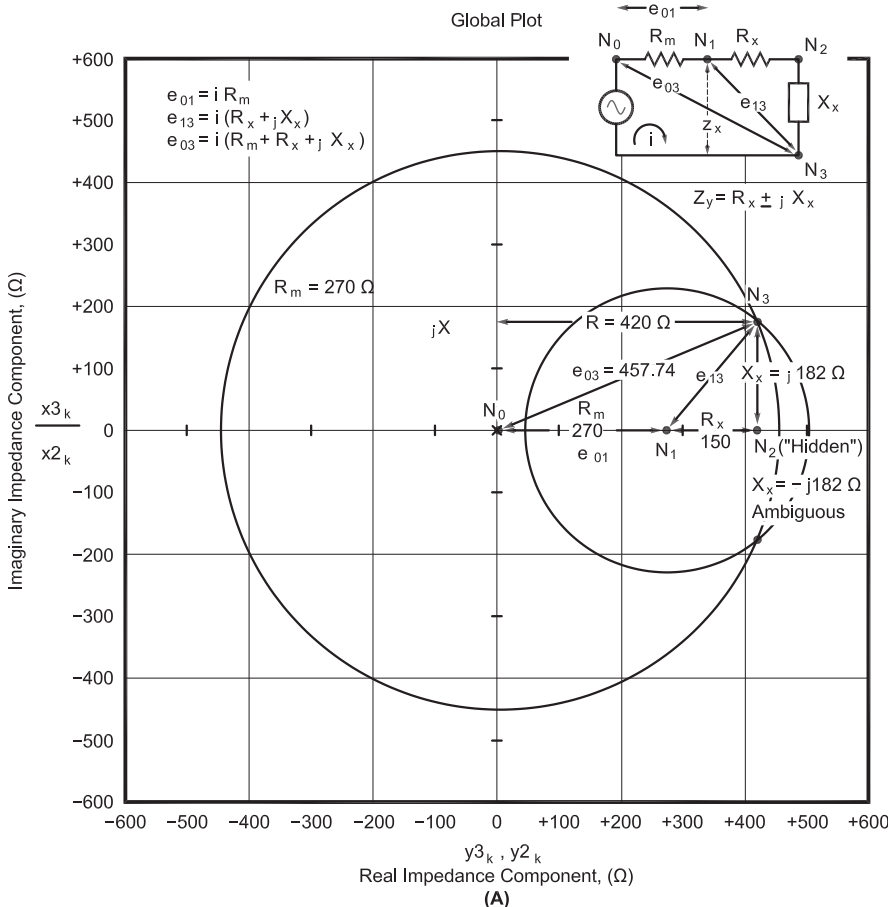
This geometric solution can be validated by somewhat more daunting algebra (see the Appendix). In either case it is clear that for maximum precision, the lengths of the  $X_x$ ,  $R_x$ , and  $R_m$  vectors should be roughly comparable. In carrying out the algebra, we see that there are three equations in three unknowns. Unfortunately, one of these equations incorporates a square root having an indeterminate sign;

the algebra thus exhibits exactly the same ambiguity as found in the geometrical construction. The equations are based upon the geometry (or vice versa, depending on your point of view) and cannot distinguish the sign of  $X_x$  if the geometry will not itself do so.

When we have *a priori* knowledge regarding the sign of  $X_x$ , all is well (as when measuring inductance, or capacitance or even ground parameters — in which the relative dielectric constant,  $k_r$ , is almost always positive).<sup>7</sup> When it comes to antennas, filters or amplifiers, we have to watch out — the proper sign is generally not known. A little reflection suggests that adding another component,  $X_m$ , to the circuit can eliminate that ambiguity, as is evident from Figure 2.

**Figure 1 — This graph shows the three-V solution for a circuit with some unknown component ( $R_x + jX_x$ ) in series with a known resistance,  $R_m$ . The plotted axes are in units of ohms for measurement values given in self consistent units (in other words, all voltages measured with the same, but otherwise arbitrary scale factor). Measurement vectors (three-V):**

$R_m = 270 \Omega$ ,  $R_x = 150 \Omega$ ,  $|X_x| = j182 \Omega$ ,  $|Z_x| = \sqrt{R_x^2 + (|X_x|)^2}$ ,  
 $|Z_x| = 235.847$ ,  $N_0 = 0 + j0$ ,  $N_1 = R_m + j0$ ,  $N_2 = N_1 + R_x$ ,  $N_3 = N_2 + X_x$ ,  $N_2 = 420 \Omega$ ,  $N_3 = 420 + j182 \Omega$ .  
 For  $i = 1 \text{ mA}$ ,  $|e_{01}| = 270 \text{ mV}$ ,  $|e_{13}| = 235.847 \text{ mV}$ ,  $|e_{03}| = 457.738 \text{ mV}$ . Hence, by calculation,  $R_x = 150 \Omega$ ,  $X_x = j182 \Omega$ . The expanded plot given at B shows that the intersections at  $420 \pm j180$  correspond to an actual  $Z_x$  of  $R_x = 420 \pm j180 \Omega$ .



QX0707-Eddy01

Note that it makes no difference where in the circuit we introduce this new  $X_m$ . From Kirchhoff's law it is evident that so long as all vectors are plotted tip to tail, their vector sum is unchanged. We merely rearrange the component subscripts. While it was assumed in the previous example that one end of  $R_m$  was grounded and that the other end was connected to the  $X_x$  component of  $Z_x$ , we can in fact scramble the order of these components any way we wish and still come up with the correct answer. Accordingly, the location of  $X_m$  in the diagram is quite arbitrary.

Almost immediately we realize that if  $X_m$  has the sign of  $X_x$ , the net circuit impedance,  $|Z_x| = |R_x + j(X_m + X_x)| = (|e_{04}|/|i|)$  will increase with  $X_m$  in the circuit, and conversely, if  $X_m$  and  $X_x$  have opposite signs, that total impedance will decrease when  $X_m$  is added. Quickly, then, this procedure resolves the issue of the  $X_x$  sign. If, however, we carry out a separate calculation using the three variables,  $|e_{13}|$ ,  $|e_{34}|$ , and  $|e_{14}|$ , we will have an independent solution, but now ambiguous with respect to  $R_x$  (instead of  $X_x$ ). Rather than sorting out and rejecting inappropriate ambiguities, we could solve directly the combined equations involving all four voltage magnitudes for the unambiguous  $R_x$  and  $X_x$ , as shown in the Appendix. Finally, we note that either or both  $R_m$  and  $X_m$  can themselves be complex. While the arithmetic becomes more difficult, we see that twisting either or both the  $R_x$  and  $X_m$  vectors in known fashion does not alter the feasibility of the exact solution with either the geometrical or algebraic solutions, as is likewise shown in the Appendix.

In swept-frequency operation, the unknown impedance,  $Z_x$ , after only a few measurements, can be modeled (approximately) in terms of dominant poles and zeros. This enables interpolation with wider frequency steps (and hence, higher average sweep rate). Furthermore, the iterative inversion of the nonlinear matrix is facilitated by using relaxation techniques that utilize *a priori* estimates of the solution, which greatly decrease the computational burden. When the difference,  $\epsilon$  between estimated  $R_x$  and actual  $R_x$ , is small, a binomial expansion converges quickly, thereby facilitating the process.

In my own basement workshop I have not as yet attempted swept-frequency operation and continue to use the full four-V solution obtained point-by-brutal-point, computed entirely by hand (with the aid of a calculator, but using an empirical acceleration factor when inverting the matrix). When the solution is automated, it is quickly evident that the time required to integrate the measured voltage is far less than the four-V computation time with even slow-clock 16-bit processors.

These actual nonlinear equations are indeed messy, but the complications are not fundamental. I fear that presentation of all the gory details would only deter the faint of

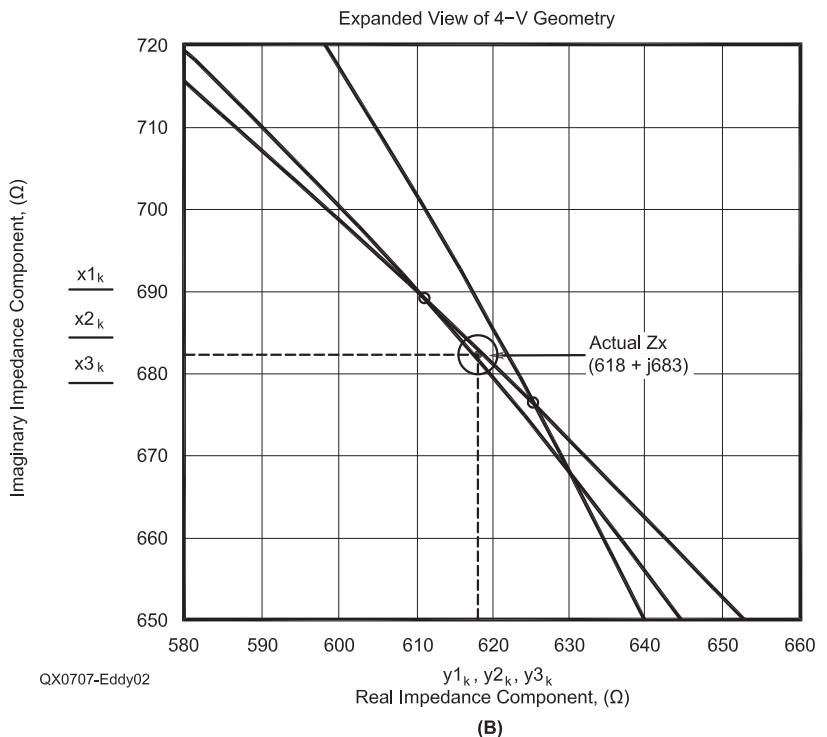
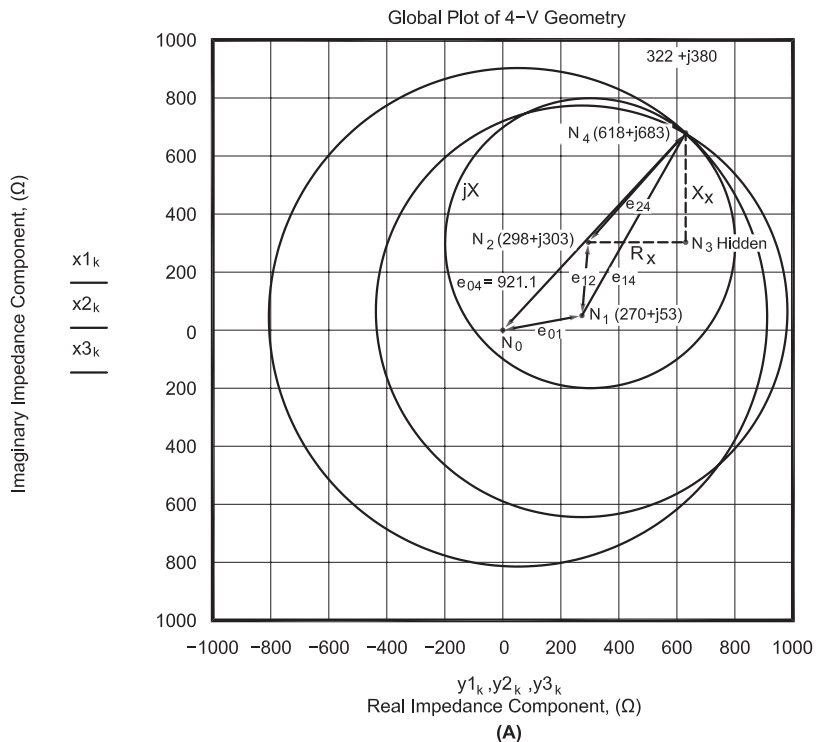


**Figure 2** — The graph of Part A is a geometrical demonstration of the inherent ambiguity removal in a series-connected four-V measurement system. It is the response of the series connected network consisting of an unknown impedance,  $Z_x (R_x + jX_x)$ , a measurement resistor,  $R_m$  (with a small reactive component) and a known reactance  $X_m$  (with a small resistive component). Measurement vectors (four-V),  $N_0 = 0$ ,  $N_1 = 270 + j53$ ,  $N_2 = 298 + j309$ ,  $N_4 = 618 + j683$ . For  $i = 1\text{mA}$ ,  $|e_{01}| = 275.2\text{ mV}$ ,  $|e_{12}| = 251.6\text{ mV}$ ,  $|e_{24}| = 496.8\text{ mV}$ ,  $|e_{04}| = 921.1\text{ mV}$ . Hence,  $Z_x = 320 + j380\ \Omega$ . Part B shows the expanded view of point  $N_4$ .



heart, leave eyes glazed over, while running the risk of my leaving out one or more special cases. The remaining space is thus more profitably devoted to the practical issues of: 1) defining the  $R_m$  and  $X_m$  parameters, and 2) measuring the voltage magnitudes.

### Real Resistors, Inductors and Capacitors

As frequency increases, component values become increasingly “soft and squishy.” Capacitors become inductors, and inductors flit back and forth between capacitive and inductive reactance; resistors end up having a little bit of everything. In the previous geometrical analysis, this complication is simply accommodated by rotating the  $R_m$  and/or  $X_m$  vectors as necessary. While the algebra is thereby complicated, the geometrically-constructed circles remain substantially the same.

In the 1960s I made a series of measurements using then widely available Allen-Bradley (A-B) 1/4-W resistors, which confirmed a simplistic theoretical model of their inductance and capacitance. Both theory and measurement (see Figures 3 through 5) suggested that their impedance could be modeled with a shunt capacitance of 0.43 pF and with the frequency-invariant resistance placed in series with an inductance of 13 nH. As confirmed by experiment (see Figure 5), the absolute value  $|Z_c|$  of a nominal 270  $\Omega$  composition A-B resistor was essentially flat out to nearly 1 GHz, but it exhibited a phase response corresponding to the delay introduced by an ideal 1/4-inch, 270- $\Omega$  transmission line.

A near flat 50- $\Omega$  magnitude frequency response can be achieved with either five 250- $\Omega$  resistors of near zero lead length in a radial, cartwheel configuration. Conversely, a flat 5-k $\Omega$  response can be attained using twenty 250- $\Omega$  resistors butted together in series. Resistors less than 250  $\Omega$  or greater than 300  $\Omega$  appear increasingly reactive. Common sense and limited experience suggest that these exact numbers are highly dependent upon proximity to and orientation with respect to the ground plane and other components.

The large number of inductor and capacitor design configurations available in the marketplace preclude any simple numerical generalizations. There have been many attempts to estimate distributed capacitance of solenoidal coils, but none of those I have looked into yield terribly accurate results, perhaps in part because of the difficulty in including effects of nearby shields and/or ground planes. Q estimates based upon total volume and elevation height over an infinite ground plane are more reliable. But still, most practical coils employ ferrite or carbonyl cores whose permeability and loss vary significantly with frequency (and not in readily predictable fashion). Capacitor series inductance is more readily estimated from the geometry, but the

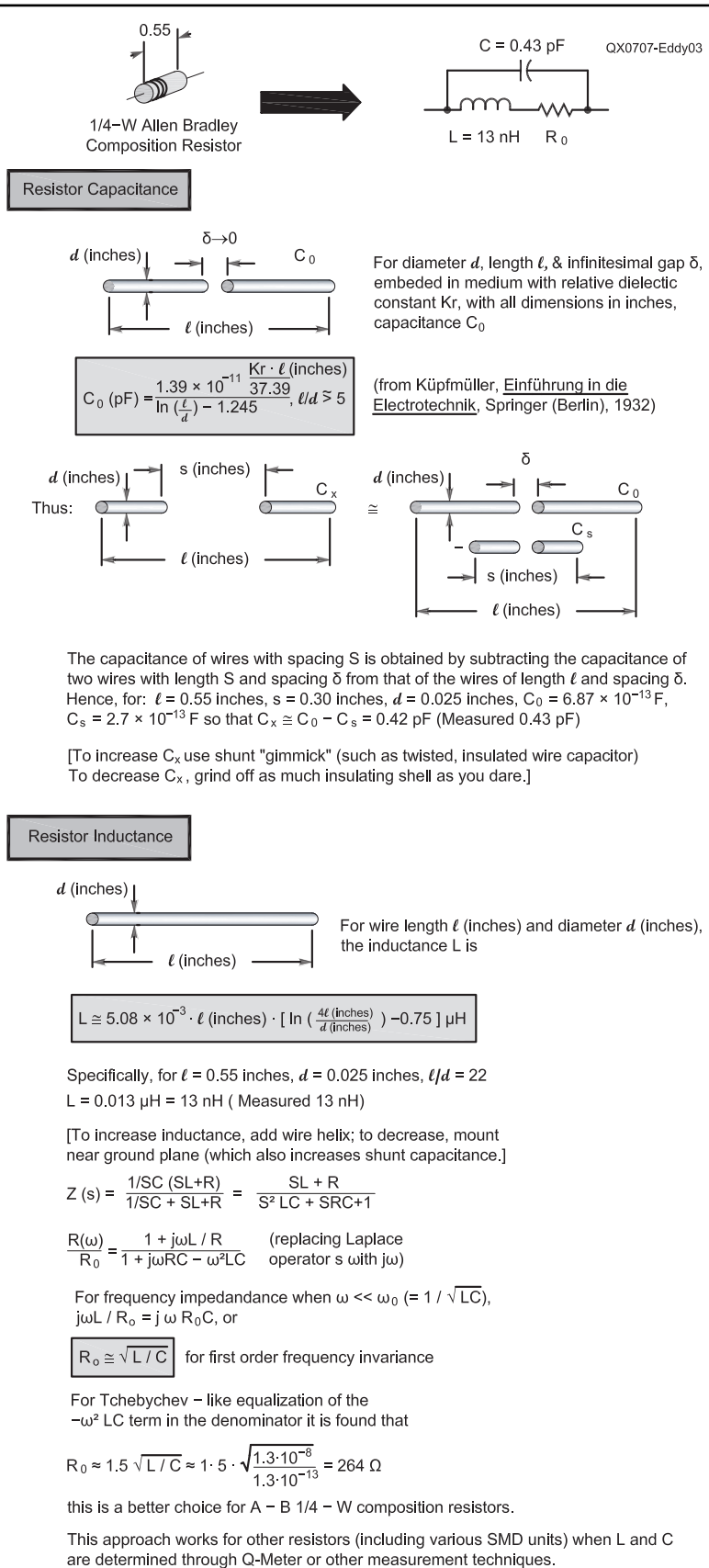


**Figure 3 — This drawing shows a composition resistor (the author used 1/4-W Allen-Bradley resistors in his measurements) equivalent circuit. The analysis shows how the equivalent capacitance and inductance are modeled and the overall impedance calculated.**

analysis is still only approximate.

There would appear to be a wide variety of manufacturer surface-mount-device (SMD) dimensional standards, but only a staggering dearth of standardized electrical specifications (perhaps partly the result of proprietary considerations).<sup>8</sup> I have made a few isolated measurements of SMD resistors and capacitors (won in a best-paper contest over ten years ago and quite possibly not representative of more widely used units) and conclude the obvious: Their self-resonant frequency or  $1/RC$  performance is at least a factor of three times better than the earlier  $1/4$  W composition resistor and their long-leaded capacitor counterparts. But I am reluctant to make strong generalizations from my limited measurements. The necessary  $C(\omega)$  measurements are readily made using Q-meter circuits with high-Q resonators operating at the frequencies of interest and observing how much the component shifts the resonant frequency, while  $R(\omega)$  is obtained from observed Q degradation. When  $R$  is large, the component should be placed in parallel; when low, in series. For the in-between cases, an inductive (or capacitive) step-down transformer can be used (a technique not that terribly different from that used by Boella back in the 1930s).

Without compensation, ordinary composition resistors in the 50 to 5 k $\Omega$  range are acceptable throughout the HF bands for use as a reference resistance without compensation or correction. Using conventional 270  $\Omega$ ,  $1/4$  W resistors (in series or parallel) but without compensation, operation up through the VHF bands yields  $\Delta R$  accuracies better than around 15  $\Omega$  when the phase shift resulting from their approximately 50-picosecond delay is acceptable. With compensation, they appear to work above 300 MHz. The highest frequency I have tried is 450 MHz. I suspect that SMD components will enable operation above 1 GHz with acceptable accuracies for many applications. Resistors and capacitors disposed radially, extending out like spokes on a wheel to a large-area ground plane, appear to minimize resistor and capacitor inductance.

### Voltage Detectors and Switched Connections

Voltage-magnitude measurements are readily made with a very-low capacitance Schottky diode such as a 1N5712 in conjunction with a high-input-impedance, low-drift op amp like an AD8603. In the steady state, detector input impedance is ultimately determined by the diode current averaged over one RF cycle. That current must therefore be held to a very low value. Detector diode linearity is increased by placing a closely-matched diode in a compensatory feedback loop. Even so, I use an empirically measured analog calibration chart to achieve even greater accuracy over a

>60-dB input dynamic range.<sup>9</sup> Square-wave modulation of the generator at a nominal 1 kHz enables autodyne conversion to a 1-kHz IF, providing an additional 20 dB or so of improvement in sensitivity by avoiding “pop-corn”  $1/f$  noise and dc drift, but at the expense of losing the spectral resolution needed for analyzing narrow-band crystal notch filters.

I must confess that when I first used this type of detector circuit, I found large unexplained shifts in apparent background noise level when the detector was moved. Because the noise greatly diminished when the fluorescent lights were turned off, I figured the high impedance circuit was picking up noise from the flickering fluorescent magnetohydrodynamic (MHD) instabilities and tried to provide better and no doubt useful shielding. I’m sure I wasted at least a couple of hours before coming late to the realization that because the diodes were in a transparent glass envelope, they were avidly absorbing photons for lunch. It took me even longer to realize that with very low junction capacitance, it doesn’t take very many picocoulombs of charge to zap a diode with an apparently rugged 30-V rating. But I was young and foolish then. Now I am no longer quite so young; I find wrist straps for me and self-shortening parking garages for the ungrounded detectors to be highly desirable.

Because the detectors are relatively in-

expensive, and their input impedances fairly high, it probably makes sense to sequentially multiplex the buffer amplified outputs from the four detectors into a PC, themselves running glitzy *Visual Basic* programs. Being inherently lazy and chintzy by nature, I have used only a single detector with three-digit LCD display. I use a crude tinker-toy manual switch for the RF connections: I have found that tiny hard-copper hooks and loops formed from oxide-resistant, gold-plated wire operating only under gravitational pressure provide reasonably reliable connections and introduce negligible excess capacitance. I have sketched possible RF switch configurations that appear to work at frequencies above 500 MHz on paper, but have not built them. I hope it is clear that I would sacrifice an arm and a leg to have a PC doing the switching, frequency-shifting, compensating, and calculation. But as I freely admit, I am lazy and have not gone much beyond unrealized daydreams of such PC glory.

### Concluding Remarks

It should be obvious that there are significant advantages in testing circuits and components at the actual desired frequencies of operation. The scaling of audio-frequency measurements to UHF is clearly fraught with difficulty. The three- and four-V impedance measurement schemes thus

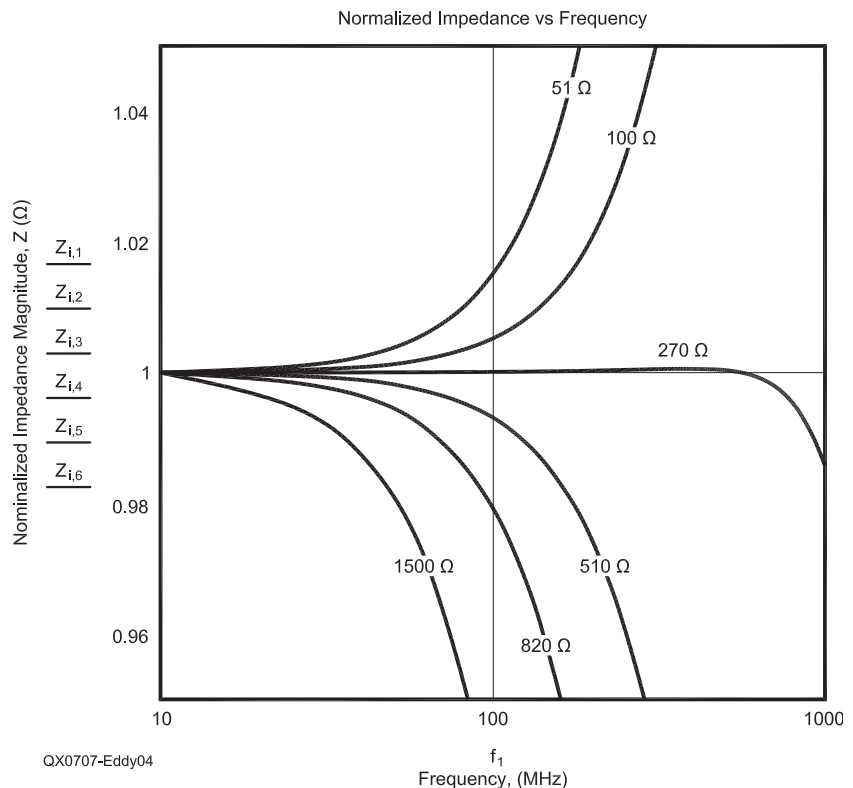


Figure 4 — This graph shows the theoretical frequency dependence of composition resistors.

have the great advantages of:

- Low cost.
- Small size (the sensor can be located next to UHF antennas without becoming part of the radiating structure, battery power and low-data-rate optical links or choked-coax with center-conductor dc power are straightforward).
- No manual nulling or frequency-dependent scaling is required.
- Greater accuracy and bandwidth capability than low-cost noise bridges.
- Readily adapted to network analysis capability.
- Perform tests at actual frequencies of interest.

Partially offsetting these advantages:

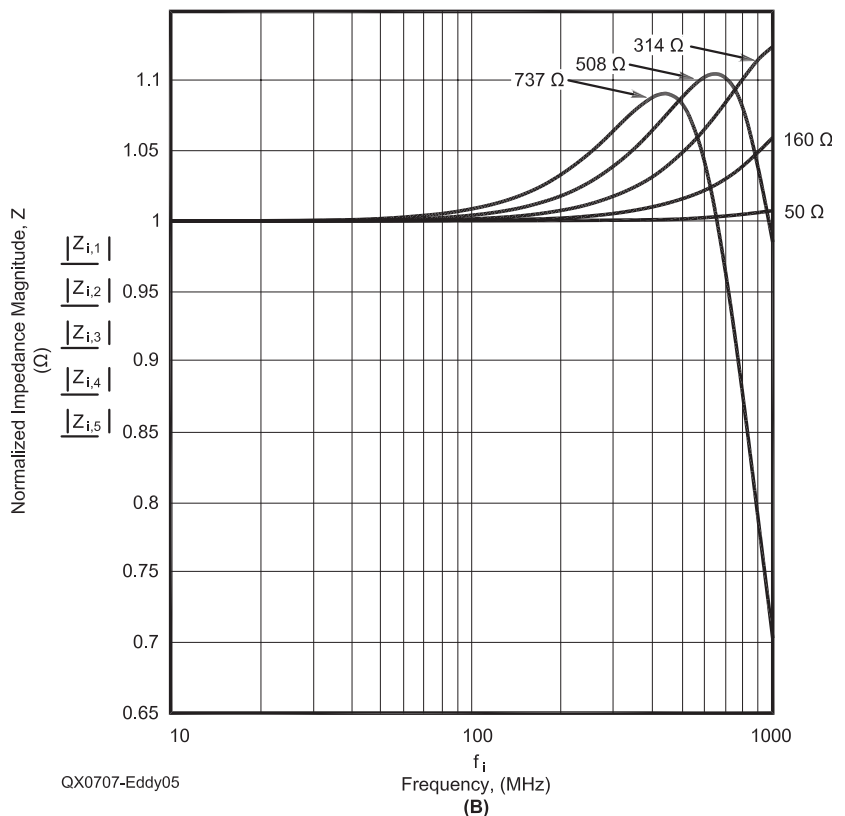
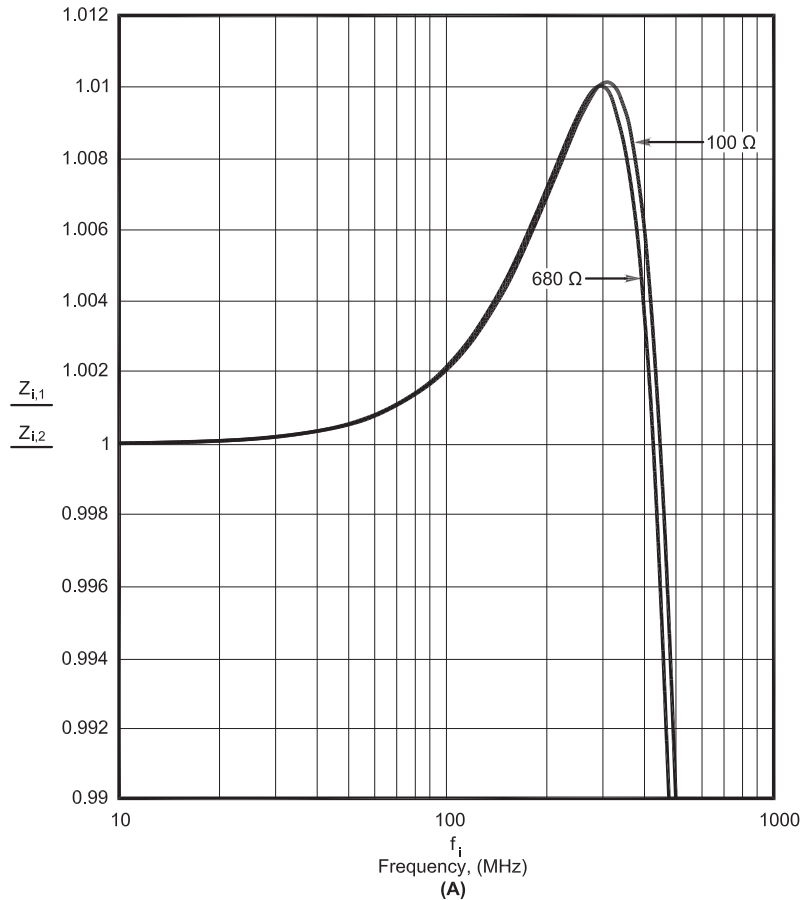
- Potential three-V ambiguities.
- Matrix inversion requirements begging for PC (as opposed to hand calculator) solution.
- Requirement for using  $R_m$  and  $X_m$  comparable to  $|Z_x|$  for maximum accuracy.
- Lack of validated cookbook designs.

I would love to see a whole panoply of amateur-designed and validated PC-based instruments providing programmable frequency and arbitrary waveform synthesis, spectrum and network analyzer capability, and so forth. I cannot help noting that sound cards are now apparently available with 24-bit A/Ds, 32-bit processing, and >100 dB dynamic range with complex sampling rates in the order of 100 kHz.<sup>10</sup> It's now costing money to dispose of still-working PCs with >100-MHz clock speeds at landfills. Whatever the merits of the voltage-magnitude impedance measurement, I cannot help thinking that by banding together, groups of amateurs can design the sorts of basic test gear every basement lab needs. But then, I've always been a dreamer.

#### Appendix: Simulation of Four-Voltage Magnitude $R_x$ and $X_x$ Measurement

In the following it will be assumed that an unknown impedance  $Z_x = R_x + jX_x$  is connected in series with a known reference reactance  $X_2$  (with some residual resistance  $R_2$ ) and a known resistance  $R_3$  (with residual reactance  $X_3$ ). It is further assumed that sneak couplings (from stray capacitance and mutual inductance) are negligible. (Although such terms can be readily incorporated at the expense of increased computational complexity, they would only serve to confuse this discussion.) It will be shown that the circuit topology shown in Figure A1 enables the unique determination

**Figure 5** — These graphs show equalized resistor responses. At A, for  $100 \Omega < R < 680 \Omega$ , a single  $\frac{1}{4}$  W composition resistor can be compensated such that  $|e_{24}| / R$  exhibits less than 1% error for  $f < 500$  MHz. At B, plots for  $L/C = R^{1.92}$ ,  $C = 0.4$  pF. See next page for 5C.



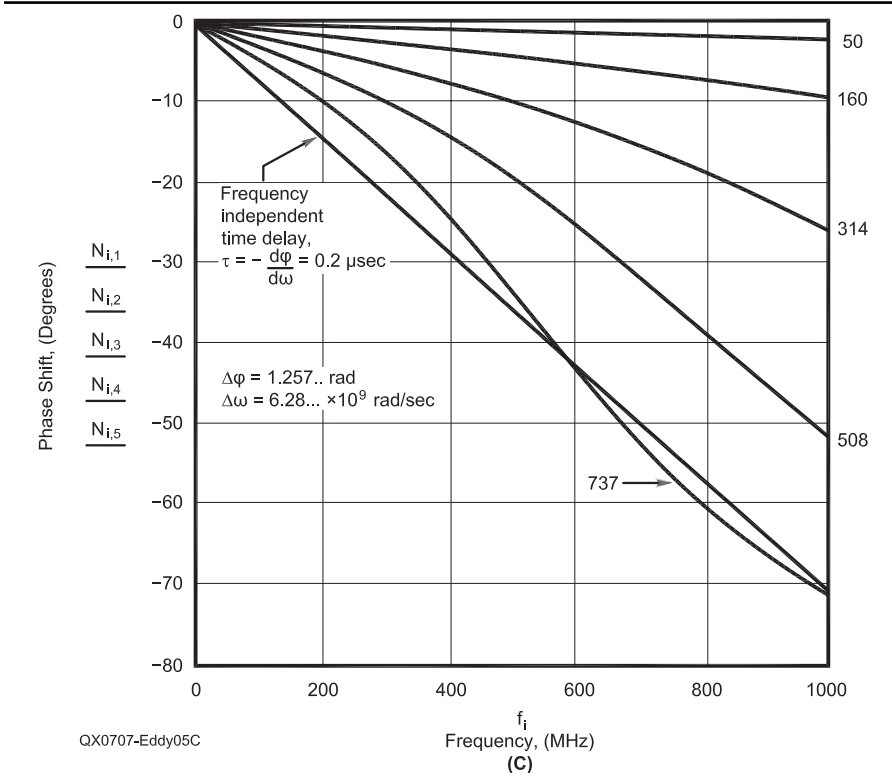


**Figure 5C — At C, inductive compensation phase response for equalized resistors. Equalization consists of adding inductance or capacitance so as to force  $L/C = R^2$ .**

of  $Z_x$  through measurement of the four voltage magnitudes,  $|V_{01}|$ ,  $|V_{02}|$ ,  $|V_{03}|$  plus any one of the following three,  $|V_{12}|$ ,  $|V_{23}|$ , or  $|V_{13}|$ , where any of these three serve to determine the current  $i$  actually flowing through the network. The use of  $i$  is reserved exclusively for current to preclude ambiguity. In the figure, the unknown impedance is assumed to be complex, of the form  $Z_x = R_x + jX_x$ , where  $j$  is the imaginary operator and  $X_x$  is a pure real quantity.

Two cases will be considered: 1)  $R_x > 0$ , and 2) sign ( $R_x$ ) unknown. The relatively infrequent case of a possibly negative resistance requires lengthier computation. With modern processors, that computation time is still less than the time required to measure the voltage magnitudes.

The source voltage  $V_{04}$  and source resistance  $Z_g$  do not enter directly into the computation. It will be shown through simulation that it is possible to uniquely determine  $Z_x$  from the four voltage magnitudes:  $|V_{01}|$ ,  $|V_{02}|$ ,  $|V_{03}|$  plus any one of the following three,  $|V_{12}|$ ,  $|V_{23}|$ , or  $|V_{13}|$ . To demonstrate this, assume the following pure real parameters (in volts and ohms as appropriate):

$$V_{03} = 10, R_x = -54, X_x = -3, R_2 = 3, X_2 = 96, R_3 = 61, X_3 = -7$$

From these parameters we first determine the voltage magnitudes that would actually be generated by the complex current,  $i$ , resulting

from an applied 10 V for  $V_{03}$ . All computed results are rounded to three significant places.

$$i = V_{03} / [R_x + R_2 + R_3 + j(X_x + X_2 + X_3)] = 0.013 - j0.1$$

From this complex current we then compute the four voltage magnitudes. We first determine the complex voltages, denoting them with a lower case  $v$ , and then from these compute the squared magnitudes (here labeled  $P$ ).

$$v_{01} = i(R_x + jX_x) = -1.065 + j6.155$$

$$v_{02} = v_{01} + i(R_2 + jX_2) = 9.989 + j7.092$$

$$v_{23} = i(R_3 + jX_3) = 0.011 - j7.092$$

$$v_{03} = v_{02} + v_{23} = 10$$

$$P_{01} = |v_{01}|^2 = 39.021$$

$$P_{02} = |v_{02}|^2 = 150.08$$

$$P_{03} = 100$$

$$P_{23} = |v_{23}|^2 = 50.2966$$

To these, we add  $P_i = |i|^2 = P_{23} / (R_3^2 + X_3^2) = 0.013$ . The actual pure-real measurement inputs to the computation are then:  $P_{01}$ ,  $P_{02}$ ,  $P_{03}$ , and  $P_i$ .

In actual practice, the measured voltage magnitudes will exhibit finite error. To determine the effects of measurement error, simply multiply these squared terms by an error term,  $k_{1,4} = (1 + \epsilon_{1,4})^2$ , where  $100 \epsilon_{1,4}$  is the percent error inherent to the voltage magnitude measurement process. In the following we set  $k_{1,4} = 1$  to establish that the processing algorithm is free from error with ideal voltage measurements.

### Processing for $R_x > 0$

Define three parameters,  $A$ ,  $B$ , and  $C$  as follows, making sure that the  $X$  terms are the known signed magnitudes (that is, do not include the  $j$  operator):

$$A = 1 / [(X_2 / X_3) - (X_2 + X_3) / (R_2 + R_3)] = 0.033$$

$$P_i = P_{23} / (R_3^2 + X_3^2) = 0.013$$

$$B = [ \{ (P_{02} - P_{01}) / P_i \} - R_2^2 - X_2^2 ] / [ 2 R_2^2 ] = -150$$

$$C = [ \{ (P_{03} - P_{01}) / P_i \} - (R_2 + R_3)^2 - (X_2 + X_3)^2 ] / [ 2 (R_2 + R_3) ] = -58.172$$

From these relations (derived from elementary circuit analysis of Figure A1), compute:

$$X_x = A(B - C) = -3.00 \text{ and } R_{xp} = \pm [ (P_{01} / P_i) - X_x^2 ]^{1/2} = \pm 54$$

It is seen that  $R_{xp}$  has indeed the correct magnitude, but that because of the square root, its sign is indeterminate. Accordingly,  $R_{xp}$  is always assumed to be a positive number. Note that the observed errors in  $X_x$  and  $|R_{xp}|$  are consistent with the number of bits employed in the numerical computations.

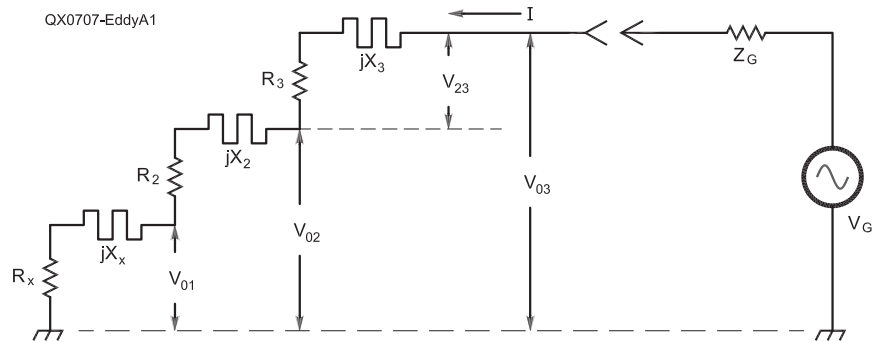


**Figure A1 — This diagram shows the assumed measurement circuit topology.**



### Unknown $R_{sp}$ Sign

When the sign of  $R_{sp}$  is not known *a priori*, new  $a$ ,  $b$  and  $c$  parameters are computed (all previously employed variables remaining unchanged).

$$a = 1 / [(R_2 / X_2) - (R_2 + R_3) / (X_2 + X_3)] = -1.454$$

$$b = [(P_{02} - P_{01}) / P_1 - R_2^2 - X_2^2] / (2 X_2) = -4.687$$

$$c = [(P_{03} - P_{01}) / P_1 - (R_2 + R_3)^2 - (X_2 + X_3)^2] / [2 (X_2 + X_3)] = -41.83$$

yielding  $R_x = a (b - c) = -54.000$  (That is, with the correct sign and magnitude, thereby validating the procedure.) Again, these foregoing  $a$ ,  $b$ ,  $c$  relations follow from elementary circuit analysis.

### Error Sensitivity

Rigorous sensitivity analysis requires far more space than is appropriate here. Nonetheless, simple simulations using the previously discussed  $k$  coefficients leads to the following rough rule of thumb: The percentage error in  $|Z_x|$  runs a bit more than twice the percentage error in the voltage measurements (for voltage measurement error much larger than the uncertainty in the reference components and for the reference impedance magnitudes roughly comparable with that of the unknown).

### Notes

<sup>1</sup>G. Steber, "An LMS Impedance Bridge," *QEX*, Sep/Oct 2005, pp 41-47.

<sup>2</sup>D. Strandlund, "Amateur Measurement of  $R + jX$ ," *QST*, June 1965, pp 24-27.

Also, see the discussion at [web.ukonline.co.uk/g3ldo/aegextra.htm](http://web.ukonline.co.uk/g3ldo/aegextra.htm) (updated 18 Mar 2002).

L. Callegaro, *et al*, "Impedance Measurement by Means of a High Stability Multiphase DDS Generator with the Three-Voltage Method," *IEEE Transactions on Instrumentation & Measurement*, 52, (4), pp 1195-1199 (2003).

<sup>3</sup>The Wheatstone bridge was actually invented by Samuel Christie in 1833. Sir Charles, with more than enough other inventions to his credit, published a paper calling attention to Christie's wonderful idea. In spite of great effort by Wheatstone to reverse this canard, the bridge has ever since been popularly (and wrongly) credited to Wheatstone. (*Encyclopedia Britannica*, 11th Ed (1910), Vol XXVIII, pp 583-584.)

<sup>4</sup>GNU and related free-ware languages (including *Fortran*, *C++*, the *GNU Scientific Library*, and others) have been made available in well-documented versions, largely by researchers in academia and large government laboratories all around the world — free from hidden ties to specific operating systems. More information, software, and at-cost manuals can be downloaded at, or ordered from, their various Internet sites.

<sup>5</sup>M. Boella, *Alta Frequenza*, 3, (2), April 1934. A rough history of the early work in this field is given in J. F. Blackburn, *Components Handbook*, Vol 17, MIT Radiation Laboratory Series, McGraw-Hill, 1949, Chapter 2, *passim*. Details on resistor design and manufacture are hopelessly obsolete, but the underlying

concepts are still valid. While there were earlier efforts in the field, Boella documented useful measurement procedures and techniques. My own earlier measurements with Allen-Bradley ¼-W composition resistors are roughly corroborated by L. Besser, *RF Design*, July 1993, p 66.

<sup>6</sup>C. P. Steinmetz (with the assistance of E. J. Berg), *Theory and Calculation of Alternating Current Phenomena*, 3rd Ed 1900, Chapters 4 and 5, Elect World and Engineer, New York, 1900. It is my uncorroborated recollection that earlier editions cover essentially the same material. Steinmetz introduced the use of complex numbers to the electrical engineering community using the *Argand diagram* in an unattributed Cartesian coordinate system. Jean Robert Argand (1768-1822) was an amateur Swiss mathematician who apparently was the first to publish (in 1806 in an anonymous book, *Essai, sur une maniere de representer les quantites imaginaires dans les constructions geometriques*, this technique for plotting complex quantities, although Gauss, Wessel, and many others had used similar and other constructions much earlier in unpublished works [as discussed in *The Oxford Biographical Dictionary of Scientists*, Second edition, R. Porter, ed, Oxford, 1994].


<sup>7</sup>In only extremely rare cases of specialized mineral deposits is  $k_r < 0$ . This fact allows use of the three-V scheme for ground parameter measurements using electrically short inverted monopoles using a circular mesh ground screen with radius comparable to monopole length.

<sup>8</sup>J. Hollomon, *Surface Mount Technology for PC Boards*, Prompt (Sams) #61060, Indianapolis, Rev 1st Ed, 1995. My own SMD experiments were carried out using a kit of undocumented parts won in a best-papers contest sponsored by *RF Design Magazine*; it is presumed, but not known, that these are representative of parts supplied by other manufacturers. The only corroborating reference I could find was a Modelithics Product Feature article, "Comprehensive Models for

RLC Components to Accelerate PCB Designs," *Microwave Journal*, May 2004 that concentrated primarily on the effects of a nearby ground plane on observed SMD parameters.

<sup>9</sup>The observed ac-in/dc-out transfer characteristic was in reasonable agreement with an Electronics Workbench Simulation carried out from 30 V<sub>p-p</sub> down to 30 mV<sub>p-p</sub> input. Below this level the required integration time became excessive.

<sup>10</sup>EMU Systems, Scotts Valley, CA 95066.

*F. N. Eddy is semi-retired. He studied applied physics at Harvard, and worked for over twenty-five years at a large not-for-profit corporation, most recently holding the position of Division Scientist. He holds numerous patents (most recent, a superconducting analog-to-digital-converter), does occasional consulting, and still putters about in his basement laboratory with particular fondness for revisiting the classic problems in physical acoustics, antenna and propagation theory, and general feedback and oscillator theory. When he could find the time he performed in various semi-professional early-music groups — with many of his instruments (that he restored) now a part of the Eddy Collection at Duke University. As part of a continuing interest in the history of science, he continues to explore early Greek and Arabic descriptions of astronomical instruments, making reproductions of some of these for modern day test and evaluation. Long since having abandoned active Amateur Radio, he nonetheless still has fond memories of operating warmly glowing push-pull 6J6 UHF transmitters and much too noisy 6C4 super-regenerative receivers cobbled together from low-cost war-surplus detritus carried home, precariously balanced on the handlebars of a bicycle!* 

## WANTED: C++ PROGRAMMER

We need a part time C++ programmer who likes to work at home but lives in the Orange County/Los Angeles area. We need to automate our test procedures, which involve RF transmitters and receivers to determine if production products pass or fail. Tests include determining RF output, current consumption, PLL lock range, frequency accuracy, and receiver sensitivity by checking each section with a fully or semi-automated test program.

We need the following:

- Someone with experience writing Visual C++ programs allowing the PC to control the test equipment with RS-232 and/or GPIB.
- You need to be familiar with RF test equipment such as spectrum analyzers, oscilloscopes, signal generators, and frequency counters.
- Be familiar with troubleshooting of RF and digital circuits.
- Be able to control relays, switches, etc. through PC I/Os with Visual C++.
- Have TCP/IP programming experience with Visual C++.
- Have CGI programming experience in any language.
- Robotic experience a plus.
- We would like to see examples and or samples of your past work.



**COMMUNICATIONS SPECIALISTS, INC.**

426 WEST TAFT AVENUE • ORANGE, CA 92865-4296

714.998.3021 • FAX 714.974.3420

US & CANADA 800.854.0547 • FAX 800.850.0547

www.com-spec.com

E-mail: [spence@com-spec.com](mailto:spence@com-spec.com)

# Introduction to Class D Tuned RF Amplification

*This article describes a 30 W CW transmitter that uses a class D amplifier.*

Jukka Vermasvuori, OH2GF

Originally published in the March 2006 issue of RADIOAMATÖÖRI, the membership journal of SRAL, the Finnish Radio Amateur League, the author translated his article for publication in QEX.

Tuned RF amplifiers with A, B or C class amplification have been around since 1920. Up to the 1950s, amplifying devices were vacuum tubes, but today solid state bipolar or field effect transistors have replaced them. In A, B and C class amplifiers, the amplifying device is handling sinusoidal type waveforms.

In the amplifier design, power efficiency is important, especially for mobile / portable use, where the used energy is taken from a battery. High efficiency with constant output power means less dc consumption and consequently less dissipated heat power means smaller heat sinks and finally smaller equipment size. The efficiency of a power amplifier device is specified as RF output power divided by dc power fed into the device. With no losses in power conversion, RF power is equal to dc power, and efficiency is 100%. The classification between working conditions is made according to the angle of current in the device. One complete sinusoid means a current angle of 360°. See Table 1.

The maximum theoretical single signal efficiency is valid for a tuned load, assuming peak RF output voltage equal to used supply voltage. Efficiency 1) is the efficiency for 90% RF swing leaving 10% unused for saturation region. Typical values for A to C stands from higher power tube amplifiers but can be used as a little pessimistic guidance for semiconductors.

In classes A, B and C, indicated figures are valid only with fully optimized drive conditions, and partial drive in A and B stages causes linear loss of efficiency. Class A and B ampli-

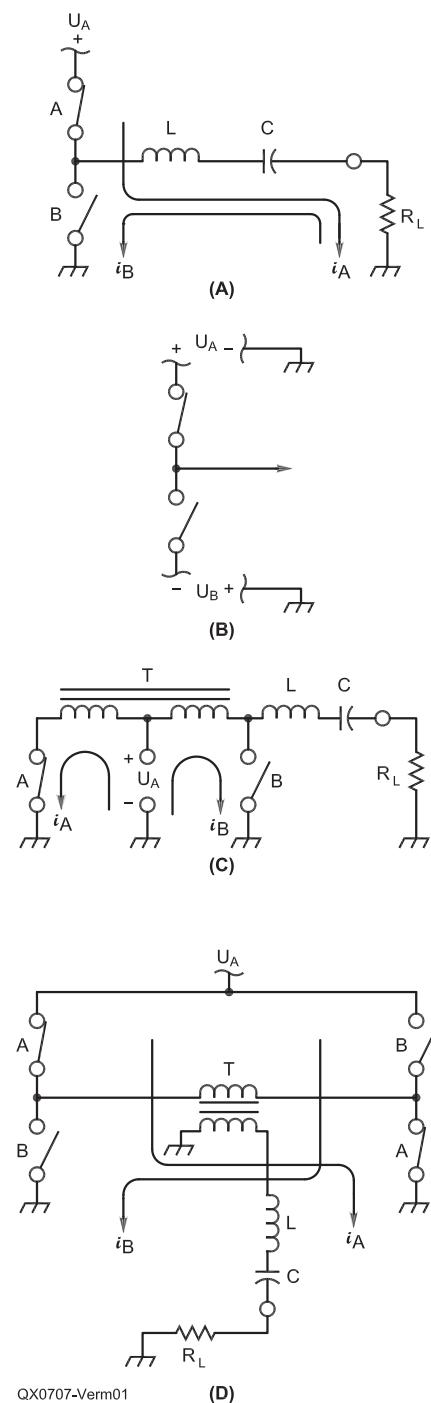
fiers are linear amplifiers used for multicarrier combinations, among others for SSB signals. Nonlinear class C amplifiers are for single signal constant carrier amplification, CW.

Classes D, E and F have been suggested for higher efficiency. In these classes the amplifying device is used as a switch in conjunction with a tuned circuit. The tuned circuit is charged from dc source with properly timed switch. With a low loss switch, high conversion efficiency can be achieved. These amplifiers are highly nonlinear, and competing with class C stages for one carrier amplification.<sup>1</sup>

## Class D

Theoretical lossless efficiency of class D is 100%. A class D amplifier is basically a square wave amplifier. The output square wave is the sum of harmonically related sinusoids according to "Mr. Fourier," and only the fundamental one is taken into use as the RF output. As the solid state switches have only two states, ON and OFF, the closed and open contacts generate a square wave. The switches are driven with constant amplitude square wave signals having the frequency of the desired output sinusoid. The generated amplified output square wave is filtered, and the desired output is a sinusoidal carrier with constant amplitude. RF output power is dependent on the magnitude of the load resistance on the desired output RF frequency presented to the switches. This resistance directly determines the dc and RF output power. Important for the proper operation is that the square wave output can "see" a proper low impedance only at the desired RF frequency and high impedance at other RF frequencies. In practice this is done with a series tuned circuit between the square wave output and the load.

Class D amplifiers are normally used for carrier amplification and are directly suitable for CW transmitters. Superimposing an audio signal on the dc supply voltage,



QX0707-Verm01

Figure 1 — Configurations of class D voltage waveform switchers.

Viputie 3  
FI-01640 Vantaa  
Finland  
oh2gf@sral.fi

<sup>1</sup>Notes appear on page 30.

however, generates a DSB AM transmission. SSB amplification is further possible by the Envelope Elimination and Restoration (EER) method by Mr. L. R. Kahn, where phase information of SSB is restored by the switch drivers or exciter oscillator and the amplitude information is added by modulating the dc supply voltage by the detected SSB envelope (valid also for class C).

### Amplifier Configurations

Figure 1 shows four different amplifier principles using ideal switches. Switches A are ON for the first part of the RF output sinusoid and B for the second half. We can feed dc energy to the square wave signal either during half of the square wave, variant A, or during two halves, variant B, C and D. (This is comparable to half wave or full wave rectification.) For several reasons it is better to divide the switching losses to two smaller units instead of one bigger one and use variants B, C or D. Variant C has the advantage of having grounded switches on one side. This makes it easier to generate the driving signal. Variant B is interesting because no transformer is needed and it might have advantages regarding overshoot generation. The disadvantage of using two opposite-polarity power supplies makes it practical only for use with ac power mains.

### Square Wave

Figure 2 shows a square wave signal. Fourier series for this waveform is:

$$U = 4 A / \pi (\cos \omega t - 1/3 \cos 3\omega t + 1/5 \cos 5\omega t - \dots) \quad [\text{Eq 1}]$$

In Figure 2 the fundamental and third harmonic plus their sum are also presented. The sum of only two components comes close to a square wave, and adding further odd harmonics makes it perfect.

The multiplier for the fundamental component is  $4 A / \pi = 1.273 \times A$ . If A is our supply voltage, 12.0 V, the peak of the sinusoid is  $12.0 \text{ V} \times 1.273 = 15.28 \text{ V}$ . This is a great advantage for class D compared to class C where you have only max. 12.0 V for the RF swing. To gain maximum efficiency, the impedance for odd harmonics,  $3\omega$ ,  $5\omega$  and so on should be infinite.

If we are loading the voltage waveform of the square wave on the fundamental sinusoid only, the switch current waveform has the form of half sinusoid. By calculating input power, you multiply half square wave voltage (constant) with half sinusoid form current and for current you should use a multiplier of 0.637 instead of 0.707 (average / RMS value).

### Example of Power Calculation for the Ideal Lossless Situation

We calculate values for one half period of the output sinusoid. If both halves are done similarly as in amplifier variant C, the

half time calculation is valid for the whole sinewave period.

$$\begin{aligned} V_{CC\text{dc}} &= 12.0 \text{ V} \\ R_{L\text{rf}} &= 5 \Omega \\ u_p &= 12 \text{ V} \times 1.273 = 15.28 \text{ V} \\ i_p &= u_p / R_{L\text{rf}} = 12.0 \times 1.273 / 5 = 3.05 \text{ A} \\ P_{\text{RF}} &= (u_p \times i_p) / 2 = (15.28 \text{ V} \times 3.05 \text{ A}) / 2 \\ &= 23.3 \text{ W} \\ P_{\text{dc}} &= V_{CC} \times i_{\text{AVE}} \\ \text{where } i_{\text{AVE}} &= i_p \times 2 / \pi \\ P_{\text{dc}} &= 12.0 \text{ V} \times 3.05 \text{ A} \times 0.637 = 23.3 \text{ W} \end{aligned}$$

The input dc power is same as the effective RF output power, and power conversion efficiency is 100%.

The current through the switch has a flow angle of  $180^\circ$ , similar to a class B amplifier. The useful RF swing, however, is 1.273 times higher than in class B. Additionally, the switching takes place during zero current cross over, so no switching losses are generated.

For comparison to class C, with a flow angle of  $120^\circ$ , you need a higher current peak value to compensate for the narrower pulse width, to reach the same equivalent current area. Semiconductors are always peak current limited, so the RF power capacity with one device in class C is smaller than in D or even B. Semiconductor circuits are relatively seldom used in Class C amplifiers.

### Practical Operating Conditions

The chosen amplifier configuration is version C. In Figure 1C, the output power is taken asymmetrically parallel from switch B. Power from the other half cycle is coming through a 1:1 transformer, T, having some additional loss. To avoid this small unbalanced symmetric output, a balanced/unbalanced transformer is recommended. This also has the advantage of doubling the impedance seen from the load side.

For the solid state switches in the following practical amplifier, HEXFET Power MOSFETs have been selected. To choose any switching device, three specifications are important to start with: 1) saturation resistance  $R_{\text{DS(ON)}}$ , 2) input, output and feed back capacitances, and 3) drain-source breakdown voltage,  $V_{\text{(BR)DSS}}$ .

Current through the switch generates dissipation voltage across the saturation resistance. Because the current has a half sinusoidal form, so does the generated voltage. This voltage reaches its maximum in the middle of the half-square wave, and causes a drop in the available peak value of the RF voltage swing. Dissipation power in the saturation resistance is:  $(u_{\text{sat p}} \times i_p) / 2$ .

Increasing the junction temperature from  $25^\circ\text{C}$  to  $90^\circ\text{C}$  increases the saturation resistance 1.5 times referenced to the  $25^\circ\text{C}$  value. A slightly over-dimensioned heat sink is a good investment.

To reach a lower saturation resistance, an FET with a larger chip size is needed. This comes only with increased capacitances. The output capacitance must be charged and discharged during every square wave voltage transition, needing dissipation energy  $W = 1/2 C U^2$ . This value is multiplied by the frequency.

The same idea applies to the input capacitance. The driver source resistance must be low enough, typically 5 to  $10 \Omega$ , to charge and discharge the sum of the internal capacitances to achieve adequately short rise and fall times of the driving voltage waveform.<sup>2</sup> The main switching device must be then chosen in conflict between lower saturation resistance and smaller capacitances.

The most unknown phenomena are the high peak value sinusoidal transients raiding

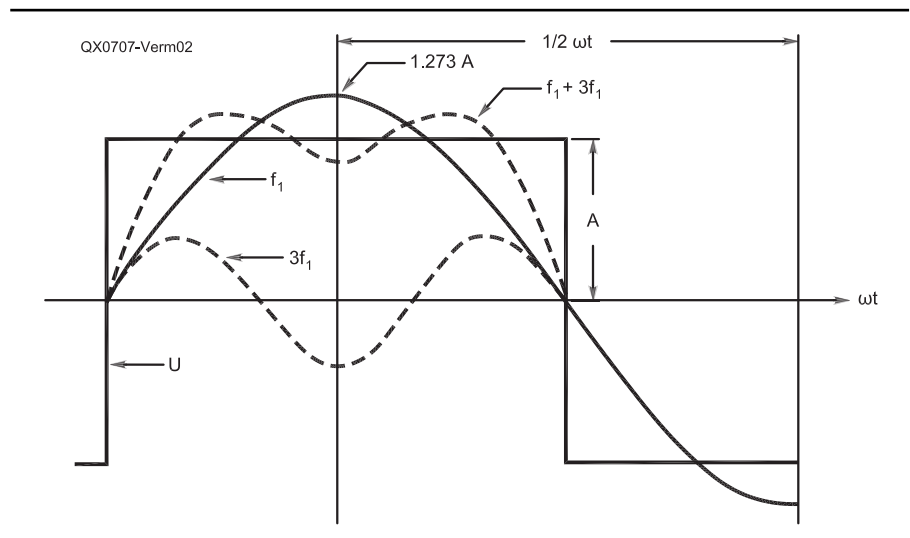


Figure 2 — Square wave waveform, shown as made up of a fundamental sine wave and odd harmonics.

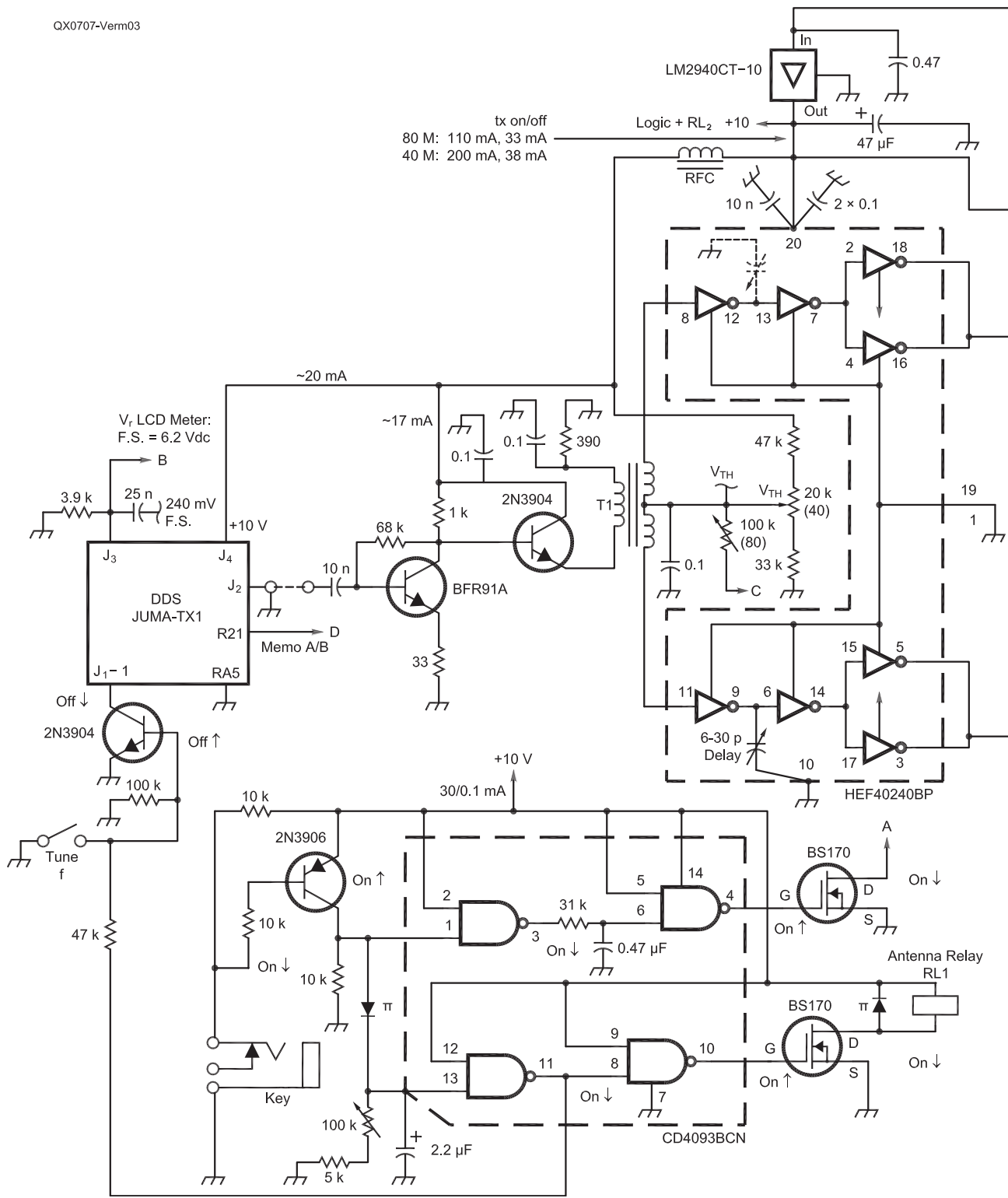


Figure 3 — Schematic diagram of class D 30 W transmitter.

on top of the drain square waveform when the switch is in the OFF condition.

Two basic switching stage internal problems exist: 1) lack of proper timing between switch A and B waveforms and 2) unavail-

able overshoot of the 1:1 transformer due to leakage inductances.

With properly timed switching, however, the most serious oscillations are generated with a reactive load, because the zero cur-

rent switching cannot be achieved. Abrupt current change causes high transients and can lead to drain-source breakdown. This is not typical only for class D operation, but also even more so with single ended class E





Charging and discharging device capacitances up to 1 nF within a few tens of nanoseconds creates high peak currents. This requires printed circuit design with an adequate ground layer and wide but short internal connections to minimize connection inductances. Several bypassing capacitors in parallel is advantageous.

### Parasitic Oscillations, Stability

FETs in class A, AB or C operation are prone to self generated spurious oscillations, leading sometimes to drain-source voltage breakdown.<sup>5</sup> This is typical in conditions where terminating elements are transformers or other inductive components. High transconductance (A / V) guarantees high gain also on spurious frequencies. Different damping methods, normally on the gate, have to be used. Using a selective antenna as a load can present high impedances on some other frequencies, leaving the amplifier unloaded. Reaching stability with a broadband dummy load is not enough. Feedback is also one method to tame the gain.

Class D seems to be easier. If the driving is done by a push-pull stage, the gate of the power switch is terminated in both ON and OFF state by the saturation resistance of the push-pull devices, usually around 5 Ω. Time for high transconductance during voltage turn over is very short and the gate is loaded with 5 Ω of one driver. In the circuit presented in Figure 1C no self oscillation has been seen.

### 30 W Field Day CW Transmitter with Class D Amplification

The following text describes a prototype transmitter, with measurements results. Suitable literature on class D amplifiers was rare and a lot of information was gained in practical work during this long project. The construction uses normal “human” sized components, needing no special tools — except the DDS. For tuning up the first time, a VOM might be adequate, as suitable measurement points have been included.

### Design Features

The supply voltage has been chosen — with Field Day conditions in mind — as 12.6 V, which is available from a normal car battery. For a higher output power, a higher supply voltage is possible with certain

limitations. The high limit depends on the FET breakdown voltage under the detuned conditions.

Class D amplifiers need a series tuned circuit to pick up the fundamental sinusoid. Dividing the output side capacitance into two adjustable parts, it is possible to match the 50 Ω load. If the antenna can present a close enough impedance, no external matching unit is needed.

A class D amplifier takes direct current according to the impedance seen by switches on output frequency. A dc Ammeter in the supply line can be used as an RF tuning indicator, giving an idea of when the tuned condition has been reached. This results in proper loading for the desired output RF power and resonance condition. Disconnecting the antenna, creates an open load condition, and drops the dc normally close to zero.

QRP operation requires a possibility to tune to the right frequency of the desired station. Low power on the offset frequency is a waste of time. A VFO is a must, and even better it must be a stable one. The solution is DDS. This transmitter uses JUMA-TX1 DDS designed by OH2NLT. Info can be found in [www.nikkemedia.fi/juma-tx1/kits-available.html](http://www.nikkemedia.fi/juma-tx1/kits-available.html). The main specifications are:  $f = 0.1 - 8.0$  MHz in steps of 10, 100, 1000 Hz and 100 kHz. There are two places for setting memories. (One is used for 3.5 MHz, the other for the 7MHz band.) The output voltage on the internal 200 Ω load is  $0.2 V_{pp}$ . Due to the DDS upper limit of 8 MHz, this transmitter is only designed for the 80 and 40 m band.

The DDS is switched off during the receiving period. For tuning to the receive frequency a “tune” switch is added.

A properly timed antenna T/R relay is used.

Continuous output power adjustment from zero to maximum makes first time adjustment of an unknown antenna safer.

This transmitter consists of the following blocks, shown in Figure 3:

- Oscillator, JUMA-TX1 DDS, Direct Digital Synthesizer.
- Linear amplifier to increase DDS output level to  $4 V_{pp}$ .
- A/D converter, one IC device with eight Schmitt trigger gates for forming two

separate driving chains to power switchers.

- Drivers for main switches creating low source resistances for fast charge and discharge of IRF510 input capacitances.
- Main switches IRF510 transistors with 1:1 balun transformers.
- Output tuned LC matching circuit.
- Amplitude modulator FET for CW keying, to form proper rise and decay times for click free CW operation. An additional function for this modulator is to decrease the supply voltage for the power switches during wrong tuning conditions. Open drain drive for the modulator FET makes it possible to increase the supply voltage over 12 V for occasional mains power supply feed. Low power stages are fed with a 10 V low-drop regulator, working even with one volt voltage difference.
- Keying waveform generation and antenna relay drive. The DDS switches off for the receive period.

### DDS Oscillator

I bought the DDS kit and built it.<sup>6</sup> The biggest problem I had was that my soldering iron was too big and hot. A thin soldering tip, proper soldering flux and narrow tin suction braid is a must.

The DDS output voltage level decreases on 7 MHz. Compensation with an RC network was not easy to do. The problem was solved by a different biasing level to the next stage on the 80/40 m bands.

### DDS Amplifier

The A/D converter’s Schmitt trigger needs  $4 V_{pp}$  drive level. Input resistance seems to be around 300 Ω so a simple two-stage amplifier was constructed with BFR91A SOT37 and emitter follower 2N3904. The measured RF levels at the 3904 emitter were  $4.75 V_{pp}$  at 3.5 MHz and  $3.80 V_{pp}$  at 7 MHz.

### A/D Converter and Digital Prestage

A single octal buffer CMOS IC HEF40240BP is used for digital signal formation. The IC forms two driver chains for output power drivers. The required 180° phase shift between the chains is realized with a three-winding broad-band transformer, T1.

The variable length pulse results from the first Schmitt trigger gate in each chain.

**Table 1**  
**Classification of Amplifier Types**

Class	$\varphi$ / degree	Max Efficiency %	Efficiency 1) %	Typical Efficiency %	Use
A	360	50	45	25-30	linear, multi carrier
B	180	78.5	71	50-65	linear, multi carrier
C	120	92	81	70-80	single carrier
D	180	100	90	82-88	single carrier

The trigger is driven with a half sinusoid RF voltage riding on a variable dc level. The IC turnover level is around half of the IC's supply voltage. By setting the levels of RF plus dc properly, the required pulse length shorter than 180° can be realized.

Equal delay for both pulse flanks is normally done by adding a series resistor and parallel capacitor to ground between two Schmitt gates. The output resistance of the previous gate is used as R of the delay circuit, so the only external component is a 30 pF trimmer capacitor added between the next gate input and ground. The chains should be symmetric, so the side for added delay must be tested on 7 MHz during tune up.

The buffer IC I used is designed for high capacitive load operation. Further improvement for lower output resistance is achieved by paralleling two gates at the outputs.

### Drivers

To have fast enough transitions in the final switch gate, low resistance drive is needed. My original idea, to use three parallel gates of 40240 for drivers, worked marginally on 3.5 MHz but was too slow for 7 MHz. The solution was a P and N FET pair in push-pull configuration. Some better IRF devices were identified, but were not available here. The "old horses," BS250/BS170, were chosen. Their saturation resistances are 9 Ω and 3.5 Ω with 0.2 A drain current, respectively. The higher resistance value of the P-type FET reflects the poorer conductivity of the P-material. Power dissipation in this case, with TO92 cases, is on the limit at 7 MHz. This forced the decrease of the supply dc level to 10 V.

### Main Switches

The choice was the HEXFET Power MOSFET, IRF510, in a TO-220AB package. The main specifications are:  
 $R_{DS(ON)}$  (at 25°C) = 0.56 Ω with 5.6 A.  
 $V_{(BR)DSS} = \min 100$  V.  
 $C_{iss} / C_{oss} / C_{rss} = 180 / 81 / 15$  pF.

The FET's have been bolted directly to two heat sinks, each 100 × 30 × 3 mm aluminium, with 27 five millimeter holes. The FET is located in one end corner in a 45° angle. The assembly is supported at the FET end by the 2 mm long source lead of the FET and at the other end with a stand-off isolator.

### Normal Operation

In a push pull stage, the switches are ON alternately. When one switch turns on fast, the drain voltage quickly falls to almost null. Low current is needed to discharge the output capacitance to null voltage. The saturation voltage is negligible. After the drain voltage change, the fundamental frequency current starts to flow in half sinusoidal form and reaches its maximum in the middle of the

square wave. The saturation voltage reaches its maximum and simultaneous half sinusoid current and voltage generates the saturation loss  $(i_p \times u_p) / 2$ . The current decays back to null and the switch opens, making the drain voltage to quickly increase again. For power loss of the switch this waveform is ideal because the voltage transition occurs during zero fundamental current. This is the other great advantage of a class D amplifier.

On the opposite side of the 1:1 dc feed transformer, voltage rises to double the supply voltage. The charge and discharge must be done from this doubled value. To charge one output capacitor, power  $P_{c_{out}} = \frac{1}{2} C U^2 f$  is needed. During one RF cycle, both switch outputs are charged once, so as seen from the power supply, double power is needed. Total dissipation in this case is 0.4 W on 3.5 MHz and 0.8 W on 7 MHz. From this it is possible to predict the "idling currents" of the switch pair: 33.5 mA at 3.5 MHz and 67 mA at 7 MHz with the balun transformer disconnected.

### Oscillations Due to Improper Timing

Typical worries of class D amplifiers are transient oscillations on top of the open drain waveform. These oscillations are not spurious oscillations due to instability of the stage. They always exist and require no power as long as they are not loaded on their frequency. They originate from the discharge of different inductance energies during switch over. In low loss surroundings, they form riding decaying sinusoidal voltage. The frequency of this sinusoid is not related to the fundamental frequency, but depends on the resonance of the output capacitances and inductances. They are, however, excited with energy from fundamental frequency voltage transitions.

The first mode of these transient oscillations depends on the switching circuit internal timing:

1) The first type reflects on the internal timing of the driver circuitry. When switch A opens, the inductance between the power supply and drain discharges its magnetic energy to the open drain, causing an opposite polarity voltage spike. This phenomenon is often used in dc/dc converters. If, however, the

opposite switch B comes ON simultaneously, the energy remains in the circuit. The first artifact is visible if the second switch comes ON with delay. A voltage spike is generated before the magnetic field is turned over.

2) A similar problem occurs if both switches are ON simultaneously for a short time. No magnetic field is generated in the 1:1 transformer due to the opposite direction of currents, and a short circuit is generated for the power supply.

Type 1 and 2 problems can be avoided by proper adjustment of the output pulse length with  $V_{TH}$  and the right spacing of pulses with delay the trimmer capacitor.

The second mode is generated from the leakage inductance of the transformer. It always exists in every transformer, and is only to be minimized by transformer construction.

See Figure 4. To these small inductances ( $L_h$ ) the polarity reversal in the main transformer function is of no help. The inductive effect forms an overshoot after the rising edge, continuing then with a decaying sinusoidal waveform. With low damping, the first swing can have a considerable amplitude.

### Oscillations Due to Switching Reactive Loads

The main, and most serious, transient generation is dependent on a reactive load of the main switches. This happens by tuning an otherwise resistive antenna load to the reactive sides. Phase shift between voltage and current creates an abrupt current switch off, with strong oscillations on the OFF-switch drain. It is obvious that maximum voltage spikes are generated with certain "optimized" detuning. Further detuning decreases the switch current, making oscillation generation smaller again.

Measurements on 7 MHz with a 12.6 V supply voltage showed 72 V peak maximum on the oscilloscope and 64 V dc from measurement point  $V_i$ , by detuning from the resistive current of 3.0 A to a detuned current of 0.6 A. The output power was 25 W down to 4 W. This was the highest peak value achieved with 12.6 V. In this prototype, maximum drain voltage peak is around six times the supply voltage used. A break down value of 100 V

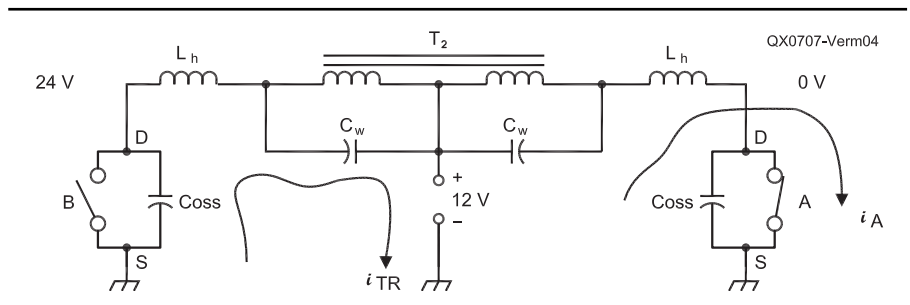


Figure 4 — Components for unloaded output switcher.  $L_h$  represents leakage inductances and  $C_w$  represents winding capacitances of 1:1 transformer, T2.

is therefore reached with a 16.7 V supply level. Below this supply voltage no additional protection is needed.

Peak rectification of the first highest very short transient peak, around 90 V, is difficult and causes loss of about 8 V between the real oscilloscope value and rectified  $V_r$  dc.

### Fighting Against Transient Oscillations

These transient sinusoidal oscillations actually cause no harm except in the case of detuning, when voltage breakdown in the switches is possible. This limits the possibilities of increasing the supply voltage for a higher RF power output.

The traditional cure is a Zener in parallel with the FET output. Measurements indicated that the type I used had excessive capacitance and seemed to be slow in action. The second idea was first to peak rectify both drain waveforms and then use a common Zener diode as a dc load. Even this did not work well. It seems obvious that the spike generation is of very low impedance and is a powerful mechanism. Hence, the countermeasures should be low impedance accordingly. It may, however, be better to accept that these phenomena belong to this type of circuitry and we must live with them.

My new idea is to reduce the RF power switch supply voltage according to the rectified spike voltage by automatic feedback. The worst spikes are generated during the detuning conditions, and with a properly tuned resistive load no countermeasures are needed. For the voltage control we already have the amplitude modulator for the CW keying formation. This feature can be added with a few extra components. With a Z marked Zener of 45 V, spikes are limited to 60 V (12.6 V supply), which is unnecessarily low. See the Zener calculation info at the end of this article. This protection cannot be very fast, due to the amplitude-modulator wave shaping for CW — several milliseconds. It works well, however, with manual detuning.

The drain waveform spikes are peak rectified to a common load resistor. The voltage on this resistor, marked as  $V_r$ , is also a good

tuning indicator. Tuning this voltage towards the minimum tells of minimum ripple on top of the square waveform on the drains, meaning a resistive load. It can be used as a load phase zero indicator during tuning. The rectified peak voltage measured with a high input resistance VOM is within a few volts of the real voltage spike around the resonance condition, and can be used for real observation of the approaching dangerous voltage level, taking into consideration a peak rectification loss of around 8 V. In the battle of oscillations no IRF510 has been lost.

The DDS LCD panel has an additional feature; a bar voltmeter with full scale sensitivity of 240 mV. This was originally used for output RF voltage measurement. I found, however, that it gave no additional information compared to the  $I_{dc}$  meter. Now it is used as a  $V_r$  meter. The  $V_r$  voltage is never below two times supply voltage, so for the LCD meter, the first 24 V is eaten out with a Zener diode, increasing the sensitivity for easier tuning.

For continuous output power adjustment with the amplitude modulator, a potentiometer has been added. This feature is useful for checking the transmitter in use, and during tune up of a new unknown antenna the first time.

With the presented safety arrangements, higher than 12 V supply voltage is now possible. Because the saturation power loss is dependent only on switch current, keeping this value constant by loading change increasing supply voltage leads linearly to higher output RF power. Dissipation power due to charging of the output capacitances follows the square of the voltage, but still remains in an acceptable proportion.

### Switch Stage Output Circuit

Due to the 1:1 transformer it is possible to take RF out from either of the switches. I measured the output as slightly asymmetrical, and this was the reason for the balanced/unbalanced transformer shown in Figure 5. Line impedance between points 1 to 3 and 2 to 4 should be equal to the load, around 6  $\Omega$ . Instead of the two-wire winding I used,

a four-wire method described below leads closer to this desired value. The two-wire version presents some extra inductance for a series tuned circuit, which can be counter tuned out by changing  $C_1$ .

The one switch RF load can be as low as 2.5  $\Omega$ , so a low dc resistance of the 1:1 transformer is important. This transformer consists of four copper wires wound together. Twelve turns of this combination is wound as a solenoid on the outer surface of U17 Siemens ferrite tube ( $D = 6$  mm,  $L = 15$  mm, color code grey). Two wires are connected in parallel to form a winding. Measurement indicated by increasing output power that the tilt on the top of the square wave becomes stronger. Normally this tilt is indicating too small a main inductance in the 1:1 transformer, but here, surprisingly, it works the other way around.

### Power Calculation in Lossy Surroundings

Table 2 shows calculation results including the influence of the saturation resistance. For the main switches, the supply voltage of 12.6 V is lowered to 12.0 V due to the loss in the fuse, the ammeter shunt resistor and saturation resistance of the amplitude modulator FET. Indicated output powers must also be lowered by the output capacitance charging dissipation of 0.4 W or 0.8 W.

Values are presented according to the different dc values. Any value can be chosen by tuning the loading capacitor  $C_2$  and slight retuning back to the resonance by  $C_1$ .

Results have been calculated with two decimals and presented here by rounding to one decimal accuracy.

### LC Tuned Matching Circuit

With the tuned circuit shown in Figure 6, the antenna impedance seen by the transmitter is matched to the desired switch load resistance. The circuit consists of a series inductance,  $L$ , and series capacitor  $C_1$  plus the output capacitor  $C_2$  in parallel with the load.  $C_1$  is the tuning and  $C_2$  the loading capacitor.

Value calculations are as follows:

Choose loaded  $Q$ . Normally 10.

$$X_{C1} = Q_L \times R_1$$

$$X_{C2} = R_L \times \sqrt{(R_1 / (R_L - R_1))}$$

$$X_L = X_{C1} + (R_1 \times R_L) / X_{C2}$$

The matching reactances should be calculated with the minimum useful  $R_1$ , so

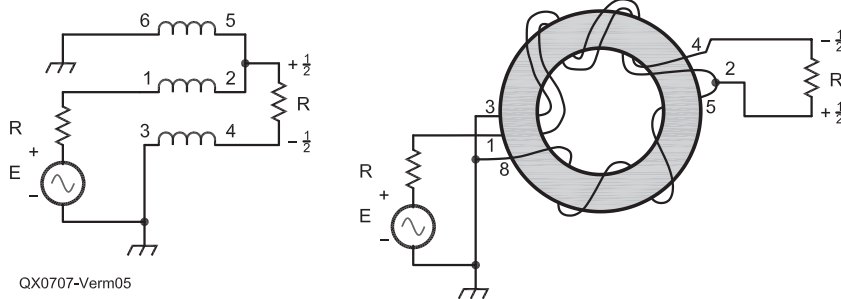


Figure 5 — Asymmetrical/symmetrical transformer. Ten turns of doubled 0.6 mm copper wire twisted together plus 10 turns of a single 0.6 mm copper wire wound on 4C4 or 4C6 toroid. The outer diameter of this toroid is 14 mm.

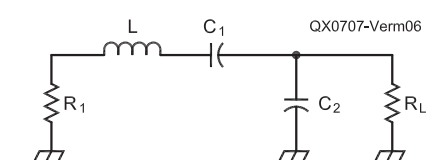


Figure 6 — Tuned matching circuit with component numbering.



with increasing  $R_1$ ,  $Q_L$  goes down.

Calculation has been done with the following values:

$I_{dc} = 3.0 \text{ A}$   
 $R_L = 50 \Omega$   
 $R_1 = 5.4 \Omega$   
 $Q = 10$ . (30 W output)  
 $X_{C1} = 54 \Omega$   
 $X_{C2} = 17.4 \Omega$   
 $X_L = 69.5 \Omega$

3.5 MHz:

$C_1 = 834 \text{ pF}$   
 $C_2 = 2590 \text{ pF}$   
 $L = 3.1 \mu\text{H}$

7 MHz

$C_1 = 417 \text{ pF}$   
 $C_2 = 1295 \text{ pF}$   
 $L = 1.56 \mu\text{H}$

Increasing  $C_2$  increases the loading and  $I_{dc}$ .

The signal going through the matching circuit has some attenuation.

Tank circuit efficiency =  $(1 - Q_L / Q_0) \times 100\%$  (See Note 7.)

Tank circuit efficiency =  $(1 - 10/150) \times 100\% = 93\%$

The first form of the coil was a traditional single solenoid with tapping for 40 m. On 40 m the short-circuited part of the total coil

became hot, meaning unnecessary losses. The second version has two separate solenoids at a  $90^\circ$  angle to each other, minimizing coupling between the coils. Now 40 m operation is cool with no extra loss. The first version might burn relay contacts because of the high short-circuit current.

For information about calculating coil turns see *The ARRL Handbook*, 2007 edition, page 4.32.

### Amplitude Modulator

A digital power amplifier can be switched on and off very fast. However, that creates strong sidebands, known as key clicks. CW

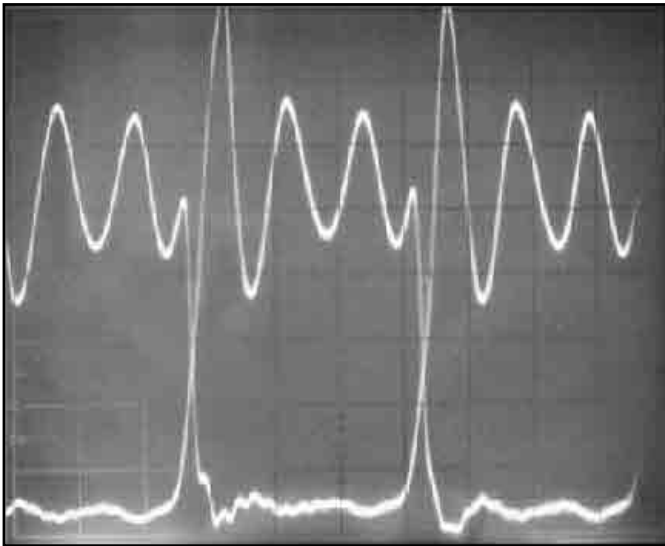


Figure 7 — Unloaded drain waveforms on 7 MHz seen with dual trace oscilloscope; 5 V/division, 20 ns/division.



Figure 8 — This oscilloscope screen shows the same waveforms as Figure 7 but on 3.54 MHz; 5 V/division, 50 ns/division.

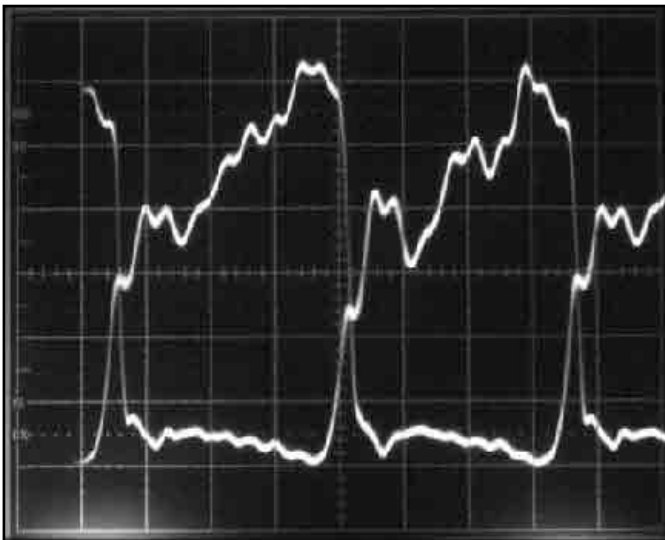


Figure 9 — Drain waveforms in normal operating condition on 7 MHz with  $I_{dc} = 2.0 \text{ A}$ ; 5 V/division, 20 ns/division.

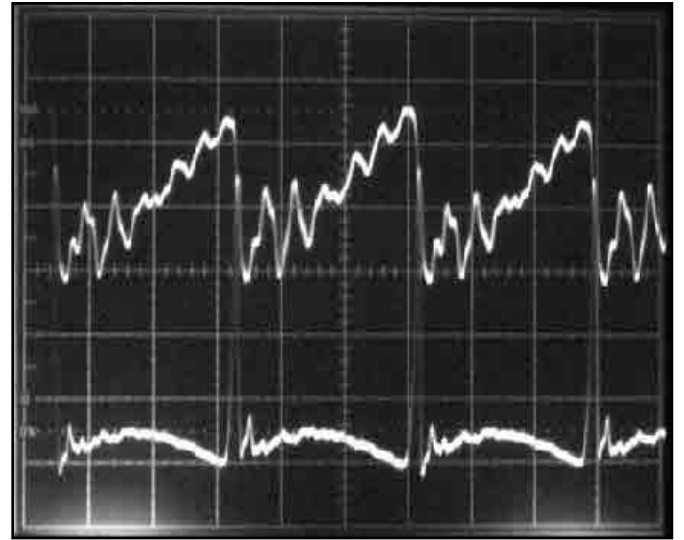


Figure 10 — This screen shows the same waveforms as Figure 9 but on 3.5 MHz with  $I_{dc} = 3.0 \text{ A}$ ; 5 V/division, 50 ns/division.

rise and fall times should be rounded to several milliseconds. The main RF switches need full drive all the time for proper efficiency, so that rounding must be done in the supply voltage by the amplitude modulator. This is done with a P-FET, IRF9Z34N in a TO-220AB case, by rounding its gate drive with an RC network. The source is connected to the supply voltage and the drain feeds the RF switches. By connecting the gate to ground, the P-FET opens and the saturation voltage of 0.4 V with 5 A remains over source to drain. Continuous output power adjustment is realized through a diode clamp from the sliding contact of the potentiometer between the supply and zero voltage (which occurs at full power). When the CW key is up, the gate drive should rise to the source voltage of 12.6 V, or if being operated from the ac mains, even higher. The keying logic works with 10 V, so a buffer with open drain must be added.

The transient high peak voltage feedback protection consists of diode rectifiers from both switch drains. This rectified peak voltage is used from front panel as  $V_r$  output and via Zener diode to raise the amplitude modulator gate towards the supply voltage. By increasing the gate potential, the FET becomes more resistive, eating part of the RF switch supply voltage.

The closing time for the antenna relay is measured from the time the coil voltage was applied to the time when the contact closes. The relay used needed 7.5 ms for this. The output power should not come on before this delay. Two gates of the CMOS-IC CD4093BCN form a 10 ms delay circuit driving the open-drain keying buffer.

One gate and diode 1N4148 form a re-

lease delay circuit, driving the gate of the FET buffer through phase reversal. An inductive spike on the relay coil is limited with a diode. With a 100 k $\Omega$  potentiometer it is possible to choose the antenna relay opening delay to suit your preferences.

### Commissioning of Class D Power Stage

Fundamental adjustments are easiest to make by disconnecting the RF load wires from the balun transformer to the switch drains. Now it is possible to see overshoot due to leakage inductances and possible transients originating

from the improper internal timing. Charging of switch output capacitors should cause 34 mA of "idling current" on 3.5 MHz and 67 mA on 7 MHz. Connect a more sensitive ammeter (100 mA full scale) to the amplitude modulator feed. Turn the output power potentiometer to max output, key down, and adjust the currents with the  $V_{th}$  potentiometers, first for 40 m and then for 80 m. With the RF drive levels on the 2N3904 emitter set to 3.80  $V_{pp}$  on 40 m and 4.75  $V_{pp}$  on 80 m, the  $V_{th}$  values were 4.53 V and 4.15 V respectively.

Connect a VOM to the  $V_r$  output and

**Table 2**  
**Power Calculation**

$I_{dc} / A$	1.7	2.0	2.4	2.8	3.0	3.2	3.0
$i_p / A$	2.7	3.1	3.8	4.4	4.7	5.0	4.7
$U_{dc} / V$	12.0	12.0	12.0	12.0	12.0	12.0	23.5
$u_{p0} / V$	15.3	15.3	15.3	15.3	15.3	15.3	29.9
$U_{sat\ 25C} / V$	1.2	1.4	1.6	1.9	2.0	2.2	2.0
$U_{sat\ 60C} / V$	1.5	1.7	2.0	2.4	2.6	2.7	2.6
$u_{pL} / V$	13.8	13.6	13.2	12.9	12.7	12.6	27.3
$P_{RF} / W$	18.5	21.3	25.0	28.4	30.0	31.6	64.2
$P_{dc} / W$	20.2	24.0	28.8	33.6	36.0	38.4	70.5
$n / \%$	90.5	88.8	86.7	84.4	83.3	82.2	91.1
$P_{diss- / 2 \times FET} / W$	1.9	2.7	3.8	5.2	6.1	6.9	6.1
$R_L / one\ sw. / \Omega$	5.2	4.3	3.5	2.9	2.7	2.5	5.8
$R_{L\ DD} / \Omega$	10.4	8.6	7.0	5.9	5.4	5.0	11.6

#### Formulas Used:

$$i_p = I_{dc} / 0.637$$

$$U_{sat\ 25C} : i_p = 2 \text{ to } 5\ A, U_g = 10\ V; R_{sat} = 0.433\ \Omega$$

$$u_{pL} = u_{p0} - U_{sat\ 60C}$$

$$P_{RF} = (i_p * u_{pL}) / 2$$

$$P_{dissipation / 2 \times FET} = (U_{sat\ 60C} \times i_p) / 2$$

$$R_L / one\ switch = u_{pL} / i_p$$

$$u_{p0} = U_{dc} \times 1.273$$

$$U_{sat\ 60C} = U_{sat\ 25C} \times 1.25$$

$$P_{dc} = U_{dc} \times I_{dc} \quad n = P_{RF} / P_{dc}$$

and per FET, 1/2 of previous

$$R_{L\ DD} = 2 \times R_L / one\ switch$$



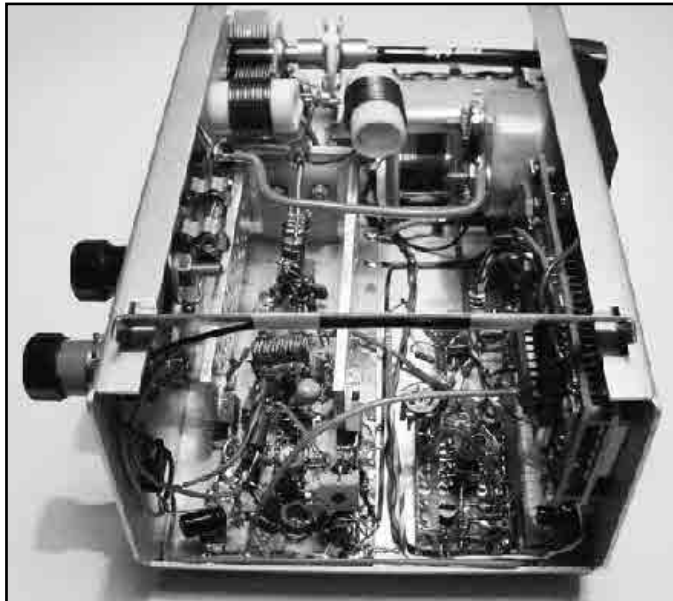
Figure 11 — Single drain waveform on 7 MHz with detuning; 10 V/division, 20 ns/division.



Figure 12 — This photo shows the prototype transmitter with the various sub units. To the left is the DDS module with LCD panel. At the top is the amplitude modulator, power control and keying circuitry. At the center of the photo is the RF unit with oversized heat sink and matching circuit components.



**Figure 13** — This photo shows the front panel view of the transmitter, assembled in the box. From left to right/top to bottom:  $V_r$  +,  $V_r$  -, Key, DDS LCD Panel, DDS Frequency Tuning, Tune Switch, 5 A dc Meter, Output Power Adjustment, Band Switch 80/40 m, PA Tune, PA Loading.



**Figure 14** — (right) Here is the completed transmitter, as the modules are mounted in the box.

minimize the reading to between 30 and 40 V with the delay trimmer capacitor. Check that the trimmer is not at minimum. If so it must be moved to the opposite side of the drive chain.

Figure 7 shows both drain waveforms simultaneously optimized on 7 MHz, as seen with a double trace Tek 475 oscilloscope via 10 to 1 high Z probes. The maximum length of the ground lead for the probe is 0.5 cm! Observe the excellent symmetry and surprisingly high overshoot on 7 MHz. Symmetry is reached with the delay trimmer also showing a simultaneous minimum in  $V_r$ . The overshoot increases with higher  $V_{th}$ , so measured current is the only useful criteria here. The time period of the overshoot oscillation is 24 ns, meaning a frequency of 41.6 MHz. The slow decay of the damped wave tells of a very low loss circuit. The 1:1 transformer uses high frequency U17 ferrite, with a recommended frequency range of 10 to 220 MHz,  $\mu_i = 10$ . Using higher  $\mu$  material may add losses on 40 MHz without causing much difference on 7 MHz.

Figure 8 is similar to the Figure 7 open load situation on 3.54 MHz. Overshoot is much smaller. With  $V_{th} = 4.15$  V “idling current” is only 17.4 mA.

Remove the more sensitive current meter that you added earlier. Connect the balun transformer to the drains again. Connect a dummy load and use the 7 MHz band.

Start to turn the output power potentiometer from minimum power = 12 V. At the 9 V level, current starts to flow in the amplitude modulator FET. As the voltage decreases from 9 to 7 V, the FET channel opens and gives close to full supply voltage to the RF switches. Rest 7 V towards null only decreases saturation resistance.

Tune  $C_1$  and  $C_2$  to maximum direct current and minimum  $V_r$  with a partial output power. Turn the power control to maximum

and adjust the load capacitor,  $C_2$  to 2.0 A dc, maximizing with  $C_1$ . Recheck the delay trimmer to minimum  $V_r$ . It should already be optimized.

Check with this output power, tuning  $V_{th}$  to minimum  $V_r$ . In opposition to the idle condition,  $V_{th}$  now influences the overshoot size, and a clear minimum can be found. The best minimum depends on the resistive load condition, so some adjustment between these controls is needed.

Figure 9 shows the drain waveforms on 7 MHz in the above 2.0 A loading condition. Overshoots have been minimized. The tilting of square wave top that I mentioned earlier is very obvious here. Because of this tilting, the typical optimum tuning  $V_r$  on 7 MHz with 3 A dc loading is 31 V.

Figure 10 is the measurement on 3.5 MHz with 3.0 A loading. The maximum saturation voltage peak is clearly visible at the middle of the square.

Figure 11 is measured on 7 MHz from one drain only. The normal condition with 2.0 A loading has been detuned by decreasing the  $C_1$  current to 1.65 A. Note the different scale factor compared to previous figures, now 10 V / division. The worst peak is 53 V on the scope and 51 V as measured at the  $V_r$  output. The oscillation frequency is very close to the one in the no load condition of Figure 7. This photo was taken in an early phase of testing, as an example of the phenomena and does not represent the worst case.

Measured output powers have been in accordance with the calculated values within the accuracy of RF power measurement methods, and the accuracy of the oscilloscope and power meter. This makes me feel that the project was a success.

### Increasing Supply Voltage

As indicated earlier, the supply level up to 16.7 V needs no special protection. The prototype has been tested with a 24 V supply without problems. To protect the Amplitude modulator FET source-to-gate breakdown of 20 V, an 18 V Zener diode has been added between the source and the junction of the 220  $\Omega$  resistor and 0.47  $\mu$ F capacitor. Increasing the supply level leads to increasing gate voltage to keep the source-gate voltage difference constant at 5 V for closing the FET switch. The value of the series Zener diode marked “Z” can be calculated as follows: Starting from the switch FET drain real peak of 95 V, after peak rectification the dc is 87 V. With a 25 V supply, the gate voltage required for closing the switch is 25 V - 5 V = 20 V. The series clamp diode needs 0.5 V, so the required Zener rating is 87 V - 0.5 V - 20 V = 66.5 V. To have some safety margin, a Zener value of 64 V is recommended. Two 32 V Zeners in series will satisfy this requirement.

The measured output power with a 24.0 V supply was 58 W. The power calculation is included in Table 2 as the last column on the right.

At resonance,  $V_r = 52.4$  V and  $I_{dc} = 3.0$  A. Oversized heat sinks are beneficial, although saturation loss is kept constant by changing loading back to 3 A. Switch output C charging loss is now four times previous 0.8 W. At 7 MHz it is 3.2 W.  $R_{L,DD}$  has been doubled, so  $Q_L$  is no longer equal to 10, changing the tank circuit efficiency figure.

Trying to push the limits with a 24 V supply gave an output of 66 W on 7 MHz, with an  $I_{dc}$  of 4.0 A and a  $V_r$  of 59 V. This is quite

a nice figure with RF power FETs costing less than \$2 US each.

### Mechanical Design

This prototype transmitter was constructed in different sub units making continuous improvement possible. Open layout improved access to measure different waveforms with scope probes. Sub units as in Figure 12 are: left, DDS with LCD panel; top, amplitude modulator, power control, keying circuitry; middle, RF unit with oversized heat sinks and matching circuit components. No printed circuit board was used. ICs were soldered up side down on copper-clad board. Source lead length of RF switch transistors must be kept to a minimum.

After finishing measurements, the sub

units have been installed in a prefabricated box, as shown in Figure 13. The box size is 18 cm wide × 7.5 cm high × 11 cm deep.

### Summary

Using this class D switcher amplifier, 30 W output can be reached with 12.6 V battery voltage, and around 60 W with a 24 V supply. See Note 5.

The circuit is simple, cost effective and after the initial timing optimization, it is easy to use. No tendency towards self oscillation has been seen even with selective resonant antenna loads. DDS works well, giving accurate frequency according to its numeric panel reading, with fine tuning possibilities.

### Notes

<sup>1</sup>M. R. Osborne, "Design of tuned transistor power amplifiers," *Electronic Engineering*, Aug 1968, pp 436-443.

<sup>2</sup>H. O. Granberg, "Applying Power MOSFETs in Class D/E Power Amplifier Design," *RF Design*, June 1985, or *Motorola RF Device Data 7-296*, or *Application Note AR141*.

<sup>3</sup>R. Lewallen, W7EL, "On Solid-State PA Matching Networks", *QST*, Technical Correspondence, Oct 1978, p 34.

<sup>4</sup>Eileen Lau, KE6VWU, et al, "High-Efficiency Class-E Power Amplifiers, Part 1 and 2," *QST* May/June 1977, pp 39-42/39-42.

<sup>5</sup>Doug DeMaw, W1FB, "Power-FET Switches as RF Amplifiers" *QST*, Apr 1989, pp 30-33.

<sup>6</sup>You can find more information about the Juma kits at the "Ham Shop" of SRAL, the Finnish Amateur Radio League. Go to [www.nikkemedia.fi/jumatax1/](http://www.nikkemedia.fi/jumatax1/) and select "Buy Juma Kits." At press time, the DDS board is part of the RX-1 and TX-1 kits. It is expected to be available soon as a separate kit.

<sup>7</sup>F. E. Terman, *Electronic and Radio Engineering*, McGraw-Hill, 1955, p 458.



*Experience Autumn in New England  
at the 2007 TAPR/ARRL Digital  
Communications Conference*

September 28-30 in Hartford, Connecticut

- Technical Sessions
- New Products and Demonstrations
- Educational Forums
- Good Food and Good Friends
- Easy Access from Bradley International Airport

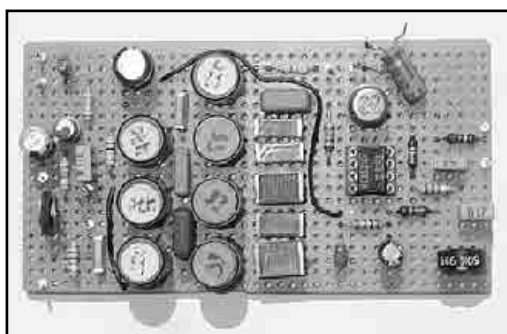
See the Digital Communications Conference site on the Web at [www.tapr.org/dcc/](http://www.tapr.org/dcc/)  
or call TAPR at 972-671-8277 to make your reservations today.



# High-Performance Audio Speech Low-Pass and CW Band-Pass Filters in SVL Design

*QRM? QRN? A good filter will shape your receiver's audio response, helping you pull in the weak signals and limiting your transmission bandwidth.*

**Werner Rahe, DC8NR**



Although competing filter technologies are replacing LC filters in many applications, passive filters still offer the best relation between performance and complexity. In this article a wide variety of audio LC filters with different complexity is shown. The filter construction is easy and inexpensive because commercially available inductors are used.

In the audio range only fixed inductors with sufficient Q are available. To simplify the filter construction, the components were computed so only standard-value inductors (SVL) are required. The normally nonstandard capacitors can be realized paralleling two or more values. All filters are standardized to the same impedance level.

## Choice of the Filter Type

With modern network synthesis, many different filter types having special response characteristics became available.<sup>1</sup> Each has

<sup>1</sup>Notes appear on page 38.

Conrad-Schulz-Weg 5  
D-82211 Herrsching am Ammersee  
Germany

its own performance, disadvantages and advantages, optimized to special goals.

Of main interest in Amateur Radio filtering applications are the more selective Chebyshev and elliptic filter approximations. Their transmission functions provide a more abrupt transition from pass-band to the stop-band than Bessel or Butterworth filters would. These filters are so-called equiripple filters. That means the amplitude response shows a uniform ripple in the passband, the stopband

or in both. The differences are illustrated in Table 1. There is more information in Note 2. The group delay of these filters is very

nonlinear and therefore it causes the signal to ring when voltage transitions occur.

Generally, filters that produce faster roll offs in the transition band exhibit poorer phase response and group delay characteristics. The reference in Note 3 gives a comparative analysis. For amateur applications, this is normally only a problem if high-order band-pass filters with small relative bandwidths are used. It can also be harmful in video or digital communication systems.

It is important to note that many designers avoid Chebyshev I transfer functions in favor of Cauer elliptic alternatives, because pole Qs are higher than with elliptic functions, causing a long settling time and considerable ringing in the step response.

**Table 1**  
**Standard Approximations with Ripple Characteristics**

<i>Approximation</i>	<i>Characteristics</i>
Chebyshev I	Equiripple in pass-band, high out-of-band rejection increasing monotonically, rippled group delay near center of band, very large group delay variation near band edges
Chebyshev II (Inverse Chebyshev)	Maximally flat in passband, sharper roll-off than Butterworth filters, equiripple in stopband, moderate group delay similar to Butterworth
Cauer (Elliptic)	Equiripple in pass-band, abrupt transition from passband into stopband, equiripple in stopband, large group delay variations

**Table 2**

**Values listed are valid for a BPF with following specifications:**  
**f<sub>0</sub> = 750 Hz, BW = 500 Hz, SF = 2.4**

<i>Approximation</i>	<i>Necessary Filter Order</i>	<i>Ripple (dB)</i>	<i>Max. Pole-Qs</i>
Butterworth	9	0	7.8
Chebyshev I	6	0.2	16
Chebyshev II	6	0	6

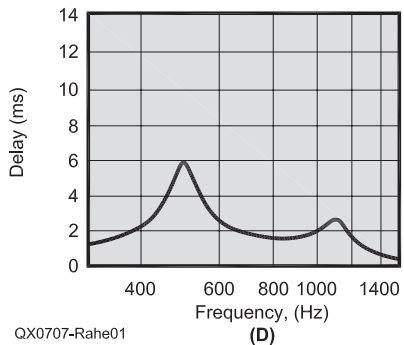
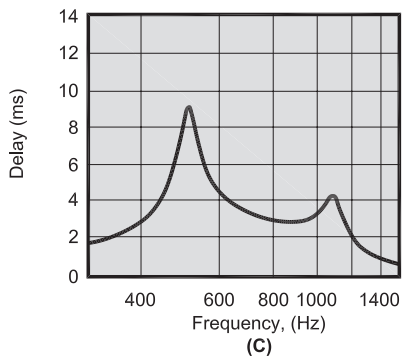
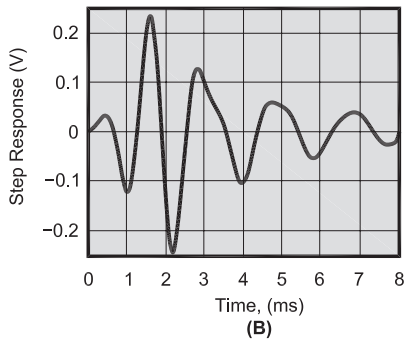
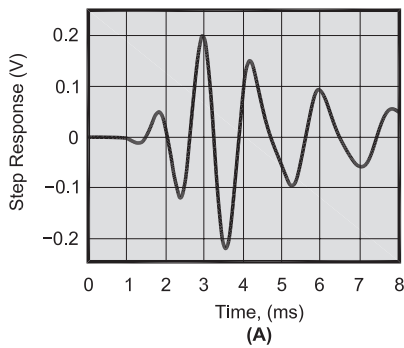


**Figure 1 — Part A shows a Butterworth BPF response;  $f_c = 750$  Hz,  $BW_{-3\text{ dB}} = 500$  Hz,  $SF_{-50/-3\text{ dB}} = 2.4$ ,  $N = 9$  (Step Response). Part B shows the response of an inverse Chebyshev BPF;  $BW_{-3\text{ dB}} = 500$  Hz,  $SF_{-50/-3\text{ dB}} = 2.4$ ,  $N = 6$  (Step Response). Part C shows the response of a Butterworth BPF (Group Delay). Part D shows the response of an inverse Chebyshev BPF (Group Delay).**

At the expense of some poorer roll off in the transition band than Cauer filters, an Inverse Chebyshev design is the best choice for CW band-pass filters, because it has the lowest section Q of all ripple filters. Until today this filter type is widely unknown to the ham community. This type has pole Qs for a given shape factor,  $BW_{as} / BW_p$ , still lower than a Butterworth design.

Differences in the step response and group delay are shown in Figure 1. Despite the fact that Chebyshev I filters are easier to design, the choice of the filter type was therefore restricted to the more complex Chebyshev II and Cauer filters.

### Filter Specifications and Use of the Tables

Filter specifications for the filters listed later on these pages define a cutoff or corner frequency as the frequency or bandwidth where the attenuation in the passband reaches  $-3\text{ dB}$ .

Chebyshev I and elliptic filters have a certain amount of amplitude variation in the passband, the so-called ripple,  $a_p$ . For these filter types, the cutoff frequency is known as the ripple frequency response,  $f_{ap}$ .  $BW_{ap}$ , the point where the response curve last passes through the maximum allowed passband ripple. In general, real filters provide passband ripples far below 3 dB. Hence for low-pass and band-pass filters  $BW_{ap}$  is always smaller than  $BW_{-3\text{ dB}}$ .

$BW_{as}$  is the bandwidth, when the amplitude response reaches the predetermined minimum attenuation limit  $a_s$ , the so-called stopband floor.

The passband ripple is related to the return

loss attenuation  $a_r$ , which is a measure of how well the filter is matched in the passband. High passband ripples create a steeper roll off in the transition band, but this advantage comes at the penalty of a poorer return loss attenuation.

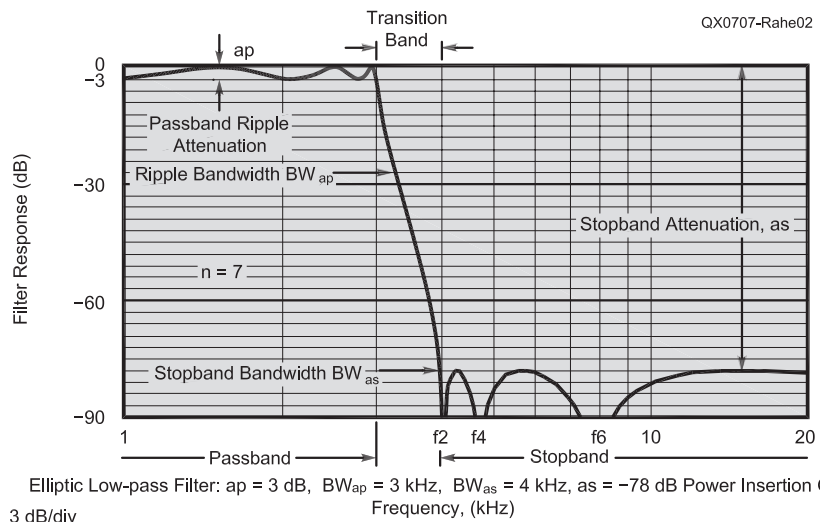
There should be a limit also for filters in the audio range at a passband ripple of preferably less than 0.5 dB, which is equivalent to an  $a_r$  of  $-9.54$  dB, a SWR of 2 or a reflection coefficient of 33.3%. The mathematical relationship can be found in the reference given at Note 4. At higher passband ripples the designs will become also more sensitive to component and impedance variations.

Filter specifications must also include a shape factor SF, which describes how fast signals roll off during attenuation. The shape factor SF is usually defined as the  $-60/-6$  dB bandwidth ratio. For the band-pass filters, the stopband ratio (SBR),  $BW_{as}/BW_{-3\text{ dB}}$ , is given additionally.

To make comparisons of the different filters more direct and to avoid a lot of diagrams the  $-3 / -6$  dB and  $-40$  dB /  $-60$  dB / ( $-80$  dB) frequencies are given in the tables. All reactance filters must be terminated with the proper values to reach the desired response.

### Filter Design and Software Solutions

To design standard value inductor filters, some restrictions are necessary. It must be noted that you are no longer free to determine bandwidth, passband ripple and stopband attenuation separately, because all these parameters are mathematically related to each other for a given filter degree. Hence, the design of an SVL filter is not a trivial task and it appears like a puzzle with only one solution.



Elliptic Low-pass Filter:  $a_p = 3$  dB,  $BW_{ap} = 3$  kHz,  $BW_{as} = 4$  kHz,  $a_s = -78$  dB Power Insertion Gain 3 dB/div

**Figure 2 — Ripple Filter Characteristics.**

The customary procedure for calculating the component values before the era of fast, cheap computer computation was to refer to one of the published tables of normalized element values for a suitable low-pass configuration.<sup>5</sup> These tables, and algorithms that are directly used today, supply order-based coefficients for a normalized low-pass filter.<sup>6</sup>

Unfortunately the tables are based on a limited number of ripple values — respectively reflection coefficients — which restricts the design selection and makes it difficult to get standard inductor values. Nevertheless, in some cases these tables can give you valuable information. For example, the stopband attenuation at which you can expect approximately standard inductor values by comparing the normalized filter coefficients.

A band-pass design may be directly obtained from the low-pass prototype by a frequency translation. But this method is very time consuming. It is easy to make calculation errors and after the design is completed, the inductor values will probably be non-standard. Hence, an appropriate computer program is a tremendous help to compute the component values.

Apart from the big and expensive analysis programs like Microwave Office (AWR), which have implemented a filter synthesis

wizard or special commercial filter programs, there are only a few freeware filter programs that can compute elliptical transfer functions.

From the DOS-era comes the *Filter Designer (FDS)* by Bob Lombardi. Unfortunately this program is not very user friendly, and it has no graphical output. The design of elliptical band-pass filters is not possible.

The *Filter Designer* developed by Neil Heckt (AADE) is very recommendable and in version 4.05, it is now free.<sup>7</sup> If you try to develop a standard value inductor filter, though, you will give up very soon, because all filter parameters must be entered new after each trial. (There are some minor bugs in calculating elliptic filters.)

In my opinion, *ELSIE* by WB6BLD (Trinity Software) is perhaps the best and most versatile one at low cost, and it exists now in a superb *Windows* version 2.10. The free student version is restricted to 7th order filters maximum, which is adequate for most purposes.

None of these programs are able to compute true Chebyshev II filters, nor do they allow the user the option of selecting the -3 dB bandwidth. Instead,  $BW_{ap}$  is used as a reference for the filter cutoff frequency. *ELSIE* cannot convert an elliptic band-pass filter in Pi-configuration to the dual T circuit, which

is often the better solution especially in the audio range (lower inductor values, lower parasitics and a better stopband attenuation in real circuits). See Note 3.

So, you can count yourself lucky if you have the opportunity to use a sophisticated commercial filter program. A very fine, but rather expensive program is *Filter Solutions* by Nuhertz Technology (APLAC). The trial version *Filter Free 4.0* is very restricted and nearly worthless (3rd order filters only).

I have not tested *FILPRO* developed by the Middle East Technical University of Ankara or the very mighty programs *PCFILT* and *S/FILSYN* by ALK Engineering.

### Simple Speech and CW Filters

For most applications, simple low-pass and band-pass filters are completely adequate either to reduce the bandwidth, improving the signal-to-noise ratio, or to suppress harmonics. Already low order filters show a good performance if the demands on out-of-band attenuation are not too strict.

Figure 3 shows some SVL designs, which are easy to implement in an unselective AF chain of your receiver or transmitter. These filters are easier to build and have a much better performance than the usually favored active RC filters. Standard values for the coils had been reached within <<1% tolerance.

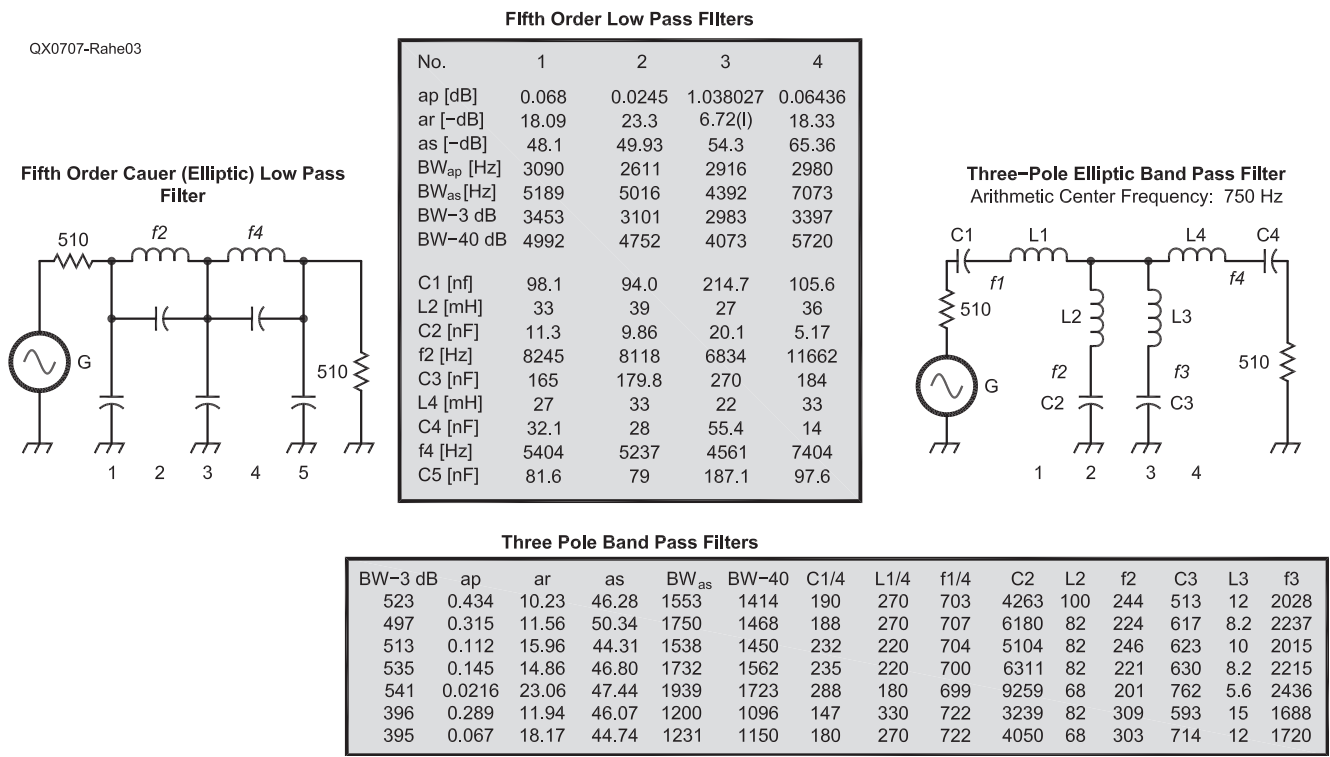
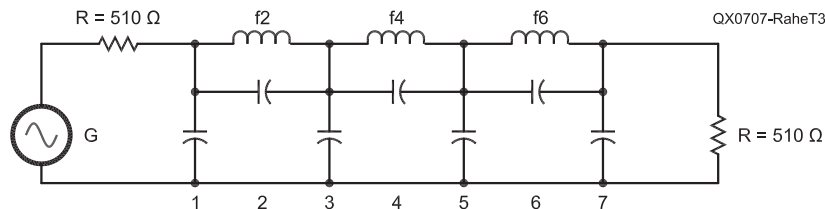


Figure 3 — Simple speech low-pass and CW band-pass filters are shown. Maximum Passband Ripple =  $a_p$ , Minimum Stopband Attenuation =  $a_s$ , Return Loss Attenuation =  $a_r$ , Passband Ripple Bandwidth (Cutoff Frequency) =  $BW_{ap}$ , and Stopband Bandwidth =  $BW_{as}$ .

**Table 3**  
**Seven-Branch Elliptic Speech Low-pass Filter**



$a_p$  = max Passband Ripple,  $a_s$  = Min Stopband Attenuation,  $a_r$  = Return Loss Attenuation  
 $BW_{ap}$  = Passband Ripple Bandwidth (Cutoff Frequency),  $BW_{as}$  = Stopband Bandwidth,

**Standard-Value Inductor Design**

$BW_{-3dB} \sim 3kHz$ ,  $Z = 510 \Omega$ ,  $SWR$  Limit = 1.55

No.	1	2	3	4	5	6	7	8	9	10
$BW_{ap}$ (Hz)	3067	3748	4637	2891	3931	3215	2796	2687	2933	3141
$a_p$ (dB)	0.028313	0.028313	0.031723	0.001046	0.126245	0.131754	0.020145	0.205461	0.003868	0.043149
$a_r$ (-dB)	21.87	21.87	21.38	36.18	15.43	15.25	23.35	13.35	30.51	20.05
$a_s$ (-dB)	45.56	45.56	47.27	62.21	67.35	68.01	70.36	74.41	87.68	90.82
$BW_{as}$ (Hz)	3684	4502	5630	4920	5508	4529	4476	3987	6590	6344
$BW_{as}/BW_{ap}$	1.2	1.2	1.22	1.7	1.4	1.41	1.6	1.48	2.25	2.02
$BW_{-6dB}$	3274	4002	4924	3544	4145	3408	3105	2834	3534	3485
$BW_{-40dB}$	3653	4465	5563	—	—	—	—	—	—	—
$BW_{-60dB}$	—	—	—	4898	5426	4452	4357	3833	5795	5482
$BW_{-80dB}$	—	—	—	—	—	—	—	—	6452	6145
$SF_{-60/-6dB}$	—	—	—	1.38	1.31	1.31	1.4	1.35	1.64	1.57
C1 (nF)	82.5	67.5	56.1	58.5	92.1	113.8	93.0	152.2	71.6	97.0
L2 (mH)	33	27	22	33	27	33	39	39	36	36
C2 (nF)	16.4	13.4	10.4	7.04	7.63	9.2	7.4	9.71	3.33	3.68
f2 (Hz)	6847	8367	10543	10438	11085	9133	9371	8179	14535	13830
C3 (nF)	133.3	109.1	90.3	142.1	138.2	170.4	174.6	221.8	162.9	176.5
L4 (mH)	22	18	15	33	22	27	36	33	39	36
C4 (nF)	82.6	67.6	51.8	30.4	36.6	44.1	33.8	46.5	14.3	16.7
f4 (Hz)	3735	4564	5710	5022	5606	4610	4566	4062	6742	6486
C5 (nF)	116.3	95.1	79.1	134.9	126.9	156.7	164.5	206.5	158.5	170.7
L6 (mH)	22	18	15	27	22	27	33	33	33	33
C6 (nF)	62.9	51.5	39.2	25.6	26.3	31.6	25.6	32.9	11.3	12.3
f6 (Hz)	4279	5229	6560	6054	6619	5447	5474	4832	8255	7904
C7 (nF)	51.7	42.3	36.5	43.2	76.9	95.4	77.6	132.5	64.3	89.2

**Low-Pass Filter Tables**

If you want to have steeper skirts, you have to decrease the stopband requirements or to increase the filter order. It has been stated that increasing the passband ripple is not a good solution.

Table 3 lists a set of seven-branch Cauer low-pass filters in a coil saving  $\pi$ -configuration (shunt-C input/output) with a -3 dB-bandwidth of around 3 kHz, arranged with increasing stopband attenuation. Thus, you can choose a design that may be the optimum for a particular application.

The designations of the inductor and capacitor listings are associated with the similarly labeled components in the schematic diagram at the top of the table. The first five lines of the table represent the design parameters.

Stefan Niewiadomski wrote an article for *ham radio* magazine in which similar filters

were presented.<sup>8</sup> They have been widely duplicated, especially for audio filtering in high-performance direct-conversion receivers.

Unfortunately, these filters were only a compromise. Probably to simplify the construction, the design has been somewhat strange, because there exists no solution to get three equal inductances in a seven-branch elliptic low-pass filter. As a result, these filters met the specifications with regard to bandwidth and stopband attenuation, but they were very poorly matched in the passband, which led to an increase in insertion loss.

Nevertheless, there exist possibilities to get at least two equal values of the required three inductances, and all meet the goal to hold standard values. The deviation of the calculated inductances to the standard values is <<1%, much better than the 10% tolerance of the fixed inductors available.

Filters 1 to 3 have extremely steep skirts, but they show only a moderate stopband attenuation.

Filter 2 is a scaled version of no. 1, with a greater bandwidth and is well suited for AM reception. Filter 3 has a further extended bandwidth.

Filter 4 is a very good matched low-pass filter with low ripple, along with good out-of-band attenuation. This filter can be scaled as well to a ripple bandwidth,  $BW_{ap}$ , of 3534 Hz ( $BW_{-6dB} = 4304$  Hz), which yields inductor values of 27 / 27 / 22 mH.

Filters 5 to 10 are developed especially for direct-conversion receivers, where high stopband attenuation is of primary interest. Filter 7 uses three different inductor values, one of them nonstandard. But this component value is available and it is also employed in filters 9 and 10.



As you can see, the shape factor, SF (BW<sub>-60</sub> / -6 dB), for these low-pass filters is better than for most eight-pole crystal filters in the HF range. This is only true with high-Q reactances, however.

### Low-Pass/High-Pass Filter

Cascading separate low-pass and high-pass filters with low SWR is one way to realize a band-pass response. Table 4 shows two low-pass designs with a bandwidth of around 1 kHz. These are well suited in combination with an appropriate high-pass filter to build a CW band-pass filter with a center frequency at about 750 Hz.

Only the first filter is a true SVL filter. No other design is possible. Otherwise you have to change the band-pass center frequency considerably. The problem is that the choice of useful component values in this inductance range is severely limited. An appropriate high-pass filter is shown in Figure 4, as design no. 2 of Table 4.

A classical Chebyshev characteristic has been chosen because of its better 60 Hz hum suppression in the stopband. Furthermore, the component values are much better to realize than in the case of elliptic versions. A fifth order filter seemed to be sufficient for this purpose.

**Table 4**  
SVL-Seven-Branch Elliptic Low-Pass Filters for Shaping the High Frequency Skirt of an Audio CW-Band-Pass Filter

Z = 510 Ω BW<sub>-3dB</sub> ~ 1 kHz

No.	1	2
BW <sub>ap</sub> (Hz)	880	942
ap (dB)	0.163871	0.043039
ar (-dB)	14.31	20.06
as (-dB)	71.2	90.75
BW <sub>as</sub> (Hz)	1272	1901
BW <sub>as</sub> / BW <sub>ap</sub>	1.44	2.0
BW <sub>-6 dB</sub> (Hz)	925	1045
BW <sub>-60 dB</sub> (Hz)	1238	1645
BW <sub>-80 dB</sub> (Hz)	—1845	
SF <sub>-6/-60 dB</sub>	1.34	1.57
C1 (nF)	438.7	323.5
L2 (mH)	120	120
C2 (nF)	31.5	12.3
f2 (Hz)	2588	4144
C3 (nF)	648.7	588.2
L4 (mH)	100	120
C4 (nF)	150.9	55.9
f4 (Hz)	1295	1943
C5 (nF)	600.3	568.8
L6 (mH)	100	110
C6 (nF)	107.4	41.05
f6 (Hz)	1536	2368
C7 (nF)	375.5	297.1

High-pass and low-pass filters should be separated with an amplifier stage to decouple the filter stages and to compensate the filter losses. In some cases such a composite filter may be the better choice than a true band-pass filter, and it has a lower number of coils for a given shape factor.

Note that the selectivity is concentrated in the more important high frequency skirt. This makes sense, because every normal BPF has attenuation poles at f = 0 and f = ∞.

As a result, for a given filter order the low frequency skirt is always steeper than the high frequency skirt. This is easier to see if you plot the amplitude response in a linear scale. Figure 5 shows the amplitude response of this excellent band-pass filter, using a logarithmic frequency scale.

### Band-Pass Filters

If you prefer true band-pass filters,

Figure 6 gives you a set of circuits with different characteristics and complexity. Their -3 dB-bandwidth of about 500 Hz is narrow enough to give good selectivity while broad enough for easy tuning. The arithmetic center frequency is fixed at approximately 750 Hz, because most transceivers use this sidetone frequency.

The design of band-pass filters is much more delicate than low-pass filters, if you want standard values for the components. Because all design parameters are dependent on each other, you cannot expect to reach exact standard values for all coils, especially at high order filters with a greater number of inductors.

This makes some compromises necessary with respect to bandwidth and center frequency. In some cases it was necessary to tune the pole frequencies for best return loss attenuation with the help of a computer, because the

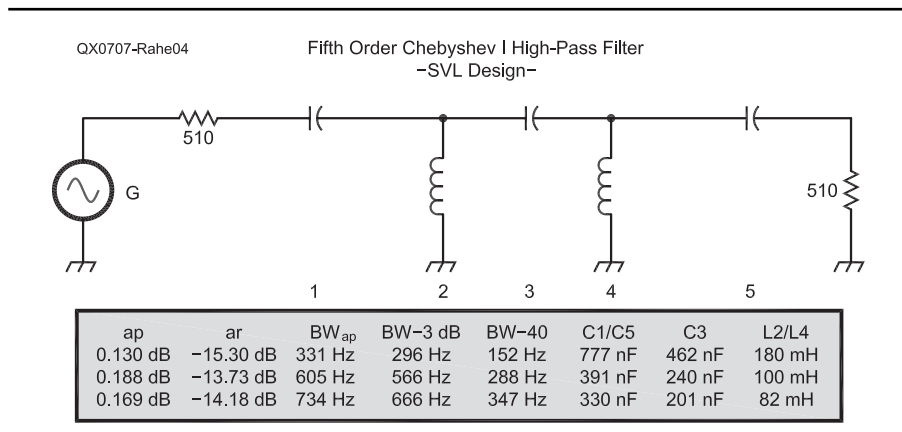


**Figure 4** — A high-pass filter design suitable for cascading with low-pass filters having the same impedance in order to create speech or CW band-pass filters.

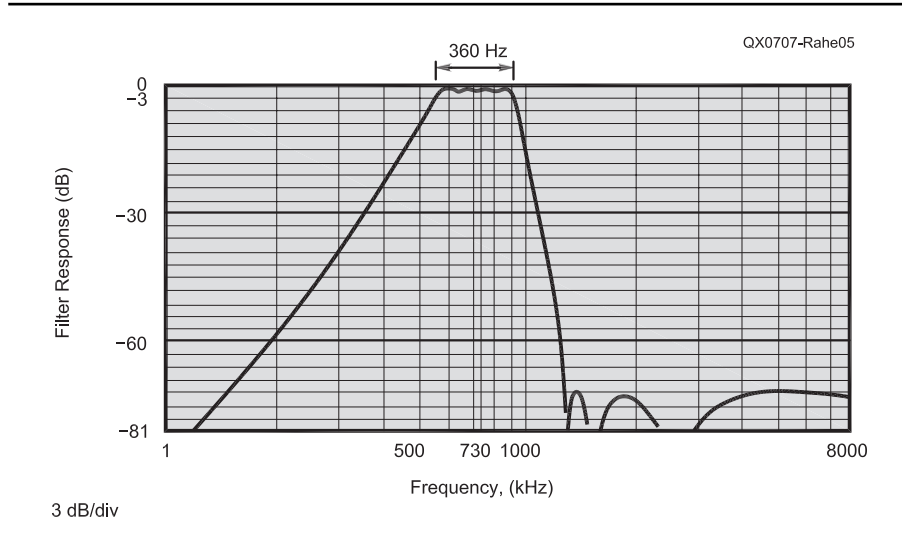


**Figure 5** — Composite BPF realized with a fifth order Chebyshev I high-pass and a seventh order elliptic low-pass filter (f<sub>c</sub> ~ 730 Hz, BW<sub>-3 dB</sub> = 360 Hz).

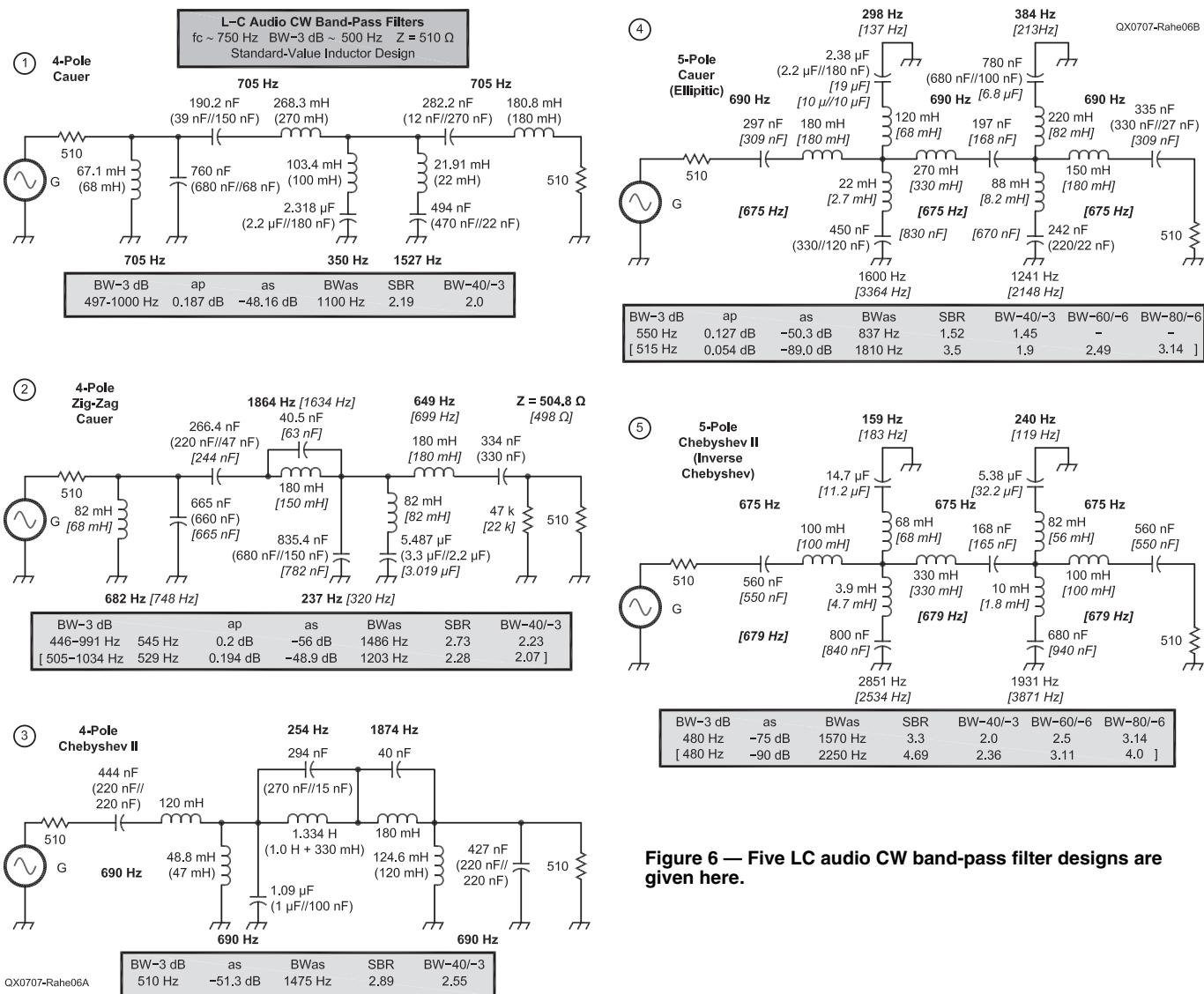


Figure 6 — Five LC audio CW band-pass filter designs are given here.

return loss attenuation is more sensitive to design errors or component tolerances than bandwidth or center frequency. A deviation of less than 5% from the standard values for the four-pole filters and <10% maximum for the five-pole filters has been reached.

No. 1 is a classical four-pole Cauer band-pass filter with steeper skirts than a simple three-pole filter. It needs five inductors, however.

Band-pass filters of even degree, derived from elliptic low-pass filters by low-pass to band-pass transformation, can be realized in most cases by a circuit with the minimum number of coils without mutual inductances. The steps of transformation are described in the reference at Note 5. Filter no. 2 is an example.

At the price of only one additional capacitor, yet only four inductors, you get a so-called zigzag band-pass filter. These filters

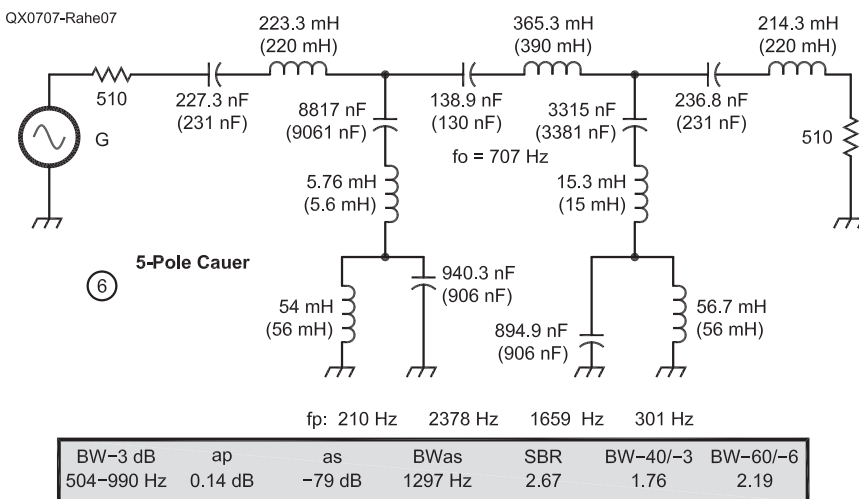


Figure 7 — This filter is a five-pole Cauer BPF design.

show a slight shape reduction and unequal terminations. This is not really a problem in most cases, however. Insertion loss in real circuits is somewhat smaller than for the conventional equivalents.

Filter no. 3 is a Chebyshev II design with good impulse response. It has the disadvantage of high inductance values. This is because no T-topology has been found with standard inductor values in this frequency range. Circuits 4 and 5 are preferably suited for direct-conversion receivers where alternatively high skirt selectivity or high stopband attenuation is needed.

These filters suffer somewhat on the high capacitor values needed for the lower stopband poles. Instead of tantalum capacitors, polyester film capacitors must be used! [WIMA MKS-2 (5%-series is recommended)].

Figure 7 shows a Cauer-BPF in another T-topology (no. 6) with high stopband attenuation and somewhat easier to realize component values.

### The Real World

The most critical quantity in passive filter circuits is the quality factor of the coils, which is given by Equation 1.

$$Q_u(f) = 2 \pi f L / R_s \quad [\text{Eq 1}]$$

$R_s$  is the loss impedance in series with the inductance,  $L$ . As you can see, most miniature inductors have a very low unloaded  $Q$  at low frequencies caused by the high dc resistance of the very thin wire used.

Only a few series of fixed inductors are available on the market suited for filter applications in the audio range. Table 5 gives an overview. Other series are commonly much worse and lead to disappointing results.

Low inductor  $Q_s$  introduce some insertion loss,  $a_i$ , and leads to finite attenuation at the pole frequencies and a distortion of the

amplitude response at the passband limits, resulting in a reduced bandwidth.

A lossy BPF shows the typical rounded passband, because the dissipative losses are greater at the band edges than at the center frequency. The passband ripple is swamped out by the losses of filter components and the stopband attenuation is reduced by the basic loss. The pole frequencies next to the cutoff are most critical.

These effects have to be taken into account in the filter design by increasing the stopband attenuation, the passband bandwidth or decreasing  $BW_{as}$  if you have to meet certain specifications in the case of lossy coils.

Figure 8 shows the typical amplitude response of a lossy filter assembled with TOKO coils 10RBH, in comparison to the lossless filter (BPF no. 4B).

The way around the distortion problem is to predistort the response, which has been presented by Zverev.<sup>10</sup> The price that must be paid for a predistorted filter to get the desired response in the case of finite inductor  $Q_s$  is a higher insertion loss and some distortion in the stopband. This procedure was not followed here, but can be tried with the mentioned reference and the help of a simulation program.

To calculate the filter losses, you can use the inductor dc resistances given in the datasheets, in series with the inductors.<sup>9</sup> This can be done with a circuit simulation program like *RFSim* or the *ARRL Radio Designer*. The method yields more realistic results than to set all inductor  $Q_s$  at a fixed value, a function that is usually implemented in most filter programs.

Figure 9 shows the amplitude response and return loss attenuation for the seven-branch elliptic low-pass filter given as no. 7 of Table 3. Figure 10 is the amplitude response and return loss attenuation of the no. 1 band-pass filter given in Figure 6. Figure 11 shows the amplitude response for the five-pole elliptic band-pass filter given as no. 6 in Figure 7.

### Measurement

In practice, the insertion loss and the definitive amplitude response is strongly dependent on the filter complexity and the unloaded  $Q_s$  of the coils. The amplitude response of the low-pass filters is therefore much more ideal than that of the band-pass filters.

That is because of the smaller number of coils and their lower losses at higher frequencies. For example, a five-branch low-pass filter

**Table 5**  
Fixed Inductor Series (See Note 9)

Manufacturer Series	TOKO 10RB (radial) ferrite shielded	Fastron 07M (radial) ferrite shielded	TOKO 10RBH (radial) ferrite shielded	TOKO 5CA 395DN SMD
Inductance Range	1 -120 mH E-12 + 36 mH	1 - 82 mH E-12	150 - 1500 mH E-12	10 - 2200 mH E-12
DC Resistance	3.4 Ω - 97 Ω	3.4 Ω - 71 Ω	75 Ω - 435 Ω	0.35 Ω - 23.5 Ω
Dimensions	d = 10.5 mm h = 14 mm	d = 9 mm h = 17.5 mm	d = 10.5 mm h = 14 mm	6.2 × 6.8 mm h = 3.3mm

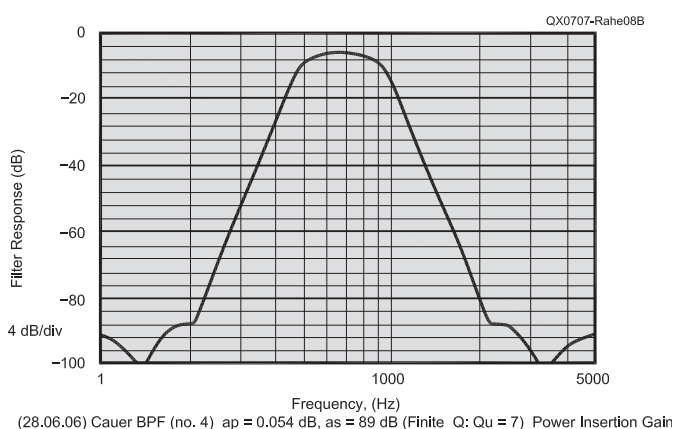
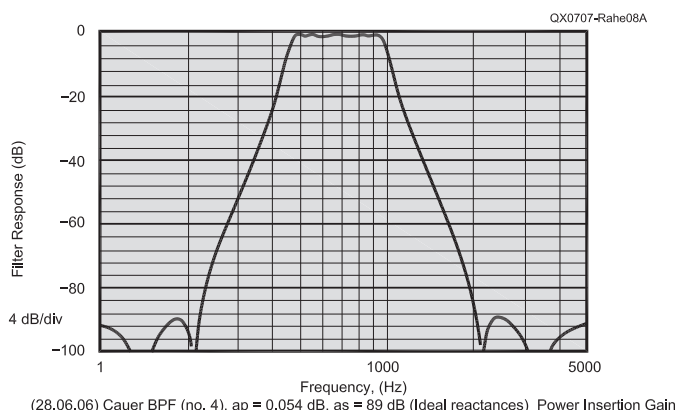


**Figure 8 — Part A shows the amplitude response of band-pass filter no. 4, with loss-less reactances. Part B shows the amplitude response of the same filter with lossy coils ( $Q_u = 7$ ). Finite  $Q$  causes an insertion loss and distorts the filter shape, but improves the time domain behavior.**

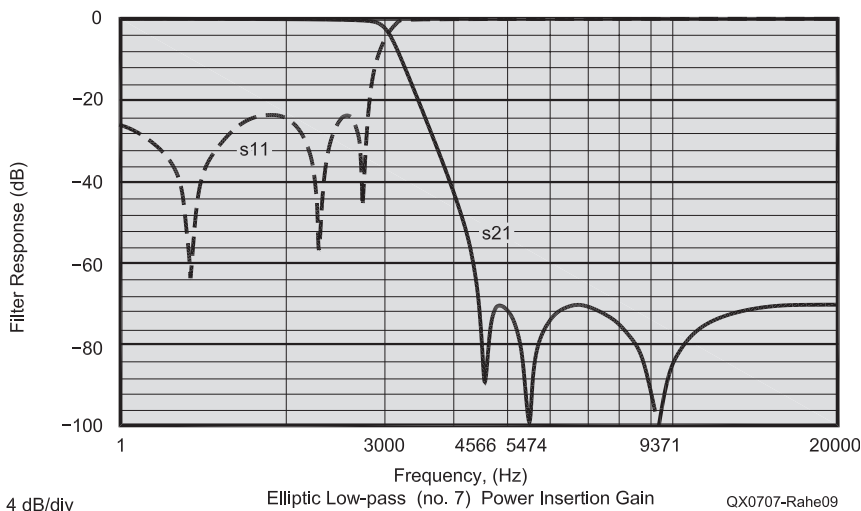


**Figure 9 — Seven-branch elliptic low-pass filter (no. 7) amplitude response and return loss attenuation.**

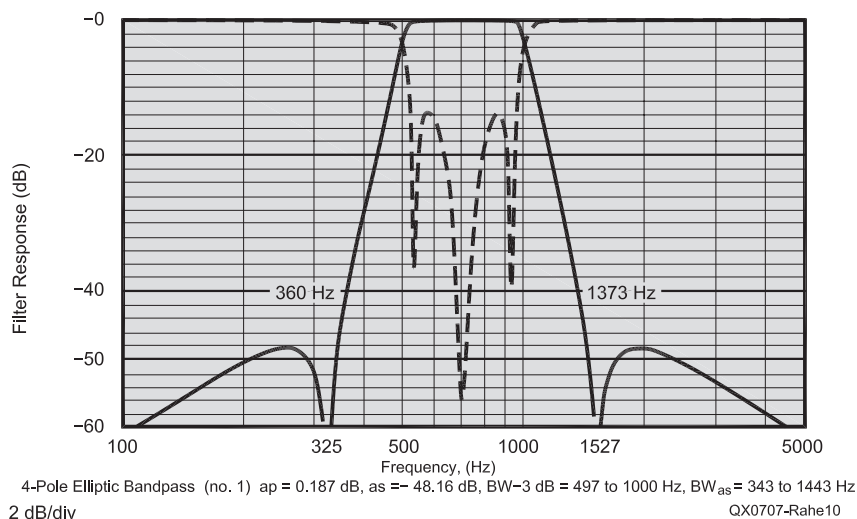


**Figure 10 — BPF no. 1 amplitude response and return loss attenuation.**

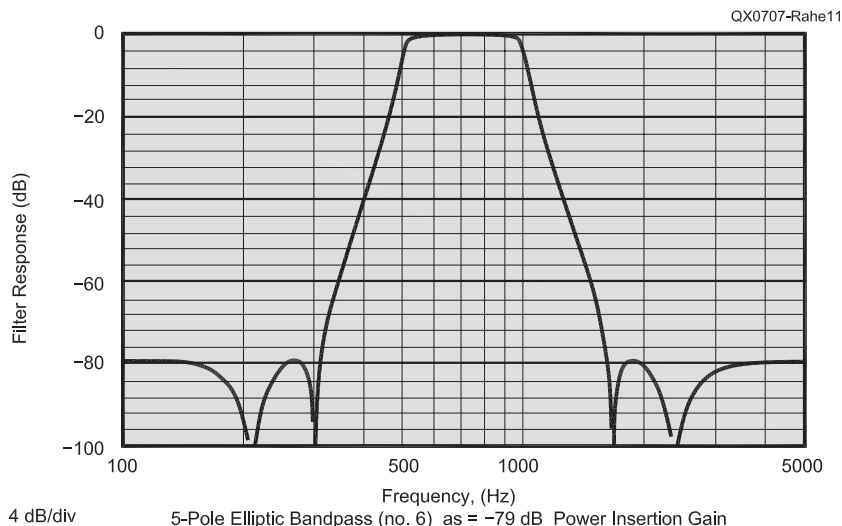


**Figure 11 — BPF no. 6 (five-pole) amplitude response.**

has an insertion loss of less than 2 dB, but a five-pole band-pass filter reaches 8 dB or a bit more if built with the Toko 10 series coils. It must be mentioned that reducing the filter bandwidth yields an increased insertion loss because of the larger inductor values needed. That is the reason why it is not opportune to choose needless small BP-bandwidths, if you don't have large high-Q inductors at hand (powdered ferrite pot-cores or toroids).

If you investigate band-pass (or high-pass) filters in the audio range, you sometimes will be aware that the measured attenuation response on the lower skirt at higher attenuation values does not agree with the computed response. This is not a fault of the filter, but is attributed to your audio-generator harmonics falling in the filter passband.

Therefore, the use of a low distortion generator is strongly recommended. (Don't use "modern" function-generator ICs; it is better to use an old-fashioned Wien-Bridge generator!) For the same reason, filters should be inserted at the beginning of the AF-chain and not at its end as frequently seen, where distortion has reached a considerable amount.

As measured, the inductors have a tolerance of  $\pm 10\%$ . If there are any doubts, you should measure both L and C and tune the resonators to the given pole-frequencies with the capacitors, since the inductance cannot be varied. Minor component tolerances mainly affect passband matching, less than bandwidth and center frequency.

### Summary

If you want to build an easy but effective audio filter for your receiver or in the audio processor of your transmitter, passive filters, realized only with L and C, are a good choice. They do not need any exotic or hard to find components, no power supply and they add no undesirable artifacts to the signal as their digital counterparts can.

### Notes

<sup>1</sup>Una-May O'Reilly, V. Aggarwal, W. O. Jin, "Filter Approximation Using Explicit Time and Frequency Domain Specifications," Gecco, 2006, Seattle, [people.csail.mit.edu/unamay/publications-dir/filter-gecco06.pdf](http://people.csail.mit.edu/unamay/publications-dir/filter-gecco06.pdf)

<sup>2</sup>Werner Rahe, DC8NR, "Steiflankige NF-CW-Filter mit Minimalaufwand Part I," *Funkamateureur*, Mar 2005.

<sup>3</sup>W. Rahe, DC8NR, "Steiflankige NF-CW-Filter mit Minimalaufwand Part II," *Funkamateureur*, Apr 2005.

<sup>4</sup>W. Rahe, DC8NR, "NF-CW-Band-pass filter mit Chebyshev- und Cauer-Charakteristik, Part I," *CQDL*, Apr 2005.

<sup>5</sup>Rudolf Saal, *Handbuch zum Filterentwurf*, Berlin, Frankfurt a.M., AEG-Telefunken, 1979.

<sup>6</sup>Pierre Amstutz, "Elliptic Approximation and Elliptic Design on Small Computers," *IEEE Transactions on Circuits and Systems*, Vol CAS-25 No. 12, 1978.

<sup>7</sup>See [www.aade.com](http://www.aade.com)




<sup>8</sup>S. Niewiadomski, "Passive Audio Filter Design," *Ham Radio*, Sep 1985.

<sup>9</sup>TOKO components are available in Germany from COMPONEX GmbH, Düsseldorf, Phone: ++49 (0)211 96491-11.

<sup>10</sup>Anatol I. Zverev, *Handbook of Filter Synthesis*, John Wiley & Sons, New York, 1967.

Werner Rahe, DC8NR, received his license in 1967. He began a technical business management course at the University of Karlsruhe and later completed an education course at the University of Erlangen-Nürnberg. He is a junior high school teacher.

Werner is co-author of the well-known bilingual VHF/UHF/ Microwave magazine DUBUS, which describes the areas of his interests in Amateur Radio. Other hobbies are windsurfing, skiing and architecture. He lives about 40 km southeast of Munich. 

## Two Big Winners from Array Solutions



### PowerMaster Watt / VSWR Meter

- Sets the benchmark for all other SWR/Watt meters to follow
- Unheard of accuracy for the price
- Fast, bright, reading meter
- Application software included
- Upgradeable via Internet
- \$430



### AIM 4170 Antenna Analyzer

- Most advanced vector impedance analyzer at a fraction of the cost
- Accurate and easy to use
- Application software included
- Lab instrument quality
- Upgradeable via Internet
- \$440

Just too many features to put in just one ad, see them on our website!

[www.arrayolutions.com](http://www.arrayolutions.com)

Phone 972-203-2008

We've got your stuff!



## We Design And Manufacture To Meet Your Requirements

\*Prototype or Production Quantities

# 800-522-2253

This Number May Not Save Your Life...

But it could make it a lot easier! Especially when it comes to ordering non-standard connectors.

### RF/MICROWAVE CONNECTORS, CABLES AND ASSEMBLIES

- Specials our specialty. Virtually any SMA, N, TNC, HN, LC, RP, BNC, SMB, or SMC delivered in 2-4 weeks.
- Cross reference library to all major manufacturers.
- Experts in supplying "hard to get" RF connectors.
- Our adapters can satisfy virtually any combination of requirements between series.
- Extensive inventory of passive RF/Microwave components including attenuators, terminations and dividers.
- No minimum order.

# NEMAL

Cable & Connectors  
for the Electronics Industry

NEMAL ELECTRONICS INTERNATIONAL, INC.

12240 N.E. 14TH AVENUE  
NORTH MIAMI, FL 33161  
TEL: 305-899-0900 • FAX: 305-895-8178  
E-MAIL: INFO@NEMAL.COM  
BRASIL: (011) 5535-2368

URL: WWW.NEMAL.COM

## NATIONAL RF, INC.



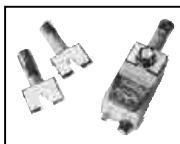
### VECTOR-FINDER

Handheld VHF direction finder. Uses any FM xcvr. Audible & LED display.  
VF-142Q, 130-300 MHz \$239.95  
VF-142QM, 130-500 MHz \$289.95



### ATTENUATOR

Switchable, T-Pad Attenuator, 100 dB max - 10 dB min BNC connectors  
AT-100, \$89.95



### DIP METER

Find the resonant frequency of tuned circuits or resonant networks—ie antennas.  
NRM-2, with 1 coil set, \$219.95  
NRM-2D, with 3 coil sets (1.5-40 MHz), and Pelican case, \$299.95  
Additional coils (ranges between 400 kHz and 70 MHz avail.), \$39.95 each



### DIAL SCALES

The perfect finishing touch for your homebrew projects. 1/4-inch shaft couplings.  
NPD-1, 3/4" x 2 3/4" inches 7:1 drive, \$34.95  
NPD-2, 5/8" x 3 3/8" inches 8:1 drive, \$44.95  
NPD-3, 5/8" x 3 3/8" inches 6:1 drive, \$49.95

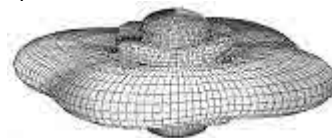
S/H Extra, CA add tax

NATIONAL RF, INC  
7969 ENGINEER ROAD, #102  
SAN DIEGO, CA 92111

858.565.1319 FAX 858.571.5909

[www.NationalRF.com](http://www.NationalRF.com)

A picture is worth a thousand words...



With the

## ANTENNA MODEL™

wire antenna analysis program for Windows you get true 3D far field patterns that are far more informative than conventional 2D patterns or wire-frame pseudo-3D patterns.

Describe the antenna to the program in an easy-to-use spreadsheet-style format, and then with one mouse-click the program shows you the antenna pattern, front/back ratio, front/rear ratio, input impedance, efficiency, SWR, and more.

An optional **Symbols** window with formula evaluation capability can do your computations for you. A **Match Wizard** designs Gamma, T, or Hairpin matches for Yagi antennas. A **Clamp Wizard** calculates the equivalent diameter of Yagi element clamps. **Yagi Optimization** finds Yagi dimensions that satisfy performance objectives you specify. Major antenna properties can be graphed as a function of frequency.

There is **no built-in segment limit**. Your models can be as large and complicated as your system permits.

**ANTENNA MODEL** is only \$90US. This includes a Web site download and a permanent backup copy on CD-ROM. Visit our Web site for more information about **ANTENNA MODEL**.

Teri Software  
P.O. Box 277  
Lincoln, TX 78948

[www.antennamodel.com](http://www.antennamodel.com)

e-mail [sales@antennamodel.com](mailto:sales@antennamodel.com)  
phone 979-542-7952

# Transmission Line Paradigm

*In the prevailing view, some fundamental facts of transmission line behavior have been stretched almost to the point of fantasy. One kernel of truth hidden inside today's nutshell of transmission line paradigm is exposed by pulling on a thread of thought connected to an 18<sup>th</sup> century gem of acoustic physics. The kernel does a good job of describing electrical behavior of transmission lines without paradigm shifts; math is the only paradigm needed.*

Richard F. Thompson, W3ODJ

“**M**athematical concepts turn up in entirely unexpected connections.”  
— Eugene P. Wigner.<sup>1</sup>  
“...a genuine understanding of ideas is not possible without an analysis of origins...” — Howard Eves.<sup>2</sup>

## Strings, Lines and Paradigms

There aren't many rational connections worth making between stretched strings and energized coax, but the physics of vibrating string motion and of transmission line voltage distribution both descend from a common mathematical ancestor. Their kinship is evident when we see visible waves on guitar strings, and speak of voltage waves on transmission lines. Mathematical waves are primal paradigms throughout physics, easy to see in the mind's eye, and once a valid conceptual connection to waves has been made, active imaginations are eager to stretch it, shift the paradigm, and enlarge the view. The original idea is simple, the stretching is plausible, and the validity of the new view seems to be obvious. *Stretch, but verify!* Sometimes the obvious is a paradigm stretched too far, and the idea is better understood in its origins at the other end of a different line of thought.

<sup>1</sup>Notes appear on page 43.

3755 Leonardtown Road  
Waldorf, MD 20601  
rftompson@earthlink.net

## A Historical Thread

Like many great technical advancements, transmission line theory has a rich history and a rich *prehistory*. It's prehistory precedes coaxial cable by a hundred years. In 1747, the French scientist Jean le Rond d'Alembert (1717-1783) derived an equation for an appropriate mathematical description of the motion of a vibrating string.<sup>3</sup> More than a century later, in 1876 the English physicist Oliver Heaviside (1850-1925) derived a similar equation to describe the electrical behavior of telegraph lines.<sup>4</sup> Their equations are both prescribed by one generic equation, called **the Wave Equation**.<sup>5</sup>

$$V_{dd} = V_{tt} / c^2 \quad [\text{Eq 1}]$$

This is a relation between rates of change, a second-order partial differential equation. It says that acceleration at every point on a vibrating elastic string is proportional to the rate of change in the string's tension at that point. The local rates of change are derived by applying known physical laws to distributed parameter models. For the telegraph, a simple electric circuit was taken as the model of a very short length of coaxial cable, and analysis of this circuit determined the change in voltage across an incremental length of cable. In either case, *c* represents the apparent swiftness (*celerity*) of mathematical waves in string or coax; it is not used here as a specific physical speed such as that of light waves in a vacuum. Such incremental *local changes* in a physical parameter are extrapolated into its *global values* by solving the wave equation.

Prescribed local rates of change are in the wave equation's genes, from which valid solutions inherit a notable determinism. After the harpist plucks a string, the present shape of the string determines how the energy stored in the string will be transformed into its future motion; *V* everywhere at the instant excitation is terminated determines *V* forever after. When all motion ceases, the string has returned to its original shape, a taut straight line of minimal energy between two fixed points; an elastic string remembers its origins. It's all in the genes.

## One Solution Fits All

The general solution of the wave equation has a surprisingly simple form. D'Alembert deduced in 1747 that a sum of any two suitably differentiable functions,  $f(x) + g(x)$ , will solve the wave equation, if the separate variables, *d* and *t*, are combined to form two new distance-time variables,  $d + ct$ ,  $d - ct$ . This gives **d'Alembert's Solution of the Wave Equation**.<sup>6</sup>

$$V(d, t) = f(d + ct) + g(d - ct) \quad [\text{Eq 2}]$$

The variables *d* and *t* represent distance and time, and as time marches on, the graphs of the functions *f* and *g* look like waves of constant shape sliding in opposite directions along a D-string, each moving with an apparent constant speed, *c*. The motions of the two wave shapes are choreographed by the imbedded synchronizing signals,  $\pm ct$ .

It is interesting to note how distance-time variables had crept into science well

before the German mathematician, Hermann Minkowski (1864-1909) provided his fundamental and revolutionary viewpoint of four-dimensional space-time in 1908. Time coordination by signal exchange was a hot topic around 1900.<sup>7</sup> Heaviside credited the English physicist George F. FitzGerald (1851-1901) with having introduced d'Alembert's 18th century synchronizing signals into 19th century electromagnetic theory, but priority probably should be given to the Danish physicist Ludwig V. Lorenz (1829-1891).<sup>8</sup>

Heaviside adapted d'Alembert's waves to successfully predict the distribution of voltage on submerged telegraph cables, and d'Alembert's solution has since become one of the fundamental formulas in transmission line theory. For Heaviside,  $V(d, t)$  was the voltage measured on the cable at distance  $d$  and time  $t$ . For d'Alembert,  $V(d, t)$  was the measured displacement of a point on the moving string. The malleable mathematical waves  $f$  and  $g$  show up in the solutions of many other physical problems as well.

### What and Where Are These "Waves?"

The two mathematical functions  $f$  and  $g$  are not part of the original physical analysis. They enter later as impromptu mathematical props that don't assume a real role in the physics. Calling them "waves" is a helpful paradigm for understanding the math, but the paradigm can't grant them physical reality; the math merely states that when the physical value  $is$  measured, it will equal the sum of these two ad hoc mathematical improvisations. Think about it — a point on a moving string has only one displacement from a fixed point at any one time. You can measure  $f + g$ , but not  $f$  or  $g$ . The analogous point about measuring voltage "waves" on a transmission line is explicitly made by Eric von Valtier, K8LV, in his recent *QEX* article on directional wattmeters.<sup>9</sup>

Caveat: Of course, if one of  $f$  or  $g$  is zero, then a direct measurement of  $f + g$  is an ambiguous measurement of either  $f$  or  $g$ , but such cases require additional information in order to resolve the ambiguity. It may be necessary to think like a mathematician in order to appreciate the view that the *nothing* we call zero is *something* that must be counted on! On a properly matched line the reflected wave function is zero, and knowing this, a direct measurement of  $f + g$  is an indirect measurement of the forward wave.

By establishing quantitative relations we can find out how things behave, but not what they are. The very fact that a pair of math functions can be used to describe either string displacement or line voltage argues that the pair's relation to physical reality is indirect; it is their bottom-line sum  $f + g$  that gets our direct attention because it

predicts what will be measured.

Voltage wave functions do not represent electromagnetic waves. They can't. Wave functions are scalar quantities that evaluate to one number, whereas electromagnetic waves are represented by pairs of vectors that evaluate to six numbers in all. Voltages on transmission lines are merely footprints left behind by electromagnetic waves as they race by, and the footprints ( $f + g$ ) don't move. Mathematical wave functions ( $f$  or  $g$ ) move in one direction. Electromagnetic waves radiate energy in every direction.

### A Classic Model for Transmission Lines

Over the years, one simple physical model has provided useful insight into the performance of no-loss and low-loss transmission lines of all shapes and sizes: parallel lines, coaxial lines, overhead power lines, submerged telegraph cables, thin-film lines in microwave integrated circuits and so on. The physical model is a small incremental length of line, which has series inductance,  $L$ , per unit length, and parallel capacitance,  $C$ , per unit length.<sup>10</sup> The distributed parameter circuit equations for this model are still known as **The Telegrapher's Equations**.<sup>11</sup>

$$V_d = -L I_t \quad [\text{Eq 3}]$$

$$I_d = -C V_t \quad [\text{Eq 4}]$$

The voltage and current equations prescribed for this model by the wave equation are:

$$\text{Voltage Equation} \\ V(d, t) = f(d + ct) + g(d - ct) \quad [\text{Eq 5}]$$

$$\text{Current Equation} \\ I(d, t) = [f(d + ct) - g(d - ct)] / Z_0 \quad [\text{Eq 6}]$$

The Current Equation is derived by pushing the Voltage Equation through the Telegrapher's Equations, and then integrating the emerging equation.<sup>12</sup>

The graphs of the mathematical wave functions race along the line at the wave speed,  $c = (LC)^{-1/2}$ , but the physical electrons responsible for the current can't keep up with the math — far from it. An individual electron's motion is rather chaotic, and its progress in the direction of the current — its drift velocity — is calculated to be much less than  $c$ .

The mathematical constant  $Z_0 = (L / C)^{1/2}$  is called the transmission line *surge impedance*, or *characteristic impedance*.  $Z_0$  is determined solely by the shape, size and electrical characteristics of the conductors and of the insulating dielectric. It is independent of the shapes and motions of the voltage wave functions  $f$  and  $g$ , and independent of whatever is energizing or terminating the line. The surge impedance of a coaxial cable is certain to have at least a small component of capacitive reactance.<sup>13</sup>

### The Heart of the Matter

It is remarkable how the Voltage Equation says that as long as the energizing voltage is differentiable, voltage inside the classic line model can be described by a sum of two time-coordinated parts:  $f + g$ . It is truly astonishing for the math to *insist*, in the Current Equation, that *the resulting current must be proportional to the difference of the same two parts*:  $f - g$ . This surprisingly simple binary decomposition is capable of predicting the often very complicated electrical behavior of transmission lines. Its gene thread has traces of DNA from: d'Alembert's vibrating string, the electrical experiments of Michael Faraday, James Clerk Maxwell's *Treatise*, Heaviside's Telegrapher's Equations, the classic transmission line model and the differential and integral calculus of Newton and Leibniz.

Transmission line theory is firmly rooted in this mathematical two-part invention, which is valid for almost any conceivable voltage. What we have here is a viable kernel for describing the voltage/current relationship in transmission lines. It is not an empirical formula derived from laboratory measurements, like Ohm's Law. It is a mathematical rule entangled in the genetic thread that should honestly be associated with names from both ends: the **Two-Function Rule (d'Alembert and Heaviside)**.

When a sufficiently differentiable voltage is applied to the classic model for transmission lines, there exist two time-synchronized mathematical functions  $f(d, t)$  and  $g(d, t)$  such that:

- The mathematical expression for voltage  $V(d, t)$  measured anywhere on the line can be represented as the *sum* of the two functions:

$$V = f + g \quad [\text{Eq 7}]$$

- The mathematical expression for current  $I(d, t)$  measured anywhere on the line is proportional to the *difference* of the *same* two functions:

$$I = (f - g) / Z_0 \quad [\text{Eq 8}]$$

- $Z_0$  is a mathematical constant.

Mind you, the Two-Function Rule doesn't provide directions for finding  $f$  and  $g$  for a particular voltage. Mathematics proves that they exist for the classic line model, however, and just knowing they exist is all that is needed to solve some problems. The Rule facilitates concise descriptions of electrical behavior in transmission lines with no distracting paradigm shifts — math *is* the paradigm.

Here are two examples where the Rule shines light on basic facts that are indistinct in the prevailing view: It is a direct consequence of the Rule that on a mismatched line, *steady-state* voltage is maximum wherever

steady-state current is minimum, and vice versa.<sup>14</sup> The Rule also readily resolves the fascinating riddle, “How can the voltage standing wave ratio, VSWR, which by definition is a ratio of line voltages measured at two different points on a standing wave, be computed from measurements taken at only one point?” But first, a further pull upon the thread.

### Is $Z_0$ Really an Impedance?

If that minus sign between  $f$  and  $g$  in the Current Equation could be changed into a plus sign, the equation would become  $I(d, t) = V(d, t) / Z_0$ , and then the mathematical constant  $Z_0$  would become an impedance by definition:  $Z_0 = V / I$ . If d’Alembert, Faraday, Maxwell, Heaviside, Newton and Leibniz are all to be trusted, then the minus sign is a minus sign, and consequently  $Z_0$  is not a voltage/current ratio. In general, characteristic impedance does not satisfy the definition of circuit impedance! Two particular cases suggest the origins of the misnomer: when the line is infinitely long, or is properly terminated, one of the functions, either  $f$  or  $g$ , is equal to zero for all values of the variable pair  $(d, t)$ , so that on these lines,  $Z_0$  does satisfy the definition of impedance. In 1887, Heaviside determined that  $Z_0$  was the constant impedance at every point on an infinitely long line.<sup>15</sup> While properly terminated lines are immensely practical, they don’t pose much of a problem. On mismatched lines,  $Z_0 = V_{\max} / I_{\max}$ , but the two  $\max$  values occur at two different places on the line.<sup>16</sup>

### A Shape to Reckon With

So, when else might a ratio like  $V(d, t) / I(d, t)$  be a workable impedance? Well, the ratio frequently becomes mathematically indeterminate,  $0 / 0$ , when digital pulses are reflected on a line. When the wave functions  $f$  and  $g$  describe nonperiodic transient shapes such as SSB, the ratio is forever changing with respect to time. Even when the waves are nonperiodic pulses of single-frequency sinusoids, the kind of waves created when we transmit a CW signal at 40 wpm, there is no workable impedance. For all these wave shapes you would need a real-time vector analyzer to monitor the voltage/current ratio.

For brick-on-the-key-CW, however, all the transients created at key-down rapidly blur into the long-term sameness of a single, sustained periodicity, so that the waves  $f$  and  $g$  rapidly take on the shapes of a Steady-State-Sinusoid (SSS) — if the CW has a T9 tone, with no frequency variation.

When SSS takes hold, the functions  $f$  and  $g$  in  $V(d, t)$  and  $I(d, t)$  can each be split into a product of two factors: one factor is a time independent phasor containing magnitude and relative phase; the other factor converts the

phasor into an instantaneous value. Our quest for impedance is fulfilled by the phasor factors: “The ratio of total phasor voltage ( $p + q$ ) to total phasor current ( $p - q$ ) at any point on the line is the definition of transmission line impedance.”<sup>17</sup> This definition appears in the most frequently computed equation in transmission line theory.<sup>18</sup> **The Transmission Line Equation (TLE)** is given as:

$$Z(d) = Z_0 [p(d) + q(d)] / [p(d) - q(d)] \text{ [Eq 9]}$$

When an SSS energizes a mismatched transmission line, TLE says that a measurable impedance  $Z(d)$  exists along the line, which varies with distance but not with time, and so in general,  $Z(d) \neq Z_0$ . The celebrated Smith Chart is actually a normalized nomograph of TLE.<sup>19</sup> TLE has been translated into computer coded Smith Charts, which greatly reduce the toil and error of line calculations. The phasors  $p$  and  $q$  in TLE are independent of time; they are all shape and no motion, and so they aren’t waves.

**Caution!** TLE is tightly tied to the steady-state-sinusoid (SSS) assumption by a short rope, and if you think TLE is valid when transients are present, you are stretching the rope. If you put your trust in TLE-based software calculations when transients may do a mischief, you should verify that the software doesn’t break the rope.

### Standing Waves

At best, the unaided eye sees a vibrating string as a swath of blurred motion. Sometimes the width of the swath alternates between a minimum and a maximum value at fixed points along the string, and the stationary boundary of the blur is called a standing wave. An analogous pattern of voltage maxima and minima can occur on a mismatched transmission line.

If a steady-state sinusoid energizes a transmission line that is terminated in a non-reactive load, then d’Alembert’s two voltage wave functions may be chosen as  $f = g = \text{sine}$ , and the solution of **The Wave Equation** may be written as:

$$V(d, t) = A \sin(d + ct) + B \sin(d - ct) \text{ [Eq 10]}$$

Equation 10 is numerically equal to:

$$V(d, t) = 2 A \sin(d) \cos(ct) + (B - A) \sin(d - ct) \text{ [Eq 11]}$$

Equation 11 can be derived from Equation 10 via an elementary trigonometric identity,  $\sin(\alpha + \beta) + \sin(\alpha - \beta) = 2 \sin(\alpha) \cos(\beta)$ , and so it follows that both equations return the same voltage value  $V(d, t)$  when they are given the same variable values  $(d, t)$ .

The minimum and maximum values of voltage,  $V(d, t)$ , can be derived from Equation 11. Minimum voltage occurs at *nodes*,

where the standing wave vanishes (where  $d$  is a multiple of  $\pi$ ), and so the minimum voltage amplitude is just the amplitude of the traveling wave,  $V_{\min} = |B - A|$ . The maximum voltage occurs at *antinodes* where and when the standing wave is largest (where  $d$  is a multiple of  $\pi / 2$  and when  $ct$  is a multiple of  $\pi$ ), and so  $V_{\max} = |2A + (B - A)| = |A + B|$ . Successive nodes and antinodes are  $1/4 \lambda$  apart.

Now use the Two-Function Rule to get the current equation (put the minus sign in Equation 10 and divide by  $Z_0$ ):  $I(d, t) = [A \sin(d + ct) - B \sin(d - ct)] / Z_0$ . Using a little algebra and two trig identities,  $\sin(\pi - a) = \sin(a)$  and  $\sin(\pi + a) = -\sin(a)$ , it follows that when  $d = \pi$  (and  $ct = a$ ):

$$I(\pi, t) = [-A \sin(ct) - B \sin(ct)] / Z_0 = -(A + B) \sin(ct) / Z_0 \text{ [Eq 12]}$$

The current amplitude is taken from Equation 12 as  $|I(\pi, t)| = |(A + B) / Z_0| = I_{\max}$ . So current is maximum at  $d = \pi$ , which is where voltage is minimum. Repeating the analysis at  $d = \pi / 2$  reveals that current is minimum where voltage is maximum. Conclusion: Voltage nodes are current antinodes, and vice versa.

### Not to Worry

There is a huge paradigm shift between Equations 10 and 11. Terms that use *distance-time* variables ( $d \pm ct$ ) are *traveling waves* — shapes that move. In Equation 11, the first term,  $2A \sin(d) \cos(ct)$  is called a *voltage standing wave* because its shape doesn’t move along the transmission line; the distance and time variables  $d$  and  $t$  have been separated, and the separation drops the anchor. So we see two traveling waves in Equation 10, while in Equation 11 we see one traveling wave and one standing wave, yet regardless of how we look at it, an RF voltmeter *measures* the same voltage.<sup>20</sup>

Two alternatives, each yielding the same consequence, pose a logical dilemma. If you dwell on paradigms when you put a brick on your key, you have a choice. You can choose Equation 10 and stretch your imagination to see a voltage wave racing back toward your expensive transceiver, breaching the end of the coax, and flooding your final. Or, you can choose the equivalent Equation 11, and not worry about your rig since a field strength meter tells you that the traveling wave is certainly headed toward your antenna, but now you might worry that the standing wave could blow a hole in your coax. Either way, the beguiling waves haunting your mind are not real voltages racing through your line. Let the numbers be your paradigm. If your coax is happy with line voltages  $V(d, t)$  predicted by Equations 10 or 11, and your rig is happy with the input impedance,  $Z(d)$ , predicted by TLE, then your only concern is how much of the energy is getting to the antenna.



## “Where Does the (Steady-State) Power Go?”

The short answer is, “All steady-state energy delivered to the line by the transmitter is either dissipated inside the line or transferred to the load; none of the steady-state energy returns to the transmitter.” Jon Bloom reached a similar conclusion in a December 1994 *QEX* article. “No reflected power is dissipated in the generator for the simple reason that there is none left — it’s all delivered to the load.”<sup>21</sup> What happens to the energy inside the line depends upon real diagnostics such as the Reflection Coefficient,  $\rho = A/B$ , or the Voltage Standing Wave Ratio,  $VSWR = (A+B)/(B-A)$ , assuming  $B \geq A \geq 0$ . The total energy stored in any  $\frac{1}{4} \lambda$  of a standing wave is constant, merely interchanging between energy in the electric field of the voltages and energy in the magnetic field of the currents.<sup>22</sup> So all steady-state energy shoved into one end of a *lossless* line gets to the load, except for energy trapped in fields associated with a standing wave. On a *lossy* line, both the stored energy and the power dissipated are proportional to the length of the line.<sup>23</sup> So, on a *lossy* line, some energy will be lost on its way to the load, and some more disappears in order to maintain the constant energy level of the fields set up by a standing wave.

If energy loss is a problem, and replacing the line isn’t a solution, then the only remaining solution is to shrink the voltage standing wave, which in practice means reducing the reflection coefficient. The practical formula,  $\rho = (Z_L - Z_0) / (Z_L + Z_0)$ , says that the only practical way to reduce reflections without changing the line is to change the load impedance,  $Z_L$ . Sadly, an “antenna tuner” at the transmitter end of the line can’t change the load impedance at the other end, so twiddling knobs in the shack won’t solve the energy problem in the line; sad, but true.

## The Rule Unravels the Riddle

“VSWR is defined to be the ratio of voltages measured at *two very special places* on a transmission line, so how can VSWR be determined by a VSWR-meter, which makes measurements at *only one arbitrary place*?” The following answer does not depend upon a directional coupler’s sense (or non-sense) of direction:

The “SW” in VSWR means “Standing Wave,” and when Equation 10 holds, the voltage wave functions are  $f = A \sin(d+ct)$  and  $g = B \sin(d-ct)$ . Measured values of voltage and current will obey The Two-Function Rule:  $V = f + g$  and  $I = (f - g) / Z_0$ .

An SWR-meter makes two measurements at one arbitrary point on the line: The first measurement is proportional to  $V$ :  $M_1 = a(f + g)$ . The second measurement is proportional to  $I$ :  $M_2 = b(f - g) / Z_0$ . The proportions are set to be  $a = 1/2$  and  $b = Z_0 / 2$  so that  $M_1 =$

$(f + g) / 2$  and  $M_2 = (f - g) / 2$ . Adding and subtracting  $M_1$  and  $M_2$  creates two signals:  $M_1 + M_2 = f = A \sin(d+ct)$ , and  $M_1 - M_2 = g = B \sin(d-ct)$ . The RMS values of these two signals are  $R_1 = A / \sqrt{2}$  and  $R_2 = B / \sqrt{2}$ . The SWR meter displays the ratio  $(R_1 + R_2) / (R_2 - R_1) = (A + B) / (B - A) = SWR$ . This proves the result we wanted to demonstrate.

$M_1$  and  $M_2$  can be measured by ordinary RF voltmeters and ammeters.<sup>24</sup> Physical “directional coupling” cannot be made to the mathematical voltage waves  $f$  and  $g$ ; they must be derived via the Two-Function Rule from measured values of physical voltage and current. No mention of forward or reflected power creeps into the analysis.

Bifunctional is more functional than bidirectional. No extraneous paradigm. Neat!

## Seeing is Believing

The British physicist Oliver Joseph Lodge (1851-1940) was possibly the first person ever to actually *see* voltage waves standing on a wire. It happened around 1888, and the event is recounted as follows in Bruce Hunt’s well documented history.<sup>25</sup>

“Lodge showed ... that if the length of the wires and the oscillation time of the discharge were properly adjusted, a pattern of standing waves could be established ... He later found that with long wires and a strong discharge, the space around the wires actually glowed, so that in a darkened room, one could pick out the nodes and antinodes as clearly as if they were waves on a string.”

The discharge came from a large capacitor called a Leyden jar, and the capacitor plus the self inductance of the wires forced the resulting current to oscillate. Lodge saw standing waves several meters long, in the HF radio-spectrum. Interjecting one final comment about our theme, the end of Lodge’s description is tied off with a bit of string and a twitch upon the thread.

## Suggested Further Reading

Anyone interested in the foundations and history of communication science and technology should take a look at the following two excellent books:

*Oliver Heaviside* by Paul J. Nahin is an outstanding account of the life and times of this seminal genius. It gives readable, informative and interesting accounts of his practical knowledge of telegraphy (he worked for a short while as a telegraph operator/technician, his only job), of how interactions with his peers were colored by his creative theoretical prowess and of the rapidly changing communication technology to which he made major contributions. Some of Heaviside’s methods that were novel in 1887 are now routinely taught to electrical engineering students.<sup>26</sup> He is recognized as one of the creators of modern vector analysis.<sup>27</sup>

*The Maxwellians* by Bruce J. Hunt gives well deserved recognition to the late nineteenth century physicists who wrestled with the comprehensive but very difficult to read *Treatise on Electricity and Magnetism* (1873) compiled by James Clerk Maxwell (1831-1879). Maxwell gave compelling theoretical evidence in 1861 that light waves and electromagnetic waves had the same velocity, but apparently he never suspected that oscillating electric currents would radiate electromagnetic energy — “Maxwell’s silence about electromagnetic waves is well established.”<sup>28</sup> The Maxwellian physicists punched holes in the labyrinth of Maxwell’s math, and they let the electromagnetic radiation escape that had been trapped inside. One large hole was punched by FitzGerald in 1883,<sup>29</sup> and five years later a young German experimenter named Heinrich Rudolf Hertz (1857-1894) detected the liberated radio waves.<sup>30</sup> According to Hunt: “Well before German physicists had taken much notice of Hertz’s experiments, the British Maxwellians were hailing them as a major breakthrough.”<sup>31</sup> Radio hobbyists owe a lot to the Maxwellians.

## Notes

<sup>1</sup>Eugene P. Wigner, “The Unreasonable Effectiveness of Mathematics in the Natural Sciences,” *Communications on Pure and Applied Mathematics*, Vol. XIII (1960), p 2.

<sup>2</sup>Howard Eves, *Great Moments in Mathematics [After 1650]*, The Mathematical Association of America, 1961, p 63.

<sup>3</sup>John Stillwell, *Mathematics and Its History*, Springer-Verlag, NY, 1989, p 176.

<sup>4</sup>Paul J. Nahin, *Oliver Heaviside. The Life, Work, and Times of an Electrical Genius of the Victorian Age*, IEEE, 1988, Johns Hopkins University Press, 2002, p 45.

<sup>5</sup>John Stillwell, *Mathematics and History*, p 177.

<sup>6</sup>John Stillwell, *Mathematics and History*, p 178.

<sup>7</sup>Peter Galison, *Einstein’s Clocks, Poincaré’s Maps: Empires of Time*, W. W. Norton & Co, 2003.

<sup>8</sup>Bruce J. Hunt, *The Maxwellians*, Cornell University Press, 1991, p 43.

<sup>9</sup>Eric von Valtier, K8LV, “Dual Directional Wattmeters,” *QEX*, May/June 2006, pp 23-33.

<sup>10</sup>R. Dean Straw, N6BV, Ed, *The ARRL Antenna Book*, 21st Edition, ARRL, 2007, p 24-4. *The ARRL Antenna Book* is available from your local ARRL dealer, or from the ARRL Bookstore, ARRL order no. 9876. Telephone toll-free in the US 888-277-5289, or call 860-594-0355, fax 860-594-0303; [www.arrrl.org/shop](http://www.arrrl.org/shop); [pubsales@arrrl.org](mailto:pubsales@arrrl.org).

<sup>11</sup>Ramo, Whinnery and van Duzer, *Fields and Waves in Communication Electronics*, Third Edition, Wiley, 1994, p 216.

<sup>12</sup>Ramo, *Fields and Waves*, pp 215-217.

<sup>13</sup>Straw, N6BV, Ed, *The ARRL Antenna Book*, 21st Edition, ARRL, 2007, p 24-7.

<sup>14</sup>Ramo, *Fields and Waves*, pp 233-235.

<sup>15</sup>Paul J. Nahin, *Oliver Heaviside*, pp 231-232.

<sup>16</sup>Ramo, *Fields and Waves*, p 254.

<sup>17</sup>Ramo, *Fields and Waves*, p 230.

<sup>18</sup>Straw, N6BV, Ed, *The ARRL Antenna Book*, p 24-11.

# ATOMIC TIME

1010 Jorie Blvd. #332  
Oak Brook, IL 60523  
1-800-985-8463  
www.atomictime.com



ADWA101 - \$49.95

**14" LaCrosse Black Wall**  
WT-3143A \$26.95  
This wall clock is great for an office, school, or home. It has a professional look, along with professional reliability. Features easy time zone buttons, just set the zone and go! Runs on 1-AA battery and has a safe plastic lens.



WT-3143A - \$26.95

**Digital Chronograph Watch**  
ADWA101 \$49.95  
Our feature packed Chrono-Alarm watch is now available for under \$50! It has date and time alarms, stopwatch, backlight, UTC time, and much more!



WS-8248 - \$64.95

**LaCrosse Digital Alarm**  
WS-8248U-A \$64.95  
This deluxe wall/desk clock features 4" tall easy-to-read digits. It also shows temperature, humidity, moon phase, month, day, and date. Also included is a remote thermometer for reading the outside temperature on the main unit, approx. 12" x 12" x 1.5"

1-800-985-8463  
www.atomictime.com  
Quantity discounts available!



WS-9412U - \$19.95

**LaCrosse WS-9412U Clock** \$19.95  
This digital wall / desk clock is great for travel or to fit in a small space. Shows indoor temp, day, and date along with 12/24 hr time. approx 6" x 6" x 1"

Tell time by the U.S. Atomic Clock - The official U.S. time that governs ship movements, radio stations, space flights, and warplanes. With small radio receivers hidden inside our timepieces, they automatically synchronize to the U.S. Atomic Clock (which measures each second of time as 9,192,631,770 vibrations of a cesium 133 atom in a vacuum) and give time which is accurate to approx. 1 second every million years. Our timepieces even account automatically for daylight saving time, leap years, and leap seconds. \$7.95 Shipping & Handling via UPS. (Rush available at additional cost) Call M-F 9-5 CST for our free catalog.

- <sup>19</sup>Straw, N6BV, Ed, *The ARRL Antenna Book*, p 28-1.
- <sup>20</sup>Eric von Valtier, K8LV, "Dual Directional Wattmeters," *QEX*, May/June 2006, p 24.
- <sup>21</sup>Jon Bloom, KE3Z, "Where Does the Power Go?," *QEX*, Dec 1994, pp 17-20.
- <sup>22</sup>Ramo, *Fields and Waves*, pp 254-255.
- <sup>23</sup>Ramo, *Fields and Waves*, p 258.
- <sup>24</sup>Eric von Valtier, K8LV, "Dual Directional Wattmeters," *QEX*, May/June 2006, p 25.
- <sup>25</sup>Bruce J. Hunt, *The Maxwellians*, p 149.
- <sup>26</sup>Paul J. Nahin, *Oliver Heaviside*, p 231.
- <sup>27</sup>Paul J. Nahin, *Oliver Heaviside*, p 188.
- <sup>28</sup>Bruce J. Hunt, *The Maxwellians*, p 28.
- <sup>29</sup>Bruce J. Hunt, *The Maxwellians*, pp 39 and 149.
- <sup>30</sup>Bruce J. Hunt, *The Maxwellians*, p 157.
- <sup>31</sup>Bruce J. Hunt, *The Maxwellians*, p 158.

*Richard Thompson got his ham license while in high school, in 1948, and has held the call sign W3ODJ ever since. He has taken several DX-vacations on Grand Cayman as ZF2CD. After 56 years of "barefoot" CW DX-ing with wire antennas, he is currently using a three-element SteppIR Yagi, and stalking the HF bands for the last DXCC entity needed to put W3ODJ on the honor roll. The University of Maryland gave him a BS degree in electrical engineering in 1960, and then he switched to graduate mathematics just when the increasing availability of digital computers began to revolutionize scientific computation. He worked 31 years as a mathematician for NASA on unmanned spacecraft projects, which measured in situ planetary atmospheres and magnetic fields. He resigned from that position in 1999, and is now an emeritus at the Goddard Space Flight Center in Greenbelt, Maryland.* **QEX**

## ARRL Continuing Education Program ...where hams learn more... **Online!**

### Register Online! [www.arrl.org/cce](http://www.arrl.org/cce)

- 24/7 – access the content when and where you want.
- High Quality Experience – enhanced graphics and hyperlinks keep the material interesting.
- Online Mentoring – Individually assigned mentors coach each student toward successful completion (Technician License course is self study)

#### REVISED EMCOMM CONTENT

##### Emergency Communication Level 3 – EC-003R2

A significant rewrite that brings the course current with the Department of Homeland Security (DHS) paradigm. This course bridges the gap between basic participation and leadership. Requires prior completion of EC-001 & EC-002.

Members \$45.00, non-members \$75.00

#### GREAT VALUE FOR NEWCOMERS

##### Technician License Course – EC-010

The goal of this course is to prepare students to take, and pass, the entry-level Amateur Radio license exam. This course includes:

- ARRL publication "Ham Radio License Manual"
- One year ARRL membership including QST every month

Package Price \$69.00

#### OTHER COURSES AVAILABLE

- Antenna Design & Construction – EC-009
- Antenna Modeling – EC-004
- HF Digital Communications – EC-005
- Level 1 Amateur Radio Emergency Communications – EC-001
- Level 2 Amateur Radio Emergency Communications – EC-002
- Radio Frequency Propagation – EC-011
- VHF/UHF – Life Beyond the Repeater – EC-008
- HF Digital Communications – EC-005
- Analog Electronics – EC-012
- Digital Electronics – EC-013



The national association for  
**ARRL AMATEUR RADIO**

On Line classes for each course begin every month – Register at [www.arrl.org/cce](http://www.arrl.org/cce) and improve your skills.

QEX 7/2007

# Microsoft *Excel* for Antenna Modeling

*Antenna modeling programs are powerful tools for antenna analysis. Multiply that power by using Microsoft Excel to create data tables for your modeling program.*

**Brian B. Turner, K2SJM**

**A**ffordable, *Windows* compatible, Method-of-Moments antenna modeling software such as *EZNEC* by Roy Lewallen, W7EL, has revolutionized antenna experimentation for both the amateur and the professional. One can create a virtual antenna by entering the Cartesian coordinates (X, Y, Z) for its wires or tubing or wire mesh to emulate sheet metal and then let the software calculate the predicted characteristics. Within seconds one has important answers to questions about simple antennas. Not all antennas are simple, however. Some may consist of thousands of wires and tens of thousands of wire segments. It may take days to enter all of the coordinates in a “wires table,” followed by a run time of tens of minutes and some answers. It is then necessary to start the entry process again to create a small variation in element length or spacing. Trying to assess optimal dimensions for complicated antennas is almost self-defeating in view of the amount of time required to enter everything “by hand.”

By entering general equations in an *Excel* spreadsheet, where each cell corresponds to a wires table entry in *EZNEC*, and by changing one or a small number of global input values, an experimenter can run large numbers of models in a fraction of the time required for hand entry. For example, I recently ran 175 variations of a three-element quad antenna in a structured, systematic fashion for optimization of SWR, gain, and F/B ratio in about four hours. The *Excel* data is copied to a .txt document and imported into *EZNEC*. It is simple and fast.

Since the author has been using the Professional version of *EZNEC* in his work at two different companies over the past few

years and has been using the amateur version on his home computer for even longer, this paper will refer to different *EZNEC* functions and tabs as if they were universally available. The reader may have to adapt if using a different modeling package.

Most people are not aware of the power inherent in *Excel* spreadsheets. Although you might have entered figures in various rows or columns, you may have never used the computational capability that can be programmed into individual cells, the logical tests that may be added, nor the speed of array processing for large data sets. Let us begin a brief tutorial.

## A Brief *Excel* Tutorial

*Excel* columns are alphabetic (A, B, C, and so on) and rows are numeric (1, 2, 3 and so on). A cell is specified or labeled by its column and row, for example, **C12**, which is the cell at row 12 in the C column. Figure 1 is an example.

Simple mathematical operations such as addition, subtraction, multiplication, and division can be done by using the operators “+,” “-,” “\*” (for  $\times$ ), and “/” respectively. If, for example, you had entered the value “4” in cell **B1** and the value “5” in cell **C3**, you could type **=B1+C3** in a cell of your choice, push *Enter*, and the number “9” would appear in the cell where you wrote the equation. If

you later change the value in cell **B1** to “6” the number “11” will appear where you wrote the equation.

Similarly, you can write simple equations such as **=B1-C3**, or **=B1\*C3**, or **=B1/C3**, and the answer will appear in that cell. Please note that it is necessary to type the equal sign, “=,” to make these functions work.

When writing a string of cell designations with different operators, it may be useful to use parentheses to prevent mathematical operations occurring in the wrong order. For example, set **A1** = 5, **B1** = 2, and **C1** = 4. Let’s say you want to divide **A1** by **B1**, then multiply the result by **C1**. If you go to **D3** and write **=A1/B1\*C1**, the answer will appear as 0.625, which is wrong. It should be 10. The equation can be written correctly as either: **=A1\*C1/B1**, or **=(A1/B1)\*C1**. Either do all multiplying together and then divide, or put the division in parentheses and then multiply.

When using scientific notation for numbers such as 146 MHz, one writes it out as  $146 \times 10^6$  hertz. In an *Excel* equation it would be entered as **146\*10^6**.

To find the approximate wavelength of a frequency in meters, you can enter the frequency in cell **F6**, for example, as **146\*10^6**. Then in cell **G6**, enter **=3\*10^8/F6**, hit *Enter*, and the answer will appear as 2.05479... (meters).

	Columns			
Rows	A	B	C	D
1	A1	B1	C1	D1
2	A2	B2	C2	D2
3	A3	B3	C3	D3

Figure 1 — An example of how *Excel* columns and rows are set up to label cells.

6747 Lake Drive  
Warrenton, VA 20187  
k2sjm@arri.net

Trigonometric operations are included in *Excel*. Looking at the fourth tool bar line from the top of the screen, you will see the symbol “fx” next to an equal sign in a blank (white) field. Click on the “fx” and a pop-up window entitled “Insert Function” appears. The second field down has the instruction: “Or select a category.” Click on the checkmark for a drop down menu of all the functions available. This is probably the most important menu in *Excel*. Select “Math & Trig.” The new menu starts with *ABS* and ends with *TRUNC*. Click on any function, and an explanation appears beneath the window.

A couple of caveats are in order. The trigonometric functions, such as sine, cosine, tangent and so on (*SIN*, *COS*, *TAN*) use radians for arguments, not degrees. If you have created an antenna on paper that has one wire at an angle to another and you want to specify the end coordinates by trigonometry, you must convert the degrees to radians. This is easily done via the value of Pi. To insert Pi (or its Greek letter equivalent,  $\pi$ ) into an *Excel* equation, it is written **PI()**. Always remember those parentheses. For example, enter a number of degrees, say “30,” into cell **D1**.

Then remembering that there are  $2\pi$  radians in a circle of  $360^\circ$ ,

$$2\pi = 360, \text{ or}$$

$$\pi = 180.$$

Then set up a ratio equation by putting the above into the denominator:

$$X / \pi = 30 / 180$$

Rearrange this to:

$$X = \pi \times 30 / 180$$

Since the value 30 is in cell **D1**, an equation in *Excel* style that uses the sine function, could be written:

$$=\text{SIN}(\text{PI}()*\text{D1}/180)$$

Another important submenu available under “Insert Function” is “Logical,” which gives *AND*, *FALSE*, *IF*, *NOT*, *OR*, and *TRUE* choices. These can be used to sort coordinates to be included in an antenna versus those to be excluded. For example, let’s say that you are setting up a reflector that is based on a circle and want to vary how many degrees of circle will be used. Suppose that the limits of variation are between  $270^\circ$  and  $300^\circ$ . You label a cell, such as **F8**, as the one to contain the cut-off point and let’s say you enter 285 in **F8**. For all wires that might lay between  $270^\circ$  and  $300^\circ$ , you can enter the logic, as written out, “If the value in adjacent cell (for example, **F98**) is less than or equal to the value in **F8**, then the equation of this cell (**G98**) equals **E98** times the cosine of **F98**, or else it equals zero.” In *Excel* it is written: **=IF(F98<=F8,E98\*COS(F98\*PI()/180),0)**

Then depending on the comparison of **F98** versus **F8**, either a 0 or a value will appear.

It is possible to concatenate many *AND*s and *OR*s with *IF* statements, but unless you

Row	A	B	C	D	E	F	G	H	I	J
Row 1	Cartesian Coordinate Generator 3 Element Cubical Quad Antenna									
Row 2	by Brian B. Turner									
	Enter operational frequency in MHz					146	2.05	$\lambda$ in meters	2054.8	mm
	Enter height above ground in wavelengths					5	10.3	meters	10274.0	mm
	Enter reflector wavelength factor (f1)					1.04	$x \lambda/8$	267.1		mm
	Enter driven element wavelength factor (f2)					1.03	$x \lambda/8$	264.6		mm
	Enter director wavelength factor (f3)					0.99	$x \lambda/8$	254.3		mm
	Enter spacing reflector-driven element in wavelengths					0.28	0.575	meters	575.3	mm
	Enter spacing driven element-director wavelengths					0.2	0.411	meters	411.0	mm
	Enter wire diameter in meters					0.001	1			mm
	Enter number of segments per wire					3				
Row 13										
Row 14										

Figure 2 — Top of *Excel* spreadsheet showing title and fields for entry of global values in light shading under column F.

Row	F	G	H	I	J
4	146	$3*10^8/(F4*10^6)$	$\lambda$ in meters	$G4*1000$	mm
5	5	$F5*G4$	meters	$G5*1000$	mm
6	1.04	$x \lambda/8$	$F6*14/8$		mm
7	1.03	$x \lambda/8$	$F7*14/8$		mm
8	0.99	$x \lambda/8$	$F8*14/8$		mm
9	0.28	$F9*G4$	meters	$G9*1000$	mm
10	0.2	$F10*G4$	meters	$G10*1000$	mm
11	0.001	1	mm		
12	3				

Figure 3 — Top of *Excel* spreadsheet showing the equations in various cells (darker shading) that calculate the numbers shown in Figure 2. Note that the equal signs are omitted in order to display the equations.

	End 1			End 2			Diam	Segments
	X	Y	Z	X	Y	Z		
w1	(-H6)	0	I5-H6	H6	0	I5-H6	0.001	3
w2	H6	0	I5-H6	H6	0	I5+H6	0.001	3
w3	H6	0	I5+H6	(-H6)	0	I5+H6	0.001	3
w4	(-H6)	0	I5+H6	(-H6)	0	I5-H6	0.001	3
w5	(-H7)	19	I5-H7	H7	19	I5-H7	0.001	3
w6	H7	19	I5-H7	H7	19	I5+H7	0.001	3
w7	H7	19	I5+H7	(-H7)	19	I5+H7	0.001	3
w8	(-H7)	19	I5+H7	(-H7)	19	I5-H7	0.001	3
w9	(-H8)	I9+I10	I5-H8	H8	I9+I10	I5-H8	0.001	3
w10	H8	I9+I10	I5-H8	H8	I9+I10	I5+H8	0.001	3
w11	H8	I9+I10	I5+H8	(-H8)	I9+I10	I5+H8	0.001	3
w12	(-H8)	I9+I10	I5+H8	(-H8)	I9+I10	I5-H8	0.001	3

Figure 4 — Portion of *Excel* spreadsheet showing layout of equations related to wires 1 to 12.



have programming experience, it is not recommended.

**Procedure**

The procedure that links *Excel* to a program such as *EZNEC* is as follows:

1. Rather than thinking in terms of numerical Cartesian coordinates for an antenna, think of the general algebraic and trigonometric equations you could use to generate the coordinates. An example will be given later.

2. Think of the “global” values that must be entered into those equations to generate a real number (X, Y, and Z for both ends of each wire). These are the parameters that you will vary to generate different wire lengths and spacings.

3. Near the top of the spreadsheet, give it a name and a date. Set aside some cells for entering the global values. Please Refer to Figure 2 for examples. I often use **F5** to **F15** for this. Label each one by typing a descriptor into an adjacent cell, such as “Frequency of operation.” It is a good reminder to highlight those cells with a certain color — I like to use pale yellow to highlight the text while keeping it visible. To save time later, use other adjacent cells for related numbers, such as wavelength in meters or in millimeters for the frequency of operation. Since these are values that the software computes from the numbers you have already entered, enter the equations for calculating the values. Be sure to enter an equal sign at the beginning of each equation. Please refer to Figure 3 for examples, but note that the equal signs have been left off in order to show the equations. Highlight these cells in a different light hue.<sup>1</sup>

4. Starting at Row 21, enter wire numbers in column A, for example in cell **A21**, w1; in **A22**, w2; and so on. This will help in debugging if any mistakes have been made.

5. Use whatever columns you need to keep things straight in your head. I recently finished a coordinate generator for a planar log spiral antenna that uses columns A to I for such housekeeping. The data columns go beyond these.

6. Then set aside the number of columns needed to match the input format of the application software. Eight (8) columns are needed to match the *EZNEC* format of X, Y and Z for End 1; X, Y and Z for End 2; Wire Diameter, and Number of Segments per wire. Label them in rows 19 and 20 above where the equations will be entered. See Figure 4 for how this is done. For clarity in examples, let us suppose that we are starting with Column D.

7. In **D21**, enter the equation or cell label for the X-coordinate for End 1 of Wire 1. Do not type the equal sign yet. Please refer to Figure 3 again. In **E21**, enter the equation or cell label for the Y-coordinate of End 1 of

Wire 1, and so forth for all the coordinates for End 1 of Wire 1. Leave the End 2 coordinates and “wire diameter” and “segments” columns blank. I recommend that you do the entry for all the End 1 coordinates for all wires that connect to one another before doing the End 2 coordinates.

8. In **D22**, enter the coordinate equations in the respective cells, and continue in the lower rows until all equations or cell labels for the End 1 wire coordinates have been entered. When antenna elements are continuous but are subdivided into a series of wires, especially at bends or connections, the value of X, Y and Z for End 1 will appear as the value for End 2 on the next higher line. In *Excel*, copy all the End 1 equations below the first line by left clicking and dragging the mouse across the set of End 1 equations below the first line, *Copy*, then *Paste* them into the End 2 cells beginning at the first line. This is the reason for leaving off the equal signs — without them, you can copy and paste, with them, you cannot. See Figure 4 for examples.

The reflector consists of wires 1 to 4, the driven element (DE) of 5 to 8, and the director of 9 to 12. See that End 1 values of Wire 2 appear in End 2 values of Wire 1, and so on for each group. Note also that for the last wire of each group, End 2 values are the same as End 1 values for the first wire, since these are loops that go back to the starting point.

9. Once all the equations and cell labels have been entered, go back and add an equal sign to the beginning of each. You can either double click on the cell, move the cursor to the left side of the entry, type “=,” and press *Enter*, or you can press the F2 key, scroll to the left side of the entry, and add the equal sign as before. Numbers will then appear in each cell. See Figure 5.

10. Inspect each cell to ensure that the value is reasonable. Sometimes we fat-finger the keyboard or get numbers out of order. It

is especially challenging in *Excel* sheets that have 2,000 or 3,000 rows in use.

11. Once the *Excel* X, Y, Z values look reasonable, do an array entry for each of the two blank columns. If working in millimeters, it is necessary to list wire diameter in meters; a 1-millimeter wire diameter must be listed as 0.001 meters to make things right on a later operation. If Wire Diameter has been entered as a global value in cell **F11** and Segments as a global value in cell **F12**, the array entry goes as follows. Assuming we are going to use Column J for Wire Diameter, using the mouse, left click and drag the cursor from **J21** to the end of the column adjacent to the last entry. This highlights the pertinent part of Column J. Type an equal sign and the global cell label, **=F11**, then simultaneously press the *Ctrl*, *Shift*, and *Enter* keys. The value in **F11** will then appear in all the cells that were highlighted in Column J. Next, left click and drag the cursor from **K21** to the end of Column K adjacent to the last cell of Column J. Type an equal sign and the cell label, **=F12**, then simultaneously press the *Ctrl*, *Shift*, and *Enter* keys. The value in **F12** will then appear in all the cells that were highlighted in Column K.<sup>2</sup>

12. When all eight columns are filled to satisfaction, using the mouse, go to the upper left-most cell, **D21** in this example, left click and drag to the lowest right side cell. This highlights all the cells that will go into the antenna application. Copy this highlighted area by either clicking on the *Copy* icon or on the word *Copy* in the *Edit* menu.

13. Open a blank text (.txt) document (in *Windows*, click “*Programs*,” then “*Accessories*,” then “*Notepad*”). Open the *Edit* menu, click on *Paste*, and the columns copied from the *Excel* spreadsheet will appear in the .txt document.

14. Be sure that *EZNEC* is running in the background. On the *Notepad* text document, click the *File* menu, then in the drop-down

	End 1			End 2			diameter	segments
	X	Y	Z	X	Y	Z		
w1	-267.1	0	10006.8	267.1	0	10006.8	0.001	3
w2	267.1	0	10006.8	267.1	0	10541.1	0.001	3
w3	267.1	0	10541.1	-267.1	0	10541.1	0.001	3
w4	-267.1	0	10541.1	-267.1	0	10006.8	0.001	3
w5	-264.6	575.3	10009.4	264.6	575.3	10009.4	0.001	3
w6	264.6	575.3	10009.4	264.6	575.3	10538.5	0.001	3
w7	264.6	575.3	10538.5	-264.6	575.3	10538.5	0.001	3
w8	-264.6	575.3	10538.5	-264.6	575.3	10009.4	0.001	3
w9	-254.3	986.3	10019.7	254.3	986.3	10019.7	0.001	3
w10	254.3	986.3	10019.7	254.3	986.3	10528.3	0.001	3
w11	254.3	986.3	10528.3	-254.3	986.3	10528.3	0.001	3
w12	-254.3	986.3	10528.3	-254.3	986.3	10019.7	0.001	3

**Figure 5 — Portion of *Excel* spreadsheet corresponding to Figure 4, but showing the values computed by the equations after an equal sign is entered.**

<sup>1</sup>Notes appear on page 50.

menu select *Save As*, and the *EZNEC* directory will open. Click on the *Ant* folder. Make up a name for the antenna, type it in the “*File Name*” field, then click “*Save*.”

15. Go to *EZNEC*. Click on “*Wires*.” In the *Wires* Table menu, click “*Other*,” and in its drop-down menu, select “*Import Wires from ASCII File*,” which opens a submenu. Select “*Replace Existing Wires*.” The *EZNEC* Ant directory opens. Select the name you just gave to the *Notepad* (.txt) document, and click “*Open*.” This brings the values into the *Wires* Table.

16. If you are working in meters, go to the application and run the various routines. If you are not working with meters, go back to the *Wires* Table, again click “*Other*,” and from the drop-down menu, select “*Change Units, Retain Numbers*,” which opens an annoying stupidity check box that asks if you really want to do that. Select “*Yes*” and a window opens to present a choice of radio buttons. Select the appropriate units and click “*Ok*.” Close the *Wires* Table for now.

The data from the Excel spreadsheet is now in the application. It may be useful to assign a name to the file and then run “*View Antenna*” to look for defects. If all is well, run *Source Data*, *SWR*, antenna patterns, and so on.

If defects are noticed in the view of the antenna, it will be necessary to troubleshoot or debug the *Excel* coordinate generator. Maneuvering the pointer with the mouse to an obviously wrong wire in *View Antenna* of *EZNEC* opens a temporary window that identifies the wire, the end, and its coordinates. This helps the debugging process greatly. Go directly to that wire in the *Excel* spreadsheet and examine the equations to find the problem. Once the coordinate generator has been debugged, repeat the *Copy*, *Paste*, and *Save* process.

If running a series of variations of some input parameter, it is useful to return to the .txt document, under the *Edit* menu click “*Select all*,” and then press the *Delete* key, which leaves a blank document with the name you have chosen. Then return to *Excel*, change the variable, “*Copy*” the new columns of data,

“*Paste*” them into the blank .txt document, and “*Save*” (under the former file name). Then when you jump back into *EZNEC* and open the “*Other*” choice of the *Wires* Table to “*Import From ASCII File*,” the same file name will still be present on the *File Name* line, so all that is needed is to click “*Open*.” This makes it very fast to change variables and run different models quickly.

**Example**

We want to build an optimal three-element cubical quad for the amateur 2-meter band, 144-148 MHz. From reading articles

in *The ARRL Antenna Book*, we know that the driven element (DE) will be close to one full wavelength, the reflector a little longer, and the director a little shorter.<sup>3</sup> We also know that traditional spacing between elements is roughly 0.15 to 0.25 wavelengths for the reflector to DE, and 0.12 to 0.20 for the DE to director. We intend to mount the quad on a chimney whose height we haven’t measured, so we guess it is between 5 and 10 meters above ground. This height (H) of the antenna becomes a global parameter that we can vary until we know its actual height.

Let us use a coordinate axis convention

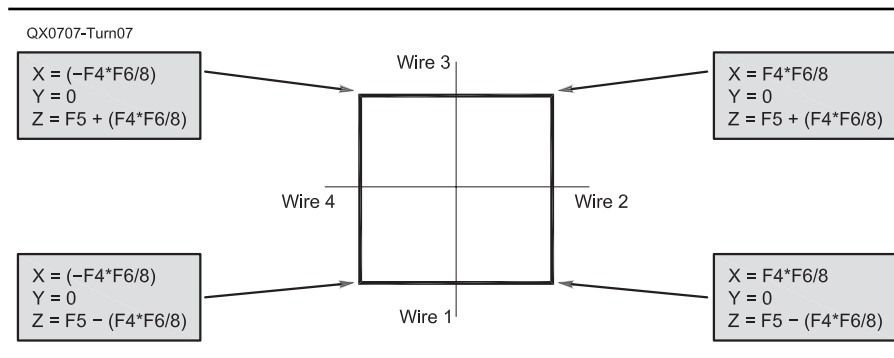


**Figure 7 — Coordinate equations for the reflector.**

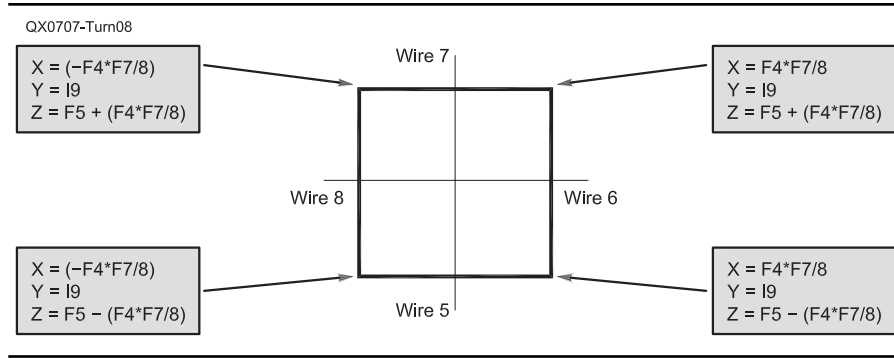


**Figure 8 — Coordinate equations for the driven element.**

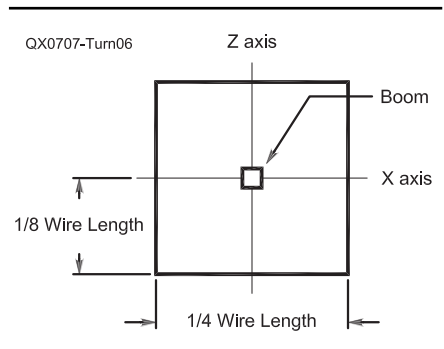


**Figure 6 — Cross section of the reflector in the XZ plane. The boom is at the height H. Y = 0.**

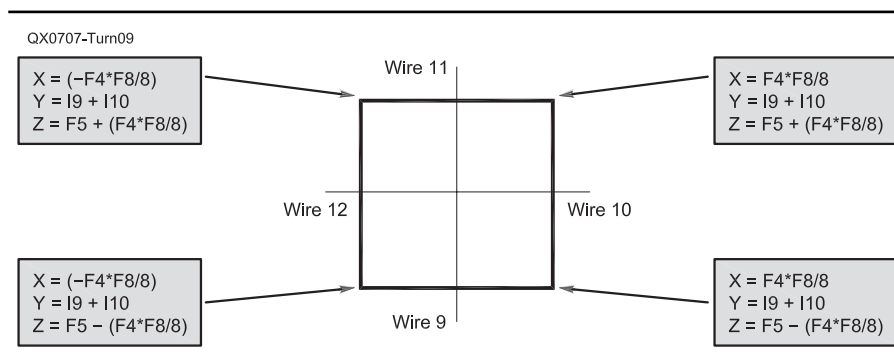


**Figure 9 — Coordinate equations for the director.**

that the X-axis lays East-West, the Y-axis North-South, and the Z-axis is vertical. Europeans use a different convention, which leads to confusion if not explicitly stated. Since we are working at VHF wavelengths, reasonably accurate measurements may be made to the nearest millimeter (mm), so that unit of measurement is chosen.

As design goals, let us specify that we want the antenna to be resonant at or near 146 MHz with an SWR not greater than 1.3:1. Also, at the band edges (144 and 148 MHz) the SWR should be 2.0:1 or less as a preference, and in any case not more than 3.0:1 as an absolute limit. Boresight gain should be at least 10 dBi at an elevation angle not to exceed 20°. Half power beamwidth should not exceed 140° in the horizontal plane and 30° in the vertical plane. Front-to-back ratio should approach 20 dB, but 15 dB is acceptable.

Let us set up the virtual antenna with the reflector in the XZ plane, that is facing North. The reflector is symmetrical about the boom. Let's say that we have chosen 5 wavelengths (10,274 mm) as the initial antenna height, H. Thus H = 10,274 mm is the value of Z at the center of the boom. The coordinates for the center of the boom at the reflector are X = 0, Y = 0, Z = 10,274, or (0,0,10274) as usually written. Please refer to Figure 6.

To perform our antenna modeling experiments, we need to vary the lengths of the wires used in the reflector, driven element, and director, as well as the spacing between elements. Since all are close to one wavelength, we can create a multiplication factor for each wire length. For example, we can start experimenting with reflector wire length that is 1.04 times one wavelength at 146 MHz, or 2137.0 mm long. Since the driven element (DE) should be (so we think at the start) about one wavelength, the DE length factor will be 1.0 at first, for a length of 2054.8 mm. Since the director is shortest, we may choose a length factor of 0.98 to start, for a wire length of 2013.7 mm. In this example, the length factors (1.04, 1.0 and 0.98) will be put into cells **F6**, **F7**, and **F8** respectively for the reflector, DE, and director.

Each of these length factors is a global parameter and integral to the coordinate generating equations.

By inspection of Figure 6, you can see that the X coordinates for the reflector are  $\pm \frac{1}{8}$  wavelength times the length factor for the reflector. Since we calculated the total length as 2137.0 mm,  $\pm \frac{1}{8} \times 2137 = \pm 267.1$  mm. Although the values could be entered directly as the value of X for the different parts of the reflector wire in an *Excel* spreadsheet, this would be some time-consuming hand entry. Thus, we enter the following equations, as appropriate:

$$X = \mathbf{F4} * \mathbf{F6} / 8 \text{ on the right side}$$

Or  $X = (-\mathbf{F4} * \mathbf{F6} / 8)$  on the left side  
Y has a value of zero (0) for the reflector because the wire is in the XZ plane.

The Z coordinate for the reflector is the global height value entered in cell **F5** plus and minus  $\frac{1}{8}$  the length of the reflector wire. Please see Figure 7.

$$Z = \mathbf{F5} + (\mathbf{F4} * \mathbf{F6} / 8) \text{ on the top}$$

$$\text{Or } Z = \mathbf{F5} - (\mathbf{F4} * \mathbf{F6} / 8) \text{ on the bottom}$$

Next the driven element X and Z are calculated in the same fashion, except that we use the global multiplication factor for the DE that is entered in cell **F7**.

$$X = \mathbf{F4} * \mathbf{F7} / 8 \text{ on the right side}$$

$$X = (-\mathbf{F4} * \mathbf{F7} / 8) \text{ on the left side}$$

$$\text{and } Z = \mathbf{F5} + (\mathbf{F4} * \mathbf{F7} / 8) \text{ on the top}$$

$$Z = \mathbf{F5} - (\mathbf{F4} * \mathbf{F7} / 8) \text{ on the bottom}$$

Since the boom runs along the Y-axis, the spacing between the reflector and the driven element becomes the Y value. We can do the calculation once in a cell near the spacing factor, or We could write out the equation for every cell having a Y value. In Figure 7 the equation is put into cell **I9** as “=**F9**\***F4**” so that for the driven element cells for the Y values it is only necessary to enter “=**I9**”.

The director is calculated similarly, except that the global multiplication factor for it is entered in cell **F8**.

$$X = \mathbf{F4} * \mathbf{F8} / 8 \text{ for the right side}$$

$$X = (-\mathbf{F4} * \mathbf{F8} / 8) \text{ for the left side}$$

$$\text{and } Z = \mathbf{F5} + (\mathbf{F4} * \mathbf{F8} / 8) \text{ for the top}$$

$$Z = \mathbf{F5} - (\mathbf{F4} * \mathbf{F8} / 8) \text{ for the bottom}$$

Since the director is located along the Y axis at a distance that is the sum of the two spacings — in other words, the reflector to DE spacing plus the DE to director spacing — the two values must be added. In Figure 8, the value for the DE to director spacing is found in cell **I10**. Thus, the equation for the sum “=**I9**+**I10**” is entered into each cell that represents a Y value for the director.

Figure 9 shows the director layout in equation form.

All that remains to be done in *EZNEC* is to specify the source wire. For horizontal polarization, select Wire 5, and for vertical polarization, either Wire 6 or Wire 8.

## Results

There are five main variables internal to the three-element quad antenna, plus height above ground as a 6<sup>th</sup> variable that affects antenna pattern. Height above ground was set at a constant 5 wavelengths (10,274 mm) for the experiment. The five internal variables are: (1) length of reflector, (2) length of driven element, (3) length of director, (4) spacing between reflector and driven element, and (5) spacing between driven element and director. When working with multiple variables, it is necessary to make certain ones constant while varying the other(s) to ascertain the effect of the limited variation. In this example, lengths of the elements (as controlled by the multiplication factors) were held constant while spacings were systematically varied. Then a new set of element lengths was chosen and held constant while the spacings were again systematically varied.

What we discover from a systematic approach is that certain variables have little effect, some have unexpected effects, and some are fairly important. This experiment was started with a multiplication factor set of (1.05, 0.98 and 0.95) for the elements, and spacings were varied from 0.10 to 0.32 in a matrix. An example of the SWR at 146 MHz is shown in Table 1. Table 1 is not a complete set of results.

Not only is the SWR unacceptably high at all spacings, an SWR plot for each individual run shows that antenna resonance is in the low 150 MHz range. These observations are a clear indication that the DE wire is too short, so it is systematically lengthened for several runs. A set of (1.01, 0.99, 0.95) shows resonance mostly in the low 150 MHz range again. A set of (1.02, 1.01, 0.98) shows resonance in the high 140 MHz values, but well above the 2-meter band. After several other sets, a set of (1.05, 1.02, 0.99) gives SWR values in the 1.2:1 to 1.9:1 range, and resonances just above 146 MHz. Set (1.05, 1.03, 0.99) gives SWR values and resonance figures that show the search is narrowing. See Table 2A, 2B, 2C, 2D, and 2E

Although spacings of 0.24 and 0.20 wavelengths look promising, front-to-back ratio is less than desired. Half power beamwidths of

**Table 1**  
**SWR for 1.05, 0.98, 0.95 Length Factors**

		Wavelength Spacing, Reflector to DE					
		0.10	0.12	0.14	0.16	0.18	0.20
Wavelength Spacing, DE to Director	0.10	4.4	5.4	6.2	6.8	7.2	7.6
	0.12	4.5	5.5	6.3	6.8		
	0.14	4.7	5.7	6.4	6.9		
	0.16	4.8	5.8	6.5	6.9	7.1	7.2
	0.18	5.0	5.9	6.5	6.8	7.0	
	0.20	5.1	6.0	6.5	6.7	6.8	

**Table 2A**  
SWR for Set (1.05, 1.03, 0.99)

Wavelength Spacing, DE to Director	Wavelength Spacing, Reflector to DE			
	0.18	0.22	0.24	0.26
0.18	1.2	1.2	1.2	1.2
0.20	1.1	1.0	1.1	1.1
0.22	1.2	1.1	1.2	1.2
0.24	1.3	1.3	1.4	1.4

**Table 2B**  
SWR at Band Edges

Wavelength Spacing, DE to Director	Wavelength Spacing, Reflector to DE			
	0.18	0.22	0.24	0.26
0.18	2.8, 2.2	2.7, 2.1	2.7, 2.0	2.7, 2.0
0.20	2.5, 2.5	2.4, 2.4	2.4, 2.4	2.4, 2.4
0.22	2.3, 2.9	2.2, 2.8	2.1, 2.7	2.1, 2.7
0.24	2.1, 3.3	1.9, 3.2	1.9, 3.1	1.9, 3.1

**Table 2C**  
Resonance in MHz

Wavelength Spacing, DE to Director	Wavelength Spacing, Reflector to DE			
	0.18	0.22	0.24	0.26
0.18	146+	146.5	146.5	146.5
0.20	146	146	146	146
0.22	145.5+	145.5	145.5	145.5
0.24	145.5	145.5	145.5	145.5

**Table 2D**  
Gain in dBi

Wavelength Spacing, DE to Director	Wavelength Spacing, Reflector to DE			
	0.18	0.22	0.24	0.26
0.18	14.4	14.4	14.4	14.4
0.20	14.5	14.5	14.5	14.5
0.22	14.6	14.6	14.6	14.5
0.24	14.6	14.6	14.6	14.6

**Table 2E**  
Front to Back Ratio in dB

Wavelength Spacing, DE to Director	Wavelength Spacing, Reflector to DE			
	0.18	0.22	0.24	0.26
0.18	14.8	13.7	12.8	12.8
0.20	13.3	12.2	11.5	11.5
0.22	11.8	10.9	10.2	10.2
0.24	10.5	9.7	9.1	9.1

121° and 21° are found for every combination of spacings, so are not shown in tabular form. A slightly longer reflector element is indicated, so a set of (1.06, 1.03, 0.99) is modeled next. Tables 3A through 3E show that progress is being made.

Most of these spacing combinations give quite good results, but F/B is just a little smaller than desired, so the set (1.07, 1.03, 0.99) is run, more out of curiosity than anything else. Tables 4A through 4E set forth the results.

Optimization decisions always involve trade-offs. What seems best to one, may not to another. A person operating in a noisy environment might tend to favor an antenna with a high F/B ratio. A person using limited transmit power might prefer higher gain. A station with a long run of lossy coax might be best served by an antenna with a low SWR. One should note that gain is essentially the same for all the different lengths and spacings, as is the half power beamwidth in both horizontal and vertical planes. Thus, they are not issues. SWR (thus resonant frequency) and F/B are the only characteristics that are much affected by changing the parameters. We found that reflector to DE spacings of 0.20 to 0.22 and DE to director

spacings of 0.18 to 0.20 work best for set (1.06, 1.03, 0.99), and 0.22 to 0.24 spacings with 0.18 to 0.20 spacings, respectively, work best for set (1.07, 1.03, 0.99). All of them meet the set of specifications that were established in the Example section near the beginning. The author would personally choose the set with wire lengths of (1.07 λ, 1.03 λ, 0.99 λ) and reflector to DE spacing of 0.22 λ and DE to director spacing of 0.18 λ.

**Conclusion**

If you are new to modeling or to the use of *Excel* spreadsheets, do not despair. It took me years of learning bits and pieces of *Excel* along the way to become fairly seasoned. In recent months, however, I have written one coordinate generator that uses over 34,000 cells that include almost 700 logical statements (for an antenna with interesting properties that basically doesn't work), a mesh model for a military HMMWV (humvee) that takes over 30,000 cells, and a mind bender of a coordinate generator for a log planar spiral antenna that uses a mere 6,000 cells and interesting mathematics.

When using some of the mega spreadsheets, processing time for the computer

grows long. Waiting a half hour for an SWR plot of 10 points can become routine. But the beauty of the beast lies in the enormous savings of time. Some of the coordinate generators may take a week of full time work to produce, but once finished, they allow me to run dozens of variations quickly.

**Notes**

<sup>1</sup>The *Excel* file for the three element cubical quad antenna used in this example is available for download from the *QEX* Web site. Go to [www.arrrl.org/qexfiles](http://www.arrrl.org/qexfiles) and look for the file **7x07\_Turner.zip**.

<sup>2</sup>Array addition, subtraction, multiplication, and division are also possible. Do an *Excel* search on "ARRAY" for a complete explanation.

<sup>3</sup>R. Dean Straw, N6BV, *The ARRL Antenna Book*, 21<sup>st</sup> edition (Newington: 2007), p 18-41. *The ARRL Antenna Book* is available from your local ARRL dealer, or from the ARRL Bookstore, ARRL order no. 9876. Telephone toll-free in the US 888-277-5289, or call 860-594-0355, fax 860-594-0303; [www.arrrl.org/shop](http://www.arrrl.org/shop); [pubsales@arrrl.org](mailto:pubsales@arrrl.org).

*Brian Turner was first licensed as KN2SJM in 1955, and upgraded to K2SJM in 1956. He has held an Amateur Extra class license since the early 1980s. He has had a diverse career path, first as a scientist with a PhD*

**Table 3A**  
SWR for Set (1.06, 1.03, 0.99)

		Wavelength Spacing, Reflector to DE			
		0.20	0.22	0.24	0.26
Wavelength	0.18	1.1	1.1	1.1	1.2
Spacing, DE	0.20	1.1	1.06	1.1	1.2
to Director	0.22	1.3	1.3	1.3	1.4

**Table 4A**  
SWR for Set (1.07, 1.03, 0.99)

		Wavelength Spacing, Reflector to DE		
		0.22	0.24	0.26
Wavelength	0.18	1.1	1.2	1.3
Spacing, DE	0.20	1.2	1.2	1.3
to Director	0.22	1.4	1.4	1.5

**Table 3B**  
SWR at Band Edges

		Wavelength Spacing, Reflector to DE			
		0.20	0.22	0.24	0.26
Wavelength	0.18	2.4, 2.2	2.4, 2.1	2.4, 2.1	2.4, 2.0
Spacing, DE	0.20	2.2, 2.5	2.2, 2.5	2.2, 2.4	2.2, 2.4
to Director	0.22	2.0, 2.9	1.9, 2.9	1.9, 2.8	1.9, 2.8

**Table 4B**  
SWR at Band Edges

		Wavelength Spacing, Reflector to DE		
		0.22	0.24	0.26
Wavelength	0.18	2.2, 2.1	2.3, 2.0	2.3, 2.0
Spacing, DE	0.20	2.0, 2.4	2.0, 2.4	2.1, 2.4
to Director	0.22	1.7, 2.8	1.8, 2.8	1.8, 2.8

**Table 3C**  
Resonance in MHz

		Wavelength Spacing, Reflector to DE			
		0.20	0.22	0.24	0.26
Wavelength	0.18	146+	146+	146.5	146.5
Spacing, DE	0.20	146	146	146	146
to Director	0.22	145.5	145.5	145.5	145.5

**Table 4C**  
Resonance in MHz

		Wavelength Spacing, Reflector to DE		
		0.22	0.24	0.26
Wavelength	0.18	146+	146+	146.5
Spacing, DE	0.20	145.5+	146-	146-
to Director	0.22	145.5-	145.5-	145.5

**Table 3D**  
Gain in dBi

		Wavelength Spacing, Reflector to DE			
		0.20	0.22	0.24	0.26
Wavelength	0.18	14.4	14.4	14.4	14.4
Spacing, DE	0.20	14.5	14.5	14.5	14.5
to Director	0.22	14.6	14.6	14.6	14.6

**Table 4D**  
Gain in dBi

		Wavelength Spacing, Reflector to DE		
		0.22	0.24	0.26
Wavelength	0.18	14.3	14.4	14.4
Spacing, DE	0.20	14.4	14.5	14.4
to Director	0.22	14.5	14.5	14.5

**Table 3E**  
Front-to-Back Ratio in dB

		Wavelength Spacing, Reflector to DE			
		0.20	0.22	0.24	0.26
Wavelength	0.18	26.9	21.6	18.6	16.6
Spacing, DE	0.20	22.5	18.6	16.3	14.7
to Director	0.22	19.0	16.2	14.4	13.1


**Table 4E**  
Front-to-Back Ratio in dB

		Wavelength Spacing, Reflector to DE		
		0.22	0.24	0.26
Wavelength	0.18	28.6	24.0	20.6
Spacing, DE	0.20	23.4	20.2	17.9
to Director	0.22	20.0	17.6	15.8

in geology (1967) with emphasis on applied physics and math, and later earning a JD (1974) and being admitted to the New York State Bar in 1975. In 1985 he went into RF engineering with a defense contractor. When the Cold War abated, he entered the wireless

phone industry as a network design engineer, consulting in several areas of the US, living in Canada for a year, and acting as the Associate Director of the European Wireless Institute in the Netherlands. He currently works for a major US defense contractor as

an RF engineer, where he does a good deal of RF propagation modeling.

Dr. Turner authored "A Programmable Calculator Azimuth-Elevation-DX Routine," which was published in *The ARRL Antenna Compendium, Volume 5*. 



## Reversible Wire Beams for Lower HF Use

Rotatable directional beams for the lower HF region (from 30 meters downward) tend to be rare, heavy and expensive. Many operators choose instead to use wire beams, despite their fixed orientation. One partial way around the limitation is to build a reversible wire beam. We can accomplish this feat with varying degrees of electrical complexity by switching sections of elements or using loading components.

In these notes, we shall examine five different but interrelated ways of achieving the goal of reversibility with the minimum of complexity. Some designs may require more real estate, but basic construction will only involve stringing and supporting elements. Any remote switching that we do will occur outside the antenna geometry. We shall look at two designs that use shorted stubs to load driver elements to become electrically long enough to serve as reflectors in 2-element beams: one Moxon rectangle and one Yagi. Then we shall look at an alternative reversible 2-element Yagi that requires three wires. The next step is to extend that technique to a 3-element Yagi with five wires. Finally, we shall reduce the wire count to four, using an idea passed along to me by Bill Desjardins, WIZY.

## Some Directional Beam Basics

Although we may apply the general ideas in these notes to any of the bands in the lower HF region (or even to 160 meters), we shall focus on 40 and 30 meters, using test frequencies of 7.15 and 10.125 MHz. 30 meters is a band that is ideal for a reversible wire beam, because we can usually manage a 50 foot height. However, the band is so narrow that we do not receive a full impression of wire-beam capabilities and limitations unless we also include 40 meters.

One limitation of horizontal beams is strictly frequency-related. The height of a beam determines to a significant measure its performance potential, and we measure the height in wavelengths. In the lower HF region, height is normally a fraction of a wavelength, since even at 30 meters, a wavelength is about 100 feet. At 40 meters, that same 100 feet is only about  $0.7 \lambda$ . Figure 1 shows selected elevation patterns at different heights from  $0.25 \lambda$  up to  $1.0 \lambda$  for a 2-element Yagi. At the lowest height, the beam is best used as a directional NVIS antenna. The lowest usable height for reliable DX work may be about  $\frac{3}{8} \lambda$ . Table 1 provides performance data at  $0.125 \lambda$  increments.

Note that the rise in forward gain is not smooth as we increase height. As well, the

front-to-back ratio fluctuates with height, reaching its maximum value at  $\frac{1}{2} \lambda$  intervals beginning at  $\frac{3}{8} \lambda$  (with the second maximum value at about  $\frac{7}{8} \lambda$ ). The value curves grow ever smoother as we exceed a  $1 \lambda$  height, but such heights are impractical for most reversible wire beam builders.

The performance we can obtain depends on the beam that we select. Most wire antenna beam builders choose a directional beam over a bidirectional antenna to obtain freedom from rearward QRM. Different beam designs are better or worse in this department. Figure 2 shows the elevation and azimuth patterns of three different beams at a height that maximizes the front-to-back ratio:  $\frac{3}{8} \lambda$ . The standard 2-element Yagi barely achieves

12 dB. The Moxon rectangle and the 3-element Yagi do far better. Similar relationships would show up at all heights, but the patterns for a height of  $\frac{3}{8} \lambda$  are simply more vivid. As we shall see, however, the front-to-back ratio will not be our only consideration if we choose to build a reversible beam.

All wire beams will fail to cover a band as wide as 40 meters. Figure 3 overlays 50  $\Omega$  SWR patterns for the three subject beams. The Moxon rectangle and the 2-element Yagi have natural 50  $\Omega$  feed point impedances. For greater gain in the 3-element Yagi, I selected a design with a 30  $\Omega$  feed point impedance and fitted it with a Regier series matching system using 50  $\Omega$  and 75  $\Omega$  cables to arrive at 50  $\Omega$ . However, the SWR curve does not

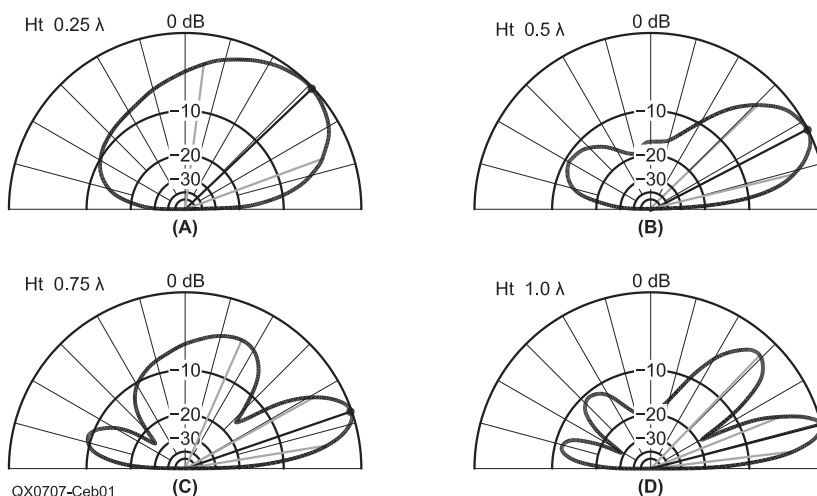
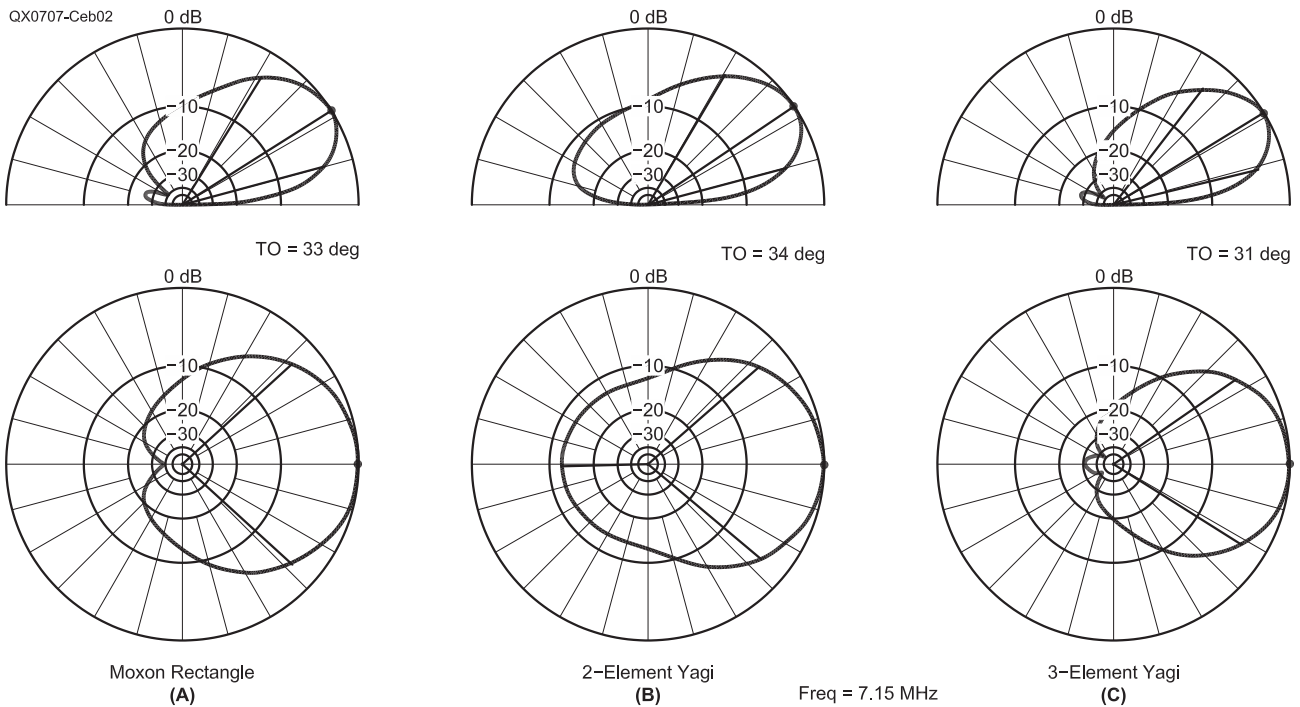


Figure 1 — Elevation patterns for a 2-element Yagi at various heights from  $0.25 \lambda$  up to  $1.0 \lambda$  showing the effects of beam height on performance.

Table 1  
Antenna Height Versus Performance for a 2-Element Yagi (Sampled at 10.125 MHz)

Height above Ground ( $\lambda$ )	Max. Gain (dBi)	TO Angle (Degrees)	Front-Back Ratio (dB)	Hor. BW (Degrees)
0.125	5.50	57	4.79	125
0.25	8.41	44	8.81	88
0.375	9.58	34	12.17	79
0.5	10.50	26	11.07	76
0.625	10.85	21	8.68	74
0.75	10.82	18	9.29	72
0.875	10.85	16	11.14	71
1.0	11.14	14	11.11	72

Notes: Maximum forward gain includes ground reflections. TO angle is the elevation angle of maximum field strength. Front-to-back ratio is the  $180^\circ$  value. Hor. BW is the horizontal beamwidth in degrees.



**Figure 2 — Elevation and azimuth patterns of three subject beams at  $\frac{1}{8} \lambda$  above ground.**

significantly change its 2:1 SWR bandwidth in the conversion. All three beams manage to cover a little over half of 40 meters. Hence, for most bands (with the exception of the 50 kHz 30 meter band), the builder will have to select a preferred portion of the band. Unlike simple dipoles, the directional beams will change their gain and front-to-back properties with frequency within any of the wider bands. Two-element (reflector-driver) beams shows a descending gain with rising frequency, while a beam with at least one director will show rising gain with increasing frequency. Perhaps the more critical parameter is the front-to-back ratio, which tends to go to pot for the subject beams at about the limits of the 2:1 SWR values.

The final factor that limits the utility of a reversible beam is geographic. Reversible beams are useful only if there are desired communications target areas at approximate 180° bearings relative to the beam. In Tennessee, a reversible beam would cover most of Europe on one side and the VK and ZL regions in the other. Only if you are comparably situated should you consider a reversible beam.

### The Survey Elements

Our short survey of techniques of easily reversing beams will use four elements. Of course, there will be text, along with a general outline of the beam under discussion. The outline graphic will also show a

QX0707-Ceb03

Comparative 50 Ω SWR Bandwidths  
Moxon Rectangle, 2-Element Yagi, 3-Element Match Yagi  
Free-Space Environment

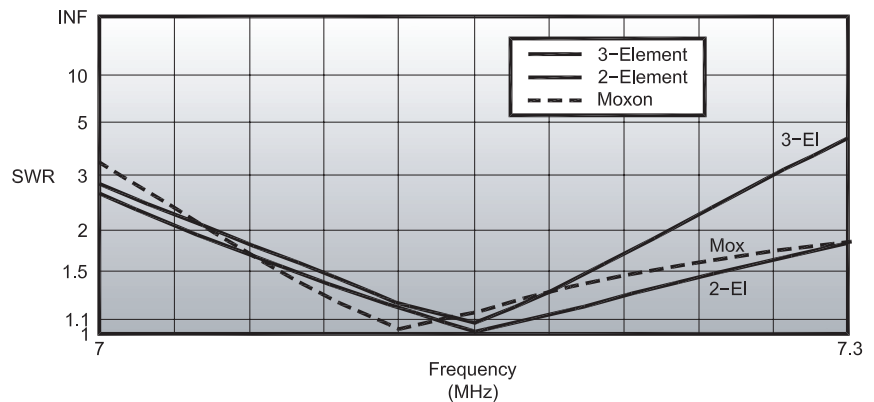


**Figure 3 — 40-meter 50 Ω SWR curves for three subject wire beams in a free space environment. The 3-element beam is matched to 50 Ω from its inherent 30 Ω feed point impedance. The other two beams have natural 50 Ω impedances. Reversible versions of these beams will not alter the basic SWR curves.**

free-space E-plane pattern for reference and comparison apart from any particular height above ground. We shall also examine parts of two tables. Table 2 lists the dimensions of each beam, while Table 3 provides free space performance data at the design frequencies.

All modeled wire beam designs in Table 2 use #12 copper wire. Design techniques call

for slightly different dimensions for the 30 and 40 meter Moxons, even when you measure the elements in terms of wavelengths. However, for the wire Yagis, you may use the same dimensions in wavelengths on both bands. If you design the Yagis for 40 meters, you may simply scale the element lengths and the spacing values for 30 meters. The failure

to compensate for the constant element diameter only lowers the resonant frequency a bit on 30 meters, but the 50 Ω SWR does not reach 1.5:1 on this narrow band. On 40 meters, the design frequency is 7.15 MHz. You may rescale the design upward or downward within the band without regard to the element diameter and not incur any adverse effects.

The free space performance values in Table 3 allow a direct comparison from one beam's potential to another's. The top section of the table provides data on the modeled performance of nonreversible forms of each beam to permit an evaluation of the performance of reversible versions. You may revise the EZNEC models to place each beam at the height that you plan to use before you reach any final conclusions.<sup>1</sup> The Yagi performance data include some special entries labeled "Unused Driver Open" and "Unused Driver Shorted." I will explain those notations as we move through the various Yagi designs.

### The Stub Loaded 2-Element Moxon Rectangle

The Moxon rectangle is a 2-element driver-reflector parasitic beam that uses two forms of element coupling to arrive at the design-frequency patterns shown in Figure 4. Not only do we have coupling between the parallel portions of the elements, but as well between the ends of the element tails. For versions of the rectangle requiring a 50 Ω feed point impedance and using a uniform element diameter throughout, a design aid is available in the form of a spreadsheet at

<sup>1</sup>Models for the antennas discussed in this "Antenna Options" column are available in EZNEC format at the QEX Web site. Go to [www.arrl.org/qexfiles](http://www.arrl.org/qexfiles) and look for 7x07\_AO.zip.

**Table 2**  
Master Dimension List for 40-Meter and 30-Meter Beams Used in These Notes. All Elements are AWG #12 Copper Wire.

#### Moxon Rectangles (See Figure 4)

40 Meters			30 Meters		
Dimension	Wavelengths	Inches	Dimension	Wavelengths	Inches
A (width)	0.3652	602.8	A (width)	0.3648	425.3
B (front-back)	0.1209	199.6	B (front-back)	0.1206	140.6
C (tails)	0.0562	92.8	C (tails)	0.0559	65.2
D (gap)	0.0085	14.0	D (gap)	0.0089	10.3

#### 2-Element Yagis (Basic and 3-Wire Back-to-Back Versions)

Dimension	Wavelengths	40 Meters	30 Meters
		Inches	Inches
Driver length	0.477	787.4	556.1
Reflector length	0.508	838.6	592.2
Spacing	0.146	241.0	170.2

#### 2-Element Yagi Stub-Loaded

Both elements	0.477	787.4	556.1
Spacing	0.155	255.9	180.7

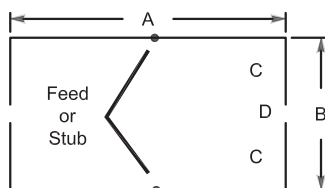
#### 3-Element Yagis (Basic and 5-Wire Back-to-Back Versions)

Dimension	Wavelengths	40 Meters	30 Meters
		Inches	Inches
Director length	0.464	766.0	540.9
Driver length	0.486	802.3	566.5
Reflector length	0.502	828.7	585.2
Spacing: dir-dr	0.174	217.2	202.8
Spacing: dr-ref	0.151	249.3	176.0
Spacing: total (basic)	0.325	536.5	378.9
Spacing: total (bk-bk)	0.650	1073.0	757.9

#### 3-Element Yagis (4-Wire Version)

Dimension	Wavelengths	40 Meters	30 Meters
		Inches	Inches
Director length	0.464	766.0	540.9
Reflector/driver length	0.502	828.7	585.2
Spacing: dir-dr/ref	0.174	217.2	202.8
Spacing: dr/ref-dr/ref	0.151	249.3	176.0
Spacing: total (dir-dir)	0.499	823.7	581.7

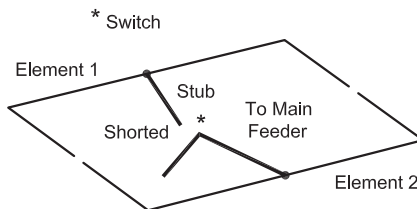
Basic Outline



(A)

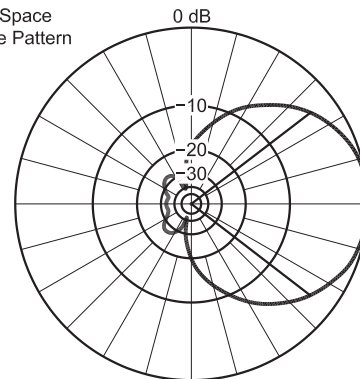
QX0707-Ceb04

Using Stubs to Reverse Directions



(B)

Free Space E-Plane Pattern



(C)

**Figure 4** — The general scheme of a reversible wire Moxon rectangle, showing the designations for its dimensions, the use of transmission line stubs to reverse directions and a free space E-plane pattern.

[www.cebik.com/trans/ant-design.html](http://www.cebik.com/trans/ant-design.html). (The spreadsheet also contains design aids for monoband quad beams and 3-element Yagis.)

Ordinarily, the Moxon rectangle reflector tails are longer than shown in Figure 4 and in Table 2. However, to make the beam reversible, we use two identical driver elements along with the prescribed gap between element tails. To the center of each element we connect a section of 50 Ω coaxial cable. At any one time, one section of cable connects to the main feed line, also a 50 Ω cable. The other section we short to form a  $j\ 65\ \Omega$  inductive reactance. On 40 meters, the stub's electrical length is 240.4 inches, while on 30 meters, the electrical length is 140.6 inches. Both lengths of coax are more than long enough to reach a center point, even using a cable with a 0.66 velocity factor (and shortening the physical length accordingly). Since the cables are for independent elements, a remote DPDT switch or relay changes each coax function. It is possible to use long lines that reach the shack for these functions. By careful calculation (including the line's velocity factor), we can determine long line lengths that will serve as the required stub. In fact, we can also make the lines long and tune out the excess inductive reactance with a capacitor. This type of system would place all switching inside the warmth of the shack. However, these refinements are beyond the scope of these introductory notes.

As shown in the performance data in Table 3, the one drawback of using stubs to reverse the direction of a wire Moxon rectangle is a decrease in the feed point impedance. The resistive impedance drops by about 8 Ω relative to an independent version of the antenna. Squaring the rectangle a small amount by shorting dimension A and increasing the tail length, C, of both elements would raise the impedance, but at a slight cost in forward gain, plus a refiguring of the required shorted stub reactance.

### The Stub Loaded 2-Element Yagi

We may apply the same technique to a 2-element Yagi, as shown in Figure 5 and in the tables. Because we wish to preserve the 50 Ω impedance of the array once we install a coax section on each driver element, we increase the element spacing from  $0.146\ \lambda$  to  $0.155\ \lambda$ . The shorted reflector stub provides  $j\ 75\ \Omega$  inductive reactance. On 40 meters, the coax length is 258.8 inches, while on 30 meters, the length is 182.3 inches. The two coaxial cable lengths allow an easy mid-point meeting for switching cable functions from driver to stub and back again.

The switched version of the antenna slightly outperforms the independent 2-element Yagi for interesting reasons. First, the physical proportions of the elements differ. Second, a loaded reflector provides slightly better

front-to-back values than a full-size reflector. Nonetheless, we would be very hard-pressed to notice the difference in operation.

Whether you choose a Moxon rectangle or a Yagi, the stub loaded switched beam provides the most compact route to a reversible beam. I have seen 3-element Yagis with switched elements, normally a function swap

between the director and the reflector. Often such beam use open stubs for the director to provide capacitive reactance to shorten the element's electrical length. The driver remains unswitched. Hence, each parasitic element switches between open and shorted modes, with potential length changes for each mode. Since these cables are weighty,

**Table 3**  
**Comparative Performance Tables: All Values for Free-Space Environment**

Antenna	Band (Meters)	Max. Gain (dBi)	Front-Back Ratio (dB)	Impedance ( $R \pm jX\ \Omega$ )
<b>Basic Antennas</b>				
Moxon	40	5.87	36.45	$53.5 + j2.5$
	30	5.88	36.69	$53.9 + j3.1$
2-El. Yagi	40	5.62	10.16	$49.8 - j1.0$
	30	5.67	10.25	$49.4 + j2.2$
3-El. Yagi	40	7.66	25.13	$50.9 + j3.6^*$
	30	7.77	24.67	$47.2 + j3.1^*$
<b>Reversible Antennas</b>				
Moxon-Stub	40	5.92	35.69	$46.1 + j3.3$
	30	5.95	36.84	$45.6 + j3.2$
2-El. Yagi w/Stub	40	6.02	10.75	$47.2 + j1.0$
	30	5.96	10.81	$48.6 + j4.2$
2-El Yagi 3-Wire Unused Dr.	40	6.21	7.73	$48.6 + j2.4$
	30	6.24	8.01	$48.4 + j3.5$
2-El Yagi 3-Wire Shorted	40	5.62	10.07	$49.8 - j1.0$
	30	5.68	10.18	$49.4 + j2.2$
3-El Yagi 5-Wire Unused Dr.	40	7.67	24.15	$32.2 + j1.0^*$
	30	7.78	25.01	$30.4 + j2.5^*$
3-El Yagi 5-Wire Shorted	40	7.73	26.79	$32.2 + j1.0^*$
	30	7.84	27.33	$30.4 + j2.6^*$
3-El Yagi 4-Wire	40	7.73	22.77	$35.4 + j53.5^*$
	30	7.84	22.99	$33.5 + j52.9^*$

Notes: Basic 3-element Yagi impedance is after application of a Regier series match. Impedance values for reversible 3-element Yagis are prior to matching. Front-to-back values are for 180°.

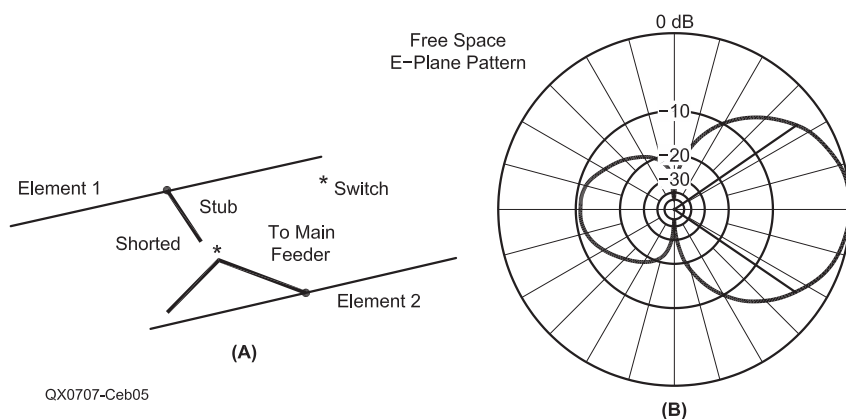


**Figure 5 — The general scheme for a reversible wire 2-element Yagi using transmission line stubs to reverse directions, with a free space E-plane pattern.**



some designs have used lumped components. In most cases, the switch systems are more complex than the ones used for the 2-element beams. As well, few Yagi 3-element designs provide peak performance with equal spacing between each pair of elements, and very often they also require a matching network to raise a low feed point impedance (perhaps 25 Ω) to the main feed line value. We may keep our switching simple if we have enough land to add some further wire elements.

### The 3-Wire 2-Element Yagi

One way to simplify switching is to begin with a common reflector element. For 2-element Yagis, we then add a driver on each side of the reflector. As shown in Table 2, the spacing of the elements returns to the value of the independent beam. The net result, as shown in Figure 6, is essentially two 2-element Yagis with a common reflector. Instead of switching stub lines for loading, this design simply switches the feed line. We can handle this task at the antenna level or we can bring the two feed lines to the shack and use a simple mechanical switch.

The 2-element reflector-driver Yagi has a limitation. As shown by the modeled data in Table 3, the performance changes according to whether the unused driver is shorted across the feed point or left open. The open connection provides the better front-to-back ratio. (The free-space E-plane pattern in Figure 6 shows the results of an open unused driver.) When the front-to-back ratio depends wholly on a reflector element, the unused element exerts a greater effect on the reflector performance (that is, on the current magnitude and phase angle), than when we have a parasitic beam with at least one director.

Obtaining an open condition in the unused driver is a simple matter electrically if we switch at the antenna level. However, the arrangement may prove to be mechanically complex. We may also achieve the desired condition with a switch at the shack end of the feed lines if we attend to the cable lengths. If the feed lines are an odd multiple of a quarter-wavelength, then shorting the unused line will produce an open circuit at the feed point. An even multiple of a quarter-wavelength will require an open line end to yield an open circuit at the feed point. (In calculating the line lengths, of course, be sure to include the line's velocity factor.)

### The 5-Wire 3-Element Yagi

The 3-wire reversible beam for 2-element Yagis now becomes a 5-wire reversible beam for 3-element Yagis. Such an array requires considerable open ground, as the dimensions in Table 2 and the outline in Figure 7 reveal. In the process, we gain an advantage but acquire a disadvantage.

The "bad" news first: to make the effort of

installing a 3-element wire beam worthwhile, we need to select a design that provides significant gain over the 2-element Yagis. The data in Table 3 show that the design provides

1.5 to 2 dB additional forward gain over either 2-element beam. In the process, the feed point impedance drops to about 30 Ω. Therefore, we require a matching system to reach 50 Ω to

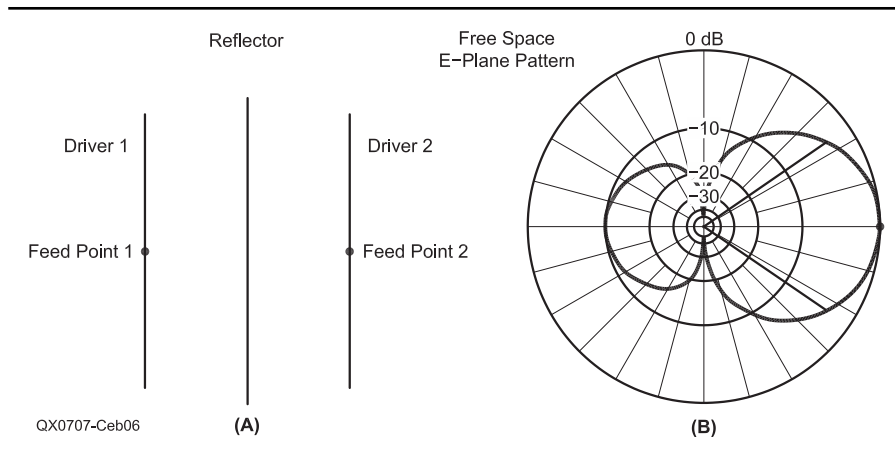


Figure 6 — The general scheme of a reversible 2-element Yagi using three wires; that is, separate drivers and a common reflector, with a free space E-plane pattern.

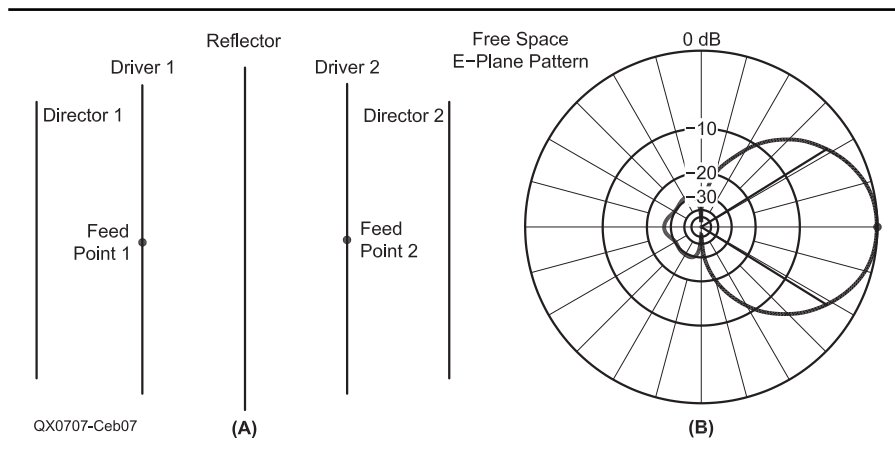


Figure 7 — The general scheme of a reversible 3-element Yagi using five wires; that is, separate drivers and directors with a common reflector, with a free space E-plane pattern.

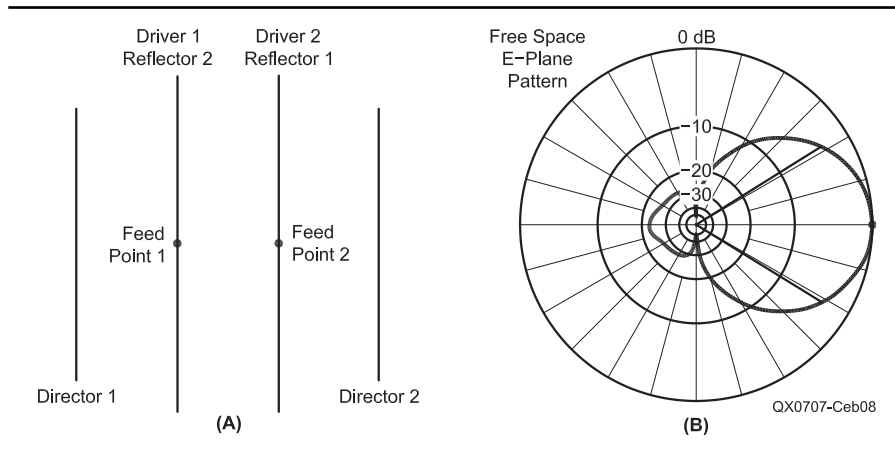


Figure 8 — The general scheme of a reversible 3-element Yagi using only four wires, with separate directors and "tradable" reflectors and drivers, with a free space E-plane pattern.



achieve the widest possible operating bandwidth. We can easily achieve the match using common 50  $\Omega$  and 75  $\Omega$  coaxial cable sections in a Regier series match. We shall not go into the required calculations for this type of match in this set of notes. However, you can download a spreadsheet that includes the Regier series match within a collection of common matching systems at [www.cebik.com/trans/ant-match.html](http://www.cebik.com/trans/ant-match.html). (The collection includes three types of series matches, the beta match, two versions of gamma-match calculations, and the match line-and-stub system. Like the antenna design aid, the spreadsheet appears in both *Quattro Pro* and *Excel* formats.) The series matching system transfers matching complexities from the feed point junction to the transmission line itself. Therefore, it adds no further weight to the system.

The "good" news is that the front-to-back ratio of a 3-element Yagi is largely a function of the director and not the reflector element. Therefore, as is clear from the data in Table 3, the state of the unused feed point makes almost no difference to the array performance in either direction. With a series match in place, it is likely that switching at the shack may be the easiest way to handle directional changes for the array.

#### The 4-Wire 3-Element Yagi

W1ZY determined that he did not have the real estate needed for the 5-wire beam. He also reasoned that he could feed the driver with parallel transmission line and use his antenna tuner to arrive at the impedance needed by his equipment. Therefore, he opted for the scheme shown in Figure 8. As the free-space E-plane pattern suggests, he lost no performance in his truncated 4-wire version of the reversible 3-element Yagi.

The dimensions in Table 2 reveal that the elements consist of two directors and two "reflectors." I place the word reflector in quotation marks, because each of these two elements trades functions as we swap directions. One of the two elements becomes a reflector. The element between it and a director becomes the driver. The driver length makes little difference to beam performance. (In fact, J-poles have been used as 3-element Yagi drivers.) Driver length becomes critical only if we are seeking a particular feed point impedance. In this design for a reversible beam, parallel feed line allows the use of a driver impedance with a considerable reactive component. Therefore, we may do the work of five elements with only four and still obtain full 3-element Yagi performance in each direction.

For optimal performance, we must observe some cautions with the 4-wire reversible beam. First, in order to function correctly as a reflector, the unused driver must be shorted across the feed point by a relay or by a precisely cut line. With the reflector open at the center, the

beam loses almost a full dB of forward gain and most of the high front-to-back ratio shown in the free-space E-plane pattern in Figure 8.

Second, as the SWR increases at the feed point, even low-loss parallel lines begin to show detectable losses. The values at the feedpoint (about  $35 + j 50 \Omega$ ) are not fatal. But losses over a 100-foot length of line may exceed 0.5 dB. As well, the values that appear at the tuner terminals may exceed its matching range. At 40 meters, the use of one of the modern low-loss coax cables may prove able to equal parallel line loss, with an easier match at the tuner. In addition, low-loss coax lines need no spacing between each other to prevent unwanted coupling. Nevertheless, in both cases, the lines require cutting to a length that — with the switching system used — will ensure a closed circuit at the active reflector (inactive driver) center.


#### Conclusion

We have looked at five of many variations on the theme of creating a reversible horizontal wire beam for the lower HF region. The options that we explored are among the simplest electrically, although some of them required a considerable open area for implementation. The chief goal of these notes has been to show that for the budget minded operator with a penchant for using wire, a reversible beam is not only possible, but both feasible and practical.

However much we tried to simplify the designs, we could not eliminate all electrical complexities. A reversible beam requires a switch somewhere along the line to change

directions. As well, the unused element or the loading stub require attention to both line length and the switched condition at the line end. These matters are generally considerations that we wrestle with during installation. When operating, we may change directions as quickly as we can flip a switch.

There are numerous variations on the designs shown as examples. Perhaps the most common tendency would be to think of the elements in the form of inverted-Vs. This option has two constraints and one advantage. The advantage is the ability to provide a strong support along the centerline for the cable hanging from the elements. One of the constraints is the necessity to redesign the elements to suit the new configuration. To base the design on a few guesses derived from the linear designs shown here or elsewhere seems a bit careless when good design tools are readily available.

The second constraint concerns performance. Inverted-V elements will reduce the front-to-side ratio of the beam patterns. In addition, V elements will also lower the effective height of the antenna. In the lower HF region, we are already height-challenged with respect to obtaining a low enough elevation angle for superior DX performance. At a certain (unspecified) point, lowering the ends of a horizontal beam may elevate the takeoff (TO) angle too much. In such cases, you might wish to consider one of the many directional vertical arrays, especially below 40 meters. Reversible beams are both possible and practical, but they will not overcome the limits that we briefly examined at the beginning of these notes. 

## ELECTRONICS OFFICER TRAINING ACADEMY

### The Complete Package To Become A Marine Radio Officer/Electronics Officer

ELKINS, with its 54-year history in the radio and communications field, is the only school in the country providing all the training and licensing certification needed to prepare for the exciting vocation of Radio Officer/Electronics Officer in the Merchant Marines.

**Great Training | Great Jobs | Great Pay**



Call, Fax or Email for More Information:

**ELKINS Marine Training International**

P.O. Box 2677; Santa Rosa, CA 95405

Phone: 800-821-0906, 707-792-5678

Fax: 707-792-5677

Email: [info@elkinsmarine.com](mailto:info@elkinsmarine.com)

Website: [www.elkinsmarine.com](http://www.elkinsmarine.com)

# Upcoming Conferences

## 41st Annual Central States VHF Society Conference

July 26-29, 2007, San Antonio, TX  
Omni Hotel

### Call for Papers

The Central States VHF Society is soliciting papers, presentations, and poster displays for the 41st Annual CSVHFS Conference on 26-28 July, 2007. Papers, presentations, and posters on all aspects of weak-signal VHF and above amateur radio are requested. You do not need to attend the conference, nor present your paper, to have it published in the proceedings. Posters will be displayed during the two days of the conference.

**Topics of interest include** (but are not limited to):

**Antennas** including modeling/design, arrays and control

**Test Equipment** including homebrew, using and making measurements

**Construction** of equipment, such as transmitters, receivers and transverters

**Operating** including contesting, roving and DXpeditions

**RF power amps** including single band and multiband vacuum tube and solid-state

**Propagation** including ducting, sporadic E, tropospheric and meteor scatter, etc

**Pre-amplifiers** (low noise)

**Digital Modes** WSJT, JT65, etc

**Regulatory topics**

**EME**

**Software-defined Radio (SDR)**

**Digital Signal Processing (DSP)**

Generally, topics not related to weak signal VHF, such as FM repeaters and packet radio, are not accepted for presentation or publication. There are always exceptions, however. Please contact either Lloyd Crawford, N5GDB or Thomas Visel, NX1N at the email addresses below.

### Deadline for Submissions

For the proceedings: Monday, 7 May 2007.

For presentations to be delivered at the conference: Monday, 2 July 2007.

For notifying us that you have posters to display at the conference: Monday, 2 July 2007. Bring your poster with you on July 26.

Further information is available at the CSVHFS web site ([www.csvhfs.org](http://www.csvhfs.org)). See

“The 2007 Conference,” “Guidance for Proceedings Authors,” “Guidance for Presenters” and “Guidance for Table-top/Poster Displays.”

### Contacts:

Primary: Lloyd Crawford, N5GDB;  
[n5gdb@austin.rr.net](mailto:n5gdb@austin.rr.net)

Alternate: Thomas Visel, NX1N;  
[Thomas@neuric.com](mailto:Thomas@neuric.com)

Mail: RMG, PO Box 91058, Austin, TX  
78709-1058

## The 26th Digital Communications Conference

September 28-30, 2007, Hartford, CT

The ARRL and TAPR Digital Communications Conference is an international forum for radio amateurs to meet, publish their work, and present new ideas and techniques. Presenters and attendees will have the opportunity to exchange ideas and learn about recent hardware and software advances, theories, experimental results, and practical applications. Full information can be found at [www.tapr.org/dcc.html](http://www.tapr.org/dcc.html).

### Call for Papers

Technical papers are solicited for presentation at the ARRL and TAPR Digital Communications Conference for publication in the conference proceedings.

Annual conference proceedings are published by the ARRL. Presentation at the conference is not required for publication. Papers must be received by August 6, 2007, and should be submitted to Maty Weinberg, ARRL, 225 Main St, Newington, CT 06111 or [maty@arrl.org](mailto:maty@arrl.org). Electronic files preferred.

Topics include, but are not limited to:

- Software defined radio (SDR)
- Digital voice
- Digital satellite communications
- Global position system
- Precise timing
- Automatic position reporting system (APRS)
- Short messaging (a mode of APRS)
- Digital signal processing (DSP)
- HF digital modes
- Internet interoperability with Amateur-Radio networks
- Spread spectrum
- IEEE 802.11 and other Part 15 license-exempt systems adaptable for Amateur Radio

- Using TCP/IP networking over Amateur Radio
- Mesh and peer-to-peer wireless networking
- Emergency and Homeland Defense backup digital communications in Amateur Radio
- Updates on AX.25 and other wireless networking protocols
- Topics that advanced the Amateur Radio art.

## Microwave Update 2007

October 18-20, 2007

### Call For Papers


Any topics related to microwave theory, construction, communication, deployment, propagation, antennas, activity, transmitters, receivers, components, amplifiers, communication modes, LASER and practical experiences welcome. Abstracts should be submitted by June 1 and completed papers and articles by August 15, 2007.

Please submit your papers, articles and abstracts to W2PED, [pdrexler@hotmail.com](mailto:pdrexler@hotmail.com) or to N2UO, [lu6dw@yahoo.com](mailto:lu6dw@yahoo.com) in Microsoft Word or as an Adobe PDF file. Diagrams, photos and illustrations should be in black and white. Hard copies may be mailed to Paul E. Drexler, 28 West Squan Rd, Clarksburg, NJ 08510.

### Microwave Update 2007 Details

Microwave Update 2007 will be held at historic Valley Forge, near Philadelphia, Pennsylvania. Thursday sightseeing or possible surplus tour. Conference Friday and Saturday; Flea Market Friday night, Vendors on site; Banquet Saturday night; Door prizes and raffles; Hospitality room. Hosted by the Pack Rats — Mt Airy VHF Radio Club. Spouses, friends and family invited. Alternative family/spouse programs available.

\$79 early-bird registration until 9/1 includes Conference, proceedings and banquet; \$89 from 9/1-10/1; \$99 thereafter. Extra banquet Tickets \$39. Special hotel rate \$92 per night. Full info and registration at [www.microwaveupdate.org](http://www.microwaveupdate.org).

Questions to chairpersons Philip Theis, Jr, K3TUF, e-mail [Phil@k3tuf.com](mailto:Phil@k3tuf.com) or David Fleming, KB3HCL, e-mail [kb3hcl@arrl.net](mailto:kb3hcl@arrl.net). 

# Letters to the Editor

## A Low Budget Vector Network Analyzer for AF to UHF (Mar/Apr 2007)

Dear Doug,

Some time ago you asked me to write some additional explanations on the alias concept for my vector network analyzer, described in the Mar/Apr 2007 issue of *QEX*. Here is some additional text to go with that article.

— 73, Dr Thomas C. Baier, DG8SAQ, University of Applied Sciences, Prittwitzstrasse 10, 89075 Ulm, Germany; baier@hs-ulm.de

### Using Unfiltered DDS-Signals for Measuring Frequency Responses

The *QEX* article on my unique direct digital synthesizer (DDS) and PC based vector network analyzer (VNWA) design has invoked quite a few questions on how the DDS output spectra are processed to obtain accurate measurement results.<sup>1</sup> Since this was touched on only briefly in the article, a more detailed discussion is given here. The simple way my VNWA handles DDS aliasing frequencies (also called image frequencies) makes it unique.

Figure 1 shows the fundamental setup that most modern network analyzers, as well as my VNWA, use to measure the frequency response of a device under test (DUT). An RF source delivers power to the DUT whose output signal is mixed down by an LO to an IF that is filtered and analyzed. The most common realization of this setup is by using spectrally pure sine wave oscillators for both the RF and LO. This doesn't have to be the case, however. A measurement of the DUT transfer function is also possible by using a wideband noise source for the RF signal and a sine wave for the LO

signal. In this case, all frequencies are present at the output of the DUT, but the single frequency LO, in combination with the IF-filter, make sure that only the desired piece of the DUT output spectrum is analyzed by the signal analyzer, as in any heterodyne receiver.

In my VNWA design, DDS oscillators are used for the RF and LO generation. The IF filter is realized through the limited frequency response of the PC soundcard used for signal analysis (typically 10 Hz to 20 kHz transmission band) in combination with digital filtering by the PC software. Due to the sampling principle, the DDS signal sources do not deliver pure sine waves, but they do produce a step function with a predictable spectrum, which is shown here in Figure 2. (This is the same as Figure 3 in the original article.) My VNWA design does not use any kind of filtering of the DDS signals. The VNWA does *not* contain any RF filters. The only frequency selective part is the sound card used to detect the IF signals.

As already mentioned, the RF signal of a network analyzer does not necessarily have

to be a pure sine wave. Care has to be taken though, that only the desired radio frequency is mixed into the IF bandwidth with the LO signal. If this can be guaranteed by tricky frequency management like in the VNWA design under discussion, then the LO signal need not be a pure sine wave.

Figure 3 shows an example of how this can be achieved by running the RF DDS and LO DDS on unequal clock frequencies. It shows the output spectra of the RF DDS (solid) and LO DDS (dashed) dependent on the tuned RF frequency at which the measurement is intended to be performed. At any particular tuned RF frequency (examples are indicated with dashed-dotted vertical lines), there are a multitude of RF and LO spectral components. Any two of these can generate an IF in the mixer. A few IFs are indicated in Figure 3 by arrows. Note that only the desired pair of RF and LO frequencies produce the desired IF, since only these have the desired vertical distance in the graph. All other pairings produce different IFs. This works out only due to the

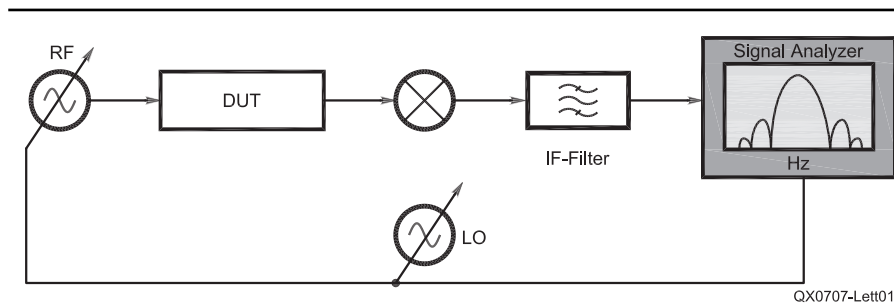


Figure 1 — Basic setup of a network analyzer.

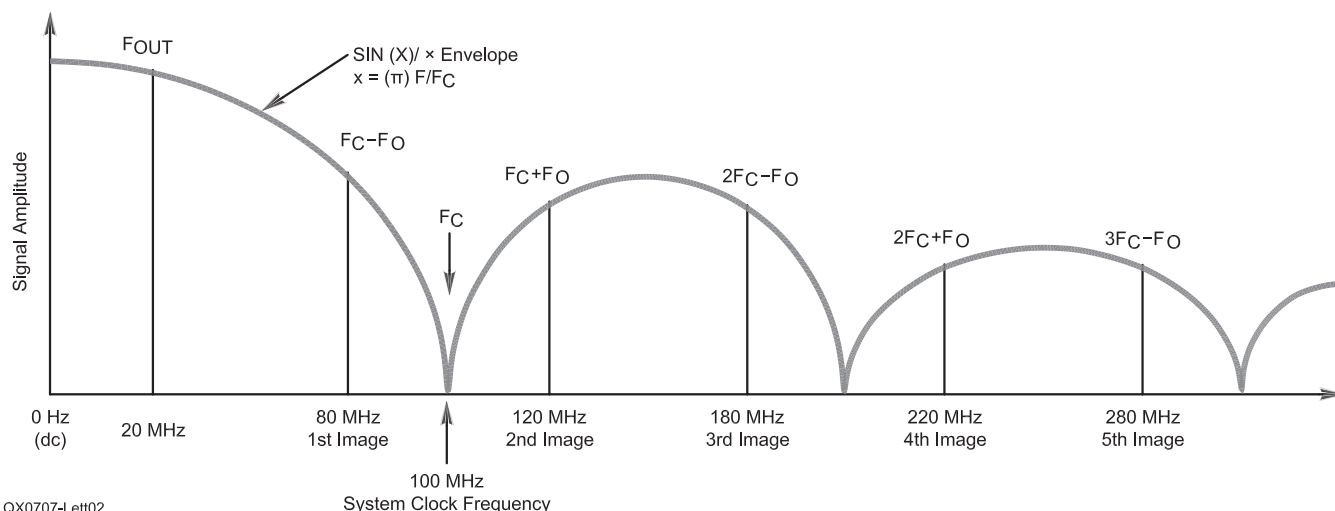


Figure 2 — Unfiltered output spectrum of a DDS clocked with 100 MHz (courtesy of Analog Devices).

**Table 1**  
Possible RF and LO Frequencies to Give the Desired IF

Example 1	Desired Frequency	Tuning Word	Fund Freq	1st Alias	2nd Alias	3rd Alias	4th Alias	5th Alias
RF DDS	20	477218588	20	160	200	340	380	520
LO DDS	40	1010580540	40	130	210	300	380	470
IF =  RF - LO			<b>20</b>	30	10	40	0	50

**Table 2**  
Possible RF and LO Frequencies to Give the Desired IF

Example 2	Desired Frequency	Tuning Word	Fund Freq	1st Alias	2nd Alias	3rd Alias	4th Alias	5th Alias
RF DDS	120	2863311530	60	120	240	300	420	480
LO DDS	140	3537031890	30	140	200	310	370	480
IF =  RF - LO			30	<b>20</b>	40	10	50	0

**Table 3**

Example 3	Desired Frequency	Tuning Word	Fund Freq	1st Alias	2nd Alias	3rd Alias	4th Alias	5th Alias
RF DDS	300	2863311530	60	120	240	300	420	480
LO DDS	320	3789677025	20	150	190	320	360	490
IF =  RF-LO			40	30	50	<b>20</b>	60	10

Example 4	Desired Frequency	Tuning Word	Fund Freq	1st Alias	2nd Alias	3rd Alias	4th Alias	5th Alias
RF DDS	370	238609294	10	170	190	350	370	530
LO DDS	390	1263225675	50	120	220	290	390	460
IF =  RF-LO			40	50	30	60	<b>20</b>	70

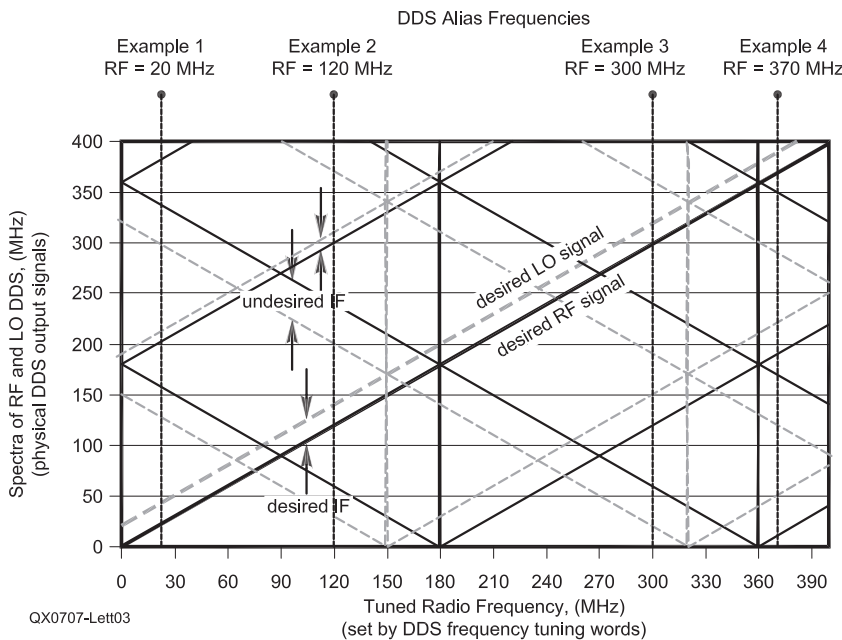


**Figure 3** — LO and RF DDS output spectra versus tuned RF. The solid traces are RF signals and the dashed traces are LO signals. The arrows indicate some possible RF-LO-mixing products. The examples are described in more detail in Tables 1-3. For better visibility, the RF clock frequency is 180 MHz, the LO clock frequency is 170 MHz and the desired IF is 20 MHz.

fact that the RF and LO DDS run on different clock frequencies. If they ran on one and the same clock frequency, every RF alias would have a matching LO alias to produce the very same IF, thus making a spectral separation of the aliases impossible.

Another question I was asked was how to set the DDS 32-bit tuning words to produce the desired alias frequencies. This is best illustrated with a few numerical examples, which are indicated in Figure 3.

The basis for calculating the tuning words is the following formula from the DDS data sheet.

$$n = \frac{f}{f_{\text{clock}}} \cdot 2^{32}$$

**Example 1:** Assume we want to measure a transmission of our DUT at 20 MHz. Thus the RF DDS needs to generate 20 MHz, the LO DDS needs to generate 20 MHz + IF = 40 MHz. With the above formula, the 32 bit tuning words can simply be calculated to yield the values in Table 1. Remember that the RF clock frequency is 180 MHz, while the LO clock frequency is 170 MHz in our example design. With these tuning words, the DDS sources produce the desired 20 MHz RF and 40 MHz LO respectively. But they also produce alias frequencies; for example the

first alias of the RF DDS is 180 MHz – 20 MHz = 160 MHz. The second alias of the LO DDS is 170 MHz + 40 MHz = 210 MHz. Comparing the aliases in Table 1, there is obviously only one pairing that yields a 20 MHz IF when mixed. Note that the table does not show all possible mixing products of the shown aliases, but only those in the vicinity of the desired IF.

Usually a DDS is used to produce less than 50% of its clock frequency. Table 2 displays example 2 where this is not the case.

The DDS tuning words can still be calculated with the above formula. The fundamental DDS frequencies are not the desired output frequencies, however. But the first aliases turn out to be exactly the wanted signals. Also here, only the desired signal pair mixes to 20 MHz IF.

Examples 3 and 4 in Table 3 demonstrate what happens when the DDS tuning words calculated with the above formula exceed the word lengths of 32 bits. In this case, the leading bits beyond bit number 32 are simply ignored. Thus, one arrives at 32 bit tuning words again. By doing this, it turns out that the DDS sources are set such that aliases produce exactly the desired frequencies. Again, only the desired pairs produce the correct IF of 20 MHz.

Finally, I would like to point to a very nice article by Sam Wetterlin, who has illustrated how, by this idea and by making the clock frequencies variable, it is possible to construct a VNWA that covers a wide frequency range without frequency gaps.<sup>2</sup>

A very small VNWA kit, which I hope will cover a frequency range up to 1 GHz is currently under development. For information on availability and pricing please visit the Web site listed in Note 1.

Thanks to Mike Alferman, WA2NAS, for straightening out my manuscript.

#### Notes

<sup>1</sup>Professor Dr Thomas C. Baier, DG8SAQ, "A Low Budget Vector Network Analyzer for AF to UHF," *QEX*, Mar/Apr 2007, ARRL; see also [www.mydarc.de/DG8SAQ/VNWA/index.shtml](http://www.mydarc.de/DG8SAQ/VNWA/index.shtml)

<sup>2</sup>Sam Wetterlin, "Using DDS Aliases to Extend the Frequency Range," [www.wetterlin.org/sam/AD9952/MultipleClockAliases.pdf](http://www.wetterlin.org/sam/AD9952/MultipleClockAliases.pdf)

#### High Speed Multi-Media Working Group

Dear Doug,

Thank you most kindly, sir, for your warm comments about the accomplishments of the League's HSMM Working Group (WG) in your editorial in the May/June 2007 issue of *QEX*. The WG's dedication and efforts are ongoing, as reflected in many radio experimenters projects.

We are particularly proud of the excellent article in your same issue of *QEX* by WG member Roderick D. Mitchell, KL1Y, "The Integration of Amateur Radio and 802.11"

and your excellent presentation thereof.

Thank you so very much for all your outstanding efforts to keep Amateur Radio on the cutting edge of modern radio and electronics technology.

— Very 73, John Champa, NCE (K8OCL), Wireless Systems Engineer, Rockwell Collins, Former Chairman, HSMM WG, 17850 Sunmeadow Dr, Apt 2303, Dallas, TX 75252; [k8ocl@hotmail.com](mailto:k8ocl@hotmail.com)

Hi John,

Thanks also for all the work you and all the members of the Working Group have done, and continue to do. I agree that Rod Mitchell's article is an interesting report on some of that work.

What else do you have to report? *QEX* stands ready to report on the WG's efforts. If you or anyone else on your group would like to write for *QEX*, please submit your articles. — 73, Larry Wolfgang, WR1B, *QEX* Managing Editor; [lvolfgang@arrl.org](mailto:lvolfgang@arrl.org)

#### Automatic Noise Figure Meter (May/June 2007)

The subject article is a good example of how a measurement problem can be solved by a little thought, without needing to buy or borrow expensive commercial equipment. Twenty or so years ago, I was faced with how to make NF measurements on some VHF and UHF very low noise amplifiers, but my university research lab was not equipped with a noise figure meter.

The solution was a calibrated noise source, a broadband amplifier, a tunable band pass filter and a power meter to measure the noise with the noise source off and then on. All these items were available in my lab. The NF was calculated from the Y factor given by the power meter. I never thought my idea was new, but I was surprised to find that the vendor for the low noise amplifiers had never thought of using my procedure. He was surprised to see that my measurements were quite accurate also.

Good article!  
— 73, John H. Bordelon, PhD, K4JIU, 1690 Hampton Oaks Bend, Marietta, GA 30066-4451; [k4jiu@arrl.net](mailto:k4jiu@arrl.net)

Hi John,

Thanks for the compliments. We're glad you liked this article.  
— 73, Larry, WR1B.

#### Components Cross Reference

Dear Sir,

I have some data to help fill a hole in the HP cross reference to JEDEC or 300-hporef. pdf. HP part number 1858-0054 is an exact match for an Intersil (RCA) CA3096 transistor array.

We found this part in an Agilent service manual. By "we" I refer to a group to which I belong that promotes classic computer stuff.

I'm also a proud ARRL member. Thanks for helping us pass along this information! — 73, Steven Canning, PO Box 1682, La Mirada, CA 90638; [cannings@earthlink.net](mailto:cannings@earthlink.net)

#### On the Crossed-Field Antenna Performance, Parts 1 and 2 (Jan/Feb and Mar/Apr 2007)

Dear Doug,

I feel the article on the Crossed-Field Antenna was far below the technical level set up to this point by *QEX*.

I know there is a great deal of discussion about the theory, but most knowledgeable antenna experts do not give this antenna any real credibility. In fact, the credit seems to go to the feed line.

I always look forward to reading *QEX* and enjoy the level of articles presented. With no empirical data or clear explanation of theory, this one just seemed out of place. It may have been better placed in the April issue.

— Doug Millar, K6JEY, ARRL Technical Advisor, 2791 Cedar Ave, Long Beach, CA 90806; [doughhelen@moonlink.net](mailto:doughhelen@moonlink.net)

Hello, Doug,

I'm dismayed to see another IEEE article reprint that takes eight editorial pages in *QEX*. I have written previously to express my disappointment at reprinting verbatim articles that appeared elsewhere. Post such a reprinted article on the ARRL Web site, if you wish, but I pay for a *QEX* subscription to learn about new things of interest to communication experimenters. I have no interest in wading through dense mathematics presented previously in a professional-society publication. I doubt most other "experimenters" will either. To make matters worse, this article's second part will take more editorial pages in a future *QEX*. This isn't the type of information I signed up to receive in the pages of *QEX*, so I intend to let my *QEX* subscription lapse.

— Jon Titus, KZ1G, 5526 West 13400 South, Suite 105, Herriman, UT 84096; [jontitus@comcast.net](mailto:jontitus@comcast.net)

Gentlemen,

We are sorry that you did not enjoy the crossed field antenna article. Direct reprints of previously published, readily available articles have been a rare occurrence in the pages of *QEX*. This research seemed to be worth sharing with *QEX* readers.

I hope you will consider sharing some of your own work with our readers. *QEX* is dedicated to sharing experimental work and ideas about a wide array of communications topics.

Jon, I hope you will also reconsider your decision to allow your subscription to lapse based on this one article. I hope you have found many other articles of interest and that you would look forward to reading more



excellent articles in the future!  
— 73, Larry, WR1B

### ARES Communications Protocol

Editor,

I am interested in investigating an improved communications and message traffic handling system for use in ARES deployment situations. I am both an Amateur Radio operator and a computer/information scientist and my experiences with existing UHF based communications systems has shown the difficulties inherent in voice-based, simplex communications and message handling.

The situation I am attempting to address is how to avoid overlapping transmissions when operating in a simplex mode (we are training for a worst-case situation with no repeater availability). The difficulty occurs when, in simplex mode, you have a network control station and remote stations, and the remote stations cannot hear each other but can communicate with the control station. The reality is that too often we have "collisions" when remote stations transmit simultaneously, and in emergencies this delay and or loss of successful communication could be fatal. One solution is for remote stations to call and wait for permission to transmit; another is a roll-call protocol. For standard voice communications, the call and wait protocol makes good sense and works well with disciplined operators. As we move to digital communications, however, there are better ways to avoid message collisions and the automated roll-call (poll-response) initiated by the control station is the one I am investigating. Packet or even character format communications would appear to be readily available. The missing pieces in this system relate to the network level protocol to control communications.

The AGW suite of software and the

AX25 Connected mode protocol appear to have almost all of the features I am seeking, although not exactly in the way I want (poll response).

Any information that your readership could provide on others who are also looking into, or working on this same or related communications protocol would be greatly appreciated.

— J.J. Hayden, KN4SH, 45 Cory Ct, Covington, GA 30016; [jjhaydeniii@earthlink.net](mailto:jjhaydeniii@earthlink.net)

### Antenna Options — NVIS Antennas for Special Needs (May/June 2007)

LB's article on discussing wide band NVIS antennas shows so clearly the obsession many have with antenna matching. Here is an antenna (terminated V) that has at least four dB more loss than an unterminated one, favored by some purely because it matches the source better. Take the unterminated version and put a 3 dB pad in front of it and the amplifier will be happy, and more RF will reach the destination! Obviously there is more to life than SWR.

I would call into question one statement, though. "Since the ... transmitter [scans] so rapidly, it does not have time for the delays associated with changing matching networks ...". There may be situations where this is true, but in general, it is very possible to design tunable matching networks using PIN diodes that can respond in microsecond time frames. For HF, it is more challenging because PIN diodes that can work down to 3 MHz are harder to come by, and will take longer to change state, but it is not impossible. High speed PIN diode devices are not likely to dominate Amateur practices anytime soon because of cost and other factors. For military applications, however, such devices provide an alternative to wideband NVIS antennas.

One of my clients manufactures tunable aircraft antennas that cover 30 to 500 MHz.

This is a blade less than a foot in any dimension! It is used with military hopping radios and can settle on a new operating frequency in 10  $\mu$ s. The radio sends the new frequency to the antenna as a digital word and the microprocessor inside selects the proper combination of PIN diodes to resonate this little blade to that frequency.

— Wilton Helm, WT6C, Embedded System Resources, 320 Old Y Rd, Golden, CO 80401; [whelm@compuserve.com](mailto:whelm@compuserve.com)

Hi Wilton,

I agree that in principle it is possible to reduce the transition time within the matching networks to the very short interval that you indicate.

Unfortunately, such tuning units are not presently available — to my knowledge — at the frequencies indicated for amateur and related NVIS services at the power levels typically used and at a price that most amateurs can pay. That is the context within which my notes were applicable.

I also agree that in principle SWR is certainly not everything, but with typical amateur transceivers the output impedance is fixed within a very small range with foldback circuits to limit final amplifier power when the SWR indication is greater than a certain threshold. Hence, the amateur need to match is a practical matter, not a theoretical one.

An alternative to high-speed matching is, of course, slower speed ALE processing, so that the speed of channel scanning matches the speed of available automatic tuner switching for ATUs that already exist or that can be developed to fit amateur budgets. Military and other services that need burst transmissions to keep channels and data secure may require the very high speed of the latest ALE processors, but the emergency services rendered by radio amateurs and many of the agencies involved in similar services do not need such security — only efficiency.

— 73, LB Cebik, W4RNL, 1434 High Mesa Dr, Knoxville, TN 37938; [Cebik@cebik.com](mailto:Cebik@cebik.com)

In the next issue of



Frequent QEX authors Paolo Antoniazzi, IW2ACD, and Marco Arecco, IK2WAQ, have written another excellent article in "Very High Q Microwave Cavities and Filters." Paolo and Marco describe the design and laboratory testing of cylindrical resonators for the 10 GHz band. With unloaded Quality Factors of 24,000 or better, these cavities are definitely worth a look! Don't miss it.



## QEX

### ARRL

225 Main Street  
Newington, CT 06111-1494 USA

For one year (8 bi-monthly issues) of QEX: **Subscribe toll-free with your credit card 1-888-277-5289**

Renewal  New Subscription

Name: \_\_\_\_\_ Call: \_\_\_\_\_

Address: \_\_\_\_\_

City: \_\_\_\_\_ State or Province: \_\_\_\_\_ Postal Code: \_\_\_\_\_

Payment Enclosed to ARRL

Charge:

Account # \_\_\_\_\_ Good thru \_\_\_\_\_

Signature \_\_\_\_\_ Date \_\_\_\_\_

Remittance must be in US funds and checks must be drawn on a bank in the US. Prices subject to change without notice.

06/01



## ELECTRONICS ENGINEERS/TECHNICIANS NEEDED!!

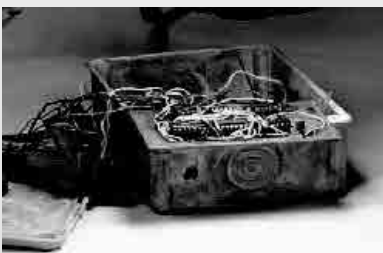
Salary potential of over \$210,000

### YOU CAN MAKE A DIFFERENCE IN THE DEFENSE OF THE NATION

You will exploit Improvised Explosive Devices (IEDs) and assist in the development of new Explosive Ordnance Disposal (EOD) tools and methods to counter emerging threats. Activities include the development of device theory of operation and basic electronic circuit analysis. The data you generate will be used by many organizations for counter terrorism operations. Extensive training is provided in preparation for periods of deployment.

You will work on a military facility within Iraq, Afghanistan, or other areas of operation. Planned deployment rotations of 3 months in theater are followed by 3 months in Indian Head MD; repeated and subject to change as required. **The successful candidate must possess a secret clearance or be able to obtain a secret clearance. TS clearance is desired.**

Please forward resume to [EODTD Employment EE.fct@navy.mil](mailto:EE.fct@navy.mil) if you are interested in applying for a position.



**All the information you need to design your own complete antenna system.**

The ARRL

# ANTENNA BOOK

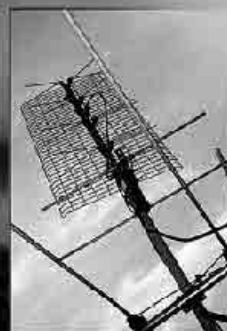
21st Edition

ARRL Order No. 9876

Only **\$44.95\***

\*shipping \$10 US/\$15.00 International

The *ultimate* reference for Amateur Radio antennas, transmission lines and propagation



Fully searchable CD-ROM included!



The ARRL  
**ANTENNA BOOK**

21st Edition



**ARRL** The national association for  
**AMATEUR RADIO**

SHOP DIRECT or call for a dealer near you.  
ONLINE [WWW.ARRL.ORG/SHOP](http://WWW.ARRL.ORG/SHOP)  
ORDER TOLL-FREE 888/277-5289 (US)

QEX 7/2007

# Big Winners from Array Solutions



## PowerMaster Watt/VSWR Meter

- Sets the leading edge for all watt/vswr meters to follow
- Unheard of accuracy for the price
- Fast Bright reading meter
- Application software included
- Upgradeable via Internet

**\$430**



## AIM 4170 Antenna Analyzer

- Most advanced vector impedance analyzer at a fraction of the cost
- Accurate and easy to use
- Application software included
- Lab instrument quality
- Upgradeable via Internet

**\$440**



OptiBeam 3 element 80 Yagi

**OB3-80+**

## OptiBeam Antennas

German Engineering means High Performance and Reliability

## Prosistel Rotators

Strongest Rotators on the Market  
Prosistel  
PST 71 DC



## AS-AYL-4

NEW 4 Direction K9AY Loop Antenna  
Hear What You've Been Missing on the Low Bands

[www.arrayolutions.com](http://www.arrayolutions.com)

Phone 972-203-2008

sales@arrayolutions.com

Fax 972-203-8811



**We've got your stuff!**



# KENWOOD

Listen to the Future

# KENWOOD SKYCOMMAND TURN IT ON!

**Kenwood SkyCommand has FCC approval.**

Allows Global communication through remote operation on HF frequencies at home or in the field utilizing Kenwood's TS-2000 series transceivers.

Kenwood's TH-D7AG or TM-D700A required for remote use.

Perfect for use in hurricane or tornado zones, as well as Search and Rescue areas for Long Distance Communications when other normal modes of communications are out.

A great tool to monitor propagation while doing other things at home!

No cables or adaptors to fool with or buy!

No software or computer required!!

Step by step setup and programming taking only minutes.

Ease of use.



*See your local dealer for details.*

**KENWOOD U.S.A. CORPORATION**

Communications Sector Headquarters

3975 Johns Creek Court, Suite 300, Suwanee, GA 30024-1265

**Customer Support/Distribution**

P.O. Box 22745, 2201 East Dominguez St., Long Beach, CA 90801-5745

Customer Support: (310) 639-4200 Fax: (310) 537-8235

**INTERNET**

Kenwood News & Products

<http://www.kenwoodusa.com>

ADS#44806



ISO 9001 Registered

UKAS Quality Management

UKAS Quality Management

UKAS Quality Management

UKAS Quality Management